Albert-Ludwigs-Universität Freiburg
Fakultät für Mathematik und Physik

Betreuung von Dr. Florian Mintert

Optimal Control of Multipartite Entanglement with Measures Optimized "On-the-Fly"

Diplomarbeit von

Mark Girard

aus

Boulder, Colorado, USA

6. August 2012

Erklärung der Selbstständigkeit

Hiermit versichere ich, die vorliegende Arbeit selbstständig verfasst und keine anderen als die angegebenen Quellen und Hilfsmittel benutzt sowie die Zitate deutlich kenntlich gemacht zu haben.

Mark Girard
Boulder, CO, USA, den 6. August 2012

Summary

Entanglement is the property of quantum states that, since the begining of the development of quantum theory, most contradicts our physical intuition, and has attracted the most attention. More recently, it has been discovered that entanglement is an essential requirement for many applications of quantum information theory. Although its importance in quantum information has been identified, a general understanding of entanglement in many-body quantum systems has yet to be developed.

Identifying whether or not a state is entangled is a difficult problem. In fact, most methods of quantifying entanglement cannot be evaluated directly and require some sort of numerically expensive optimization procedure for their evaluation. Furthermore, experimental implementations of quantum entanglement are subject to unavoidable interactions with the enviromnent which destroy the desired coherences exhibited by entangled states.

Previous work has been done to develop a method to generate multipartite entanglement in an interacting quantum system, where the entanglement produced is robust against decoherence. The time evolution of a the system can be dynamically controlled through suitably chosen, time-varying, external control fields. Highly entangled states can be produced in this manner if the target functional is chosen to be an entanglement measure. The optimal control fields that yield states that maximize this measure may be derived purely algebraically through the methods provided by control theory. This method, however, is limited to functionals that can be evaluated analytically and whose time derivatives can be easily determined. Since this is not the case for most measures of entanglement, we must resort to other techniques to achieve a similar control strategy.

In this thesis, I present a method that extends this control strategy for target functionals that must be optimized over a continuous parameter space for their evaluation. There are two properties that must be optimized simultaneously for this control scheme to succeed: the amplitude of the external control that is to be applied, and the parameters needed to evaluate the target functional. If the optimal parameters change continuously as the state evolves, then a full optimization is not necessary and the optimal adjustment to the parameters can be determined. This method optimizes entanglement measures "on-the-fly," since this optimization procedure for the functional is performed concurrently with the determination of the optimal control fields.

Zusammenfassung

Verschränkung ist die Eigenschaft von Quantenzuständen, die seit Beginn der Entwicklung der Quantentheorie unserer physikalischen Intuition zutiefst widerspricht. In neuerer Zeit wurde entdeckt, dass Verschränkung eine wesentliche Bedingung für viele Anwendungen in der Quanteninformationstheorie ist. Obwohl ihre Bedeutung in der Quanteninformation schon längst anerkannt ist, sind die allgemeinen Kenntnisse von Verschränkung in quantenmechanischen Mehrteilchensystemen bislang noch unzureichend entwickelt.

Es ist ein schwieriges Problem, zu identifizieren, ob ein Zustand verschränkt ist. Die meisten Methoden zur Verschränkungsquantifizierung können in der Praxis nicht direkt ausgewertet werden und brauchen ein numerisch aufwendiges Optimierungsverfahren zur Berechnung. Außerdem unterliegen experimentelle Realisierungen von Quantenverschränkung unvermeidbarer Wechselwirkung mit der Umwelt, die die von verschränkten Zuständen aufgewiesenen und gewünschten Kohärenzen zerstören.

In bisherigen Untersuchungen wurde eine Methode entwickelt, die gegen Dekohärenz robuste Mehrteilchenverschränkung in wechselwirkenden quantenmechanischen Systemen generiert. Die Zeitentwicklung eines Systems kann durch geeignete zeitvariierende externe Kontrollfelder dynamisch kontrolliert werden. Hoch verschränkte Zustände können auf diese Weise erzeugt werden, wenn ein Verschränkungsmaß als Zielfunktion ausgewählt wird. Die optimalen Kontrollfelder, die dieses Maß maximierende Zustände liefern, können mithilfe der Methoden optimaler Kontrolltheorie rein algebraisch hergeleitet werden. Diese Methode ist jedoch auf analytisch auszuwertende Zielfunktionen beschränkt, deren Zeitableitungen leicht bestimmt werden können. Da dies bei den meisten Verschränkungsmaßen nicht gegeben ist, müssen wir andere Methoden wählen, um eine ähnliche Kontrollstrategie zu erreichen.

In dieser Arbeit stelle ich eine Methode vor, die diese Kontrollstrategie auf Zielfunktionen ausdehnt, deren Bewertung eine Optimierung über einen stetigen Parameterraum braucht. Damit diese Kontrollstrategie gelingt, müssen zwei Eigenschaften gleichzeitung optimiert werden: die Amplitude der anzuwendenden externen Kontrolle und die für die Berechnung der Zielfunktion zu optimierende Parameter. Falls die optimalen Parameter sich während der Entwicklung des Zustandes stetig ändern, ist eine vollständige Optimierung nicht notwendig und eine optimale Änderung der Parameter kann bestimmt werden. Diese Methode optimiert Verschränkungsmaße “on-the-fly”, da das Optimierverfahren der Zielfunktion gleichzeitig mit der Bestimmung der optimalen Kontrollfelder durchgeführt werden muß.

Acknowledgements

I am very grateful for the financial support awarded to me by the German Academic Exchange Service (DAAD) for funding my studies in Germany. The friendships I've made and the good times I've had at DAAD-sanctioned events during my studies in Freiburg, especially with the local DAAD-Freundeskreis, have been incredibly rewarding.

I am sincerely thankful for Flo. More than being a wonderful and friendly advisor, his guidance has been an important part in shaping this thesis. His constructive criticism of my work, as well as his tolerance of my mistakes, have certainly helped me learn and grow. My office mates, Fede and Sol, also deserve my thanks for the pleasant discussions and entertainment they have offered.

As always, I would like to thank my family for their constant support and encouragement during the course of my studies. Above all, I am eternally indebted to Hannah, who has been a never-ending source of love and support.

Contents

Chapter 1

Introduction

The discovery of quantum mechanics at the beginning of the twentieth century heralded a new era of physics and forced physicists to revise their understanding of nature. By 1932 the foundations of quantum mechanics had been completely laid out in von Neumann's *Mathematische Grundlagen der Quantenmechanik* [1], and although quantum mechanics appeared to provide an accurate description of the physical universe, some of the puzzling features of quantum mechanics both baffled and disconcerted some physicists during the theory's early years. In their famous paper [2], Einstein, Podolsky and Rosen drew attention to some of the nonintuitive consequences of quantum mechanics, which they derided as "spooky interaction at a distance". This feature implies the existence of global states of composite systems that cannot be described as a product of states of the individual subsystems. This phenomenon, dubbed *entanglement* by Schrödinger [3], embodies the "spooky" feature of quantum machinery that lies at the center of interest in physics today.

As a nonlocal property of quantum mechanics, this lead Einstein in 1935 to question whether the quantum mechanical description of nature was complete. It wasn't until 1964 that Bell proposed a method [4] to descriminate between quantum mechanics and the theories of local realism proposed by Einstein. Bell showed that local hidden variable theories provided different predictions for measurement outcomes of certain experiments than those offered by quantum mechanics. In fact, Bell found that entangled states could exhibit *more* statistical correlations than the states allowed by hidden variable theories. Described by the so-called Bell inequalities, this conclusion finally supplied experimenters a conclusive test to determine which theory is a better description of Nature. This debate continued on theoretical ground until Aspect [5] conducted a convincing experiment in 1982 showing that the Bell inequalities were violated. This confirmed quantum mechanics as an accurate description of reality.

Although not purely a consequence of entanglement, Feynman [6] suggested

in 1982 that the nonclassical features of quantum mechaincs could be exploited in computational tasks. He pointed out that classical computers are incapable of adequately simulating large-scale quantum systems, and that one could build computers which instead worked with quantum mechanical principles. With this, the concept of the quantum computer was born.

It was not until the 1990s that it became clear that entanglement could also be used as a resource [7], especially for quantum communication protocols. In fact, present-day entanglement theory has its roots in a few key discoveries that were made during this time. Perhaps the first interesting application of entanglement was developed in the area of cryptography [8]. Ekert showed that if two distant parties share many pairs of maximally entangled qubits, they can create a perfectly secure private cryptographic key. The discovery of quantum teleportation [9] was another important moment for entanglement theory. In a teleportation protocol, two parties that share a pair of maximally entangled qubits may perfectly teleport the state of another qubit from one party to the other. Furthermore, it was discovered that the capacitity of a classical communication channel can be improved via shared entanglement between a sender and a reciever [10].

While entanglement was initially known to have many applications in quantum communication, it has been found to be very useful in other areas as well. Classical computers, for example, are inefficient at solving many problems, such as factoring large numbers. However, there exist quantum algorithms capable of solving these problems asymptotically faster than their classical counterparts [11]. The most famous example is that of Shor's factoring algorithm [12], which can factor numbers on polynomial time scales. Although it is known that entanglement is required for Shor's algorithm, the role of quantum entanglement in other computational speed-ups is not exactly known [13].

A successful quantum computer requires processing and storage of quantum information stored in qubits. Since the information in quantum states is much more fragile than classical information, error correcting codes would be necessary for a reliable quantum computer [14]. This problem is more difficult than its clasical counterpart due to the no-cloning theorem [15], which prohibits the ability to copy an unknown arbitrary state of a quantum system. Despite this, codes have been created to correct errors in quantum information protocols. Multipartite quantum entanglement seems to play a vital role in all quantum error correcting codes [11].

Recent research has focused on the importance of genuine multipartite entanglement [16], whose generation in an N-body quantum system requires all parties to interact. Genuine multipartite entangled states are known to be vital for fundamental tests of quantum physics [17, 18]. They have played an important role in development of measurement-based schemes for "one-way quantum comput-

ers" [19], which require the initial states of a system of many particles to be highly entangled. Quantum computations can then be performed though a series of succesiveive measurements [20], destroying the entanglement in the process.

Any application of quantum entanglement requires the creation and maintenance of highly entangled states of many particles. However, unavoidable interactions of the system with the environment lead to decoherence, further complicating this task. This causes information to be lost to the environment, destroying the coherences that are essential for entanglement. Now that both the importance and the role of entanglement in such tasks is well understood, the current effort in many experimental implementations of these quantum tasks is to engineer highly entangled states that will persist as long as possible against entanglement decay caused by decoherence due to environmental interactions. These problems are addressed by the framework of quantum control theory.

At its essence, quantum control confronts the problems of decoherence and imperfections within quantum systems. Interest in controlling quantum systems first arose in the 1950s with the advent of experimental nuclear magnetic resonance (NMR) spectroscopy [22]. More sophisticated control techniques emerged as research in NMR further advanced and the need for controllability in quantum computation arose [22]. Current applications of quantum control are widespread, including gate optimization for quantum computers [23, 24]. Implementation of quantum control usually manifests itself in the application of ultrafast, high-precision laser pulses, whose shapes may be manipulated to achieve desired effects in the controlled system. The mathematical framework of optimal control can be used to determine the most effective pulses for maximizing an objective [25]. Since almost any quantum system is generally too complex for optimal control to be designed analytically, numerical algorithms such as gradient ascent pulse engineering [26] are needed.

Typical optimal control schemes are devised to drive a system as close as possible to a desired target states. In this thesis, however, our goal is to create many-body entanglement that persists over long periods of time. Rather than target a specific entangled state, we can instead devise control that maximizes an entanglement measure. The problem with using an entanglement measure as the objective is that most entanglement measures cannot be straightforwardly evaluated since they require an optimization. The implementation of quantum control requires not only that the target function be repeatedly evaluated, but also that its dynamics be efficiently calculated. In this thesis, we present a method of implementing control of quantum systems where the objective is to maximize an entanglement measure. Highly entangled states are achieved by applying control that maximize the time derivatives of the measure at all times. This has already been studied in cases where the entanglement meausre can be analytically evalu-

ated [27]. We show that any measure can be used in principle if the variables over which the measure must be optimized can be continuously parameterized without constraints. Although the control fields obtained from this scheme ensure that the target funciton increases optimally at any given time during the evolution, they do not guarantee that the maximum value of the entanglement measure is reached in the end. With some of the measures that we introduce here, we show that our control scheme successfully generates states that maximize the measure. However, when certain measures are used as target funcitonals, this control scheme does not always generate an optimal state.

Furthermore, in many experimental implementations of quantum entanglement, it is difficult if not impossible to engineer and manipulate particular interactions within the system. Entanglement can arise from existing interactions between particles of a system, but creation of high levels of entanglement this way is not likely. Such systems will become unentangled just as fast as the entanglement was formed. The individual particles of a system can be controlled such that the interactions produce the desired entanglement. Once a highly entangled state is achieved, continued application of control must be applied to prevent the interactions from decreasing the amount of entanglement. We make use of the framework of quantum control theory to derive control fields that drive systems into highly entangled states, using an entanglement measure as the target to be optimized. In addition to making use of existing interactions to create entanglement, we also consider the effects of environmental interactions, and create entangled states that are most robust against specific models of decoherence.

Chapter 2

Entanglement

Before we can discuss methods with which to produce and use entanglement, we first require a mathematical description of what it is. In addition, we also need methods to quantify entanglement and to distinguish between different types. Only then can we determine how entanglement evolves due to the dynamics of the underlying quantum system. Quantum entanglement has two unfortunate yet interesting features: it is susceptible to and fragile against interactions with the environment [28], and it cannot be increased on average when systems are not in direct contact with each other [29]. The central problems in entanglement theory address not only the questions of how to characterize entanglement but how to quantify it as well.

2.1 Definition of entanglement

2.1.1 Pure states

Quantum systems can be described by a Hilbert space $\mathcal{H}$ [1], which is a complex inner-product space that is also a complete metric space [30]. For finite-dimensional systems, this is equivalent to a complex vector space $\mathcal{H} = \mathbb{C}^d$, where d is the dimension of the system. The elements of $\mathcal{H}$, which are vectors denoted by $|\psi\rangle$, represent the possible states of the corresponding system. In fact, the so-called pure states of the system have a one-to-one correspondence to the *rays* in this vector space, such that if two vectors $|\psi\rangle, |\phi\rangle \in \mathcal{H}$ satisfy $|\psi\rangle = \lambda|\phi\rangle$ where λ is a complex number, then they represent the same state.

Although some systems may be represented by infinite dimensional Hilbert spaces, the quantum systems that will be considered here are finite dimensional. Indeed, we limit outselves to the simplest case of 2-dimensional systems, whose Hilbert spaces may be spanned by a basis of two linearly independent vectors,

which may be written as $|0\rangle$ and $|1\rangle$. Such a system is canonically called a *qubit*, short for *qu*antum *bit*, in contrast to a classical bit which may only be in two possible states, 0 or 1. We will be dealing entirely with systems of qubits for the duration of this thesis, so all systems of individual particles in the remaining work will be assumed to be qubits.

We can also consider composite systems of many subsystems, e.g. systems of many qubits. The straightforward mathematical description of such systems is a Hilbert space comprised of a tensor product of the Hilbert spaces of the individual qubits,

$$\mathcal{H} = \mathcal{H}_1 \otimes \cdots \otimes \mathcal{H}_N. \tag{2.1}$$

The Hilbert space has a total dimension of 2^N, which is the product of the dimensions of the individual subsystems. It is in such systems that states with non-classical correlations arise. Such tensor vector spaces contain states that cannot be factorized into pure states of their individual components. These states are called *entangled*.

Let us consider the simplest case: A pure state $|\Psi\rangle_{AB}$ of a system of two qubits A and B, with associated Hilbert spaces $\mathcal{H}_A$ and $\mathcal{H}_B$ respectively. The state $|\Psi\rangle_{AB}$ is associated with the Hilbert space $\mathcal{H} = \mathcal{H}_A \otimes \mathcal{H}_B$, whose elements include all possible tensor products of elements in the two subspaces, such as $|0\rangle_A \otimes |0\rangle_B = |00\rangle$. Because of the superposition principle in quantum mechanics, any linear combination of these product states is also a possible state, for example

$$|\Psi\rangle_{AB} = \alpha|00\rangle + \beta|11\rangle \in \mathcal{H}. \tag{2.2}$$

A *separable* state in the composite state $\mathcal{H}$ is any state that can be written purely as a tensor product of two states from the individual subspaces, i.e.

$$|\Psi\rangle_{AB} = |\psi\rangle_A \otimes |\phi\rangle_B, \tag{2.3}$$

with $|\psi\rangle_A \in \mathcal{H}_A$ and $|\phi\rangle_B \in \mathcal{H}_B$. States in $\mathcal{H}$ that cannot be decomposed into a product, such as the example in (2.2), are said to be *entangled*. To be more precise:

Definition 1. A pure state $|\psi\rangle \in \mathcal{H}_1 \otimes \cdots \otimes \mathcal{H}_N$ of a composite quantum system is called *entangled* if and only if:

$$\begin{aligned} \forall|\phi_1\rangle \in \mathcal{H}_1, \ldots, \forall|\phi_N\rangle \in \mathcal{H}_N : \\ |\psi\rangle \neq |\phi_1\rangle \otimes \cdots \otimes |\phi_N\rangle. \end{aligned} \tag{2.4}$$

Otherwise, the state is called *separable*.

2.1.2 Mixed states

Realistically, it is not possible to completely separate a system from its environment in experiments. If there exist correlations between the system and its environment, then the state of the complete system cannot be written as a product

$$|\Psi_{se}\rangle \neq |\psi_s\rangle \otimes |\psi_e\rangle, \tag{2.5}$$

where $|\psi_s\rangle$ is a state of the system in question and $|\psi_e\rangle$ is a state of its environment. Because we do not have access to the environment, we have incomplete knowledge of the state of the system that we want to observe. The state of the system, using our incomplete knowledge, can be described by tracing out the environment

$$\begin{aligned} \rho_s &= \mathrm{Tr}_e|\Psi_{se}\rangle\langle\Psi_{se}| \neq |\psi_s\rangle\langle\psi_s| \\ &= \sum_i p_i|\psi_i\rangle\langle\psi_i|, \end{aligned} \tag{2.6}$$

with $\sum_i p_i = 1$ and $p_i \geq 0$. This describes a statistical distribution of states. In the presence of such environments, or with the presence of classical statistical uncertainty, states of the system in question are described by density matrices. The space of all possible density states of a system $\mathcal{H}$ is given by $\mathcal{P}(\mathcal{H})$,

$$\mathcal{P}(\mathcal{H}) := \{\rho \in \mathcal{B}(\mathcal{H}) | \rho \geq 0,\ \mathrm{Tr}\rho = 1\}, \tag{2.7}$$

where $\mathcal{B}(\mathcal{H})$ represents the space of all bounded linear operators on the Hilbert space $\mathcal{H}$. That is, the matrices that represent states must be positive semi-definite (i.e. having non-negative eigenvalues) and have unit trace.

With the exception of pure states, i.e. when $\rho = |\psi\rangle\langle\psi|$, there is an infinite number of unravelings into combinations of pure states that represent ρ,

$$\rho = \sum_j p_j|\psi_j\rangle\langle\psi_j|. \tag{2.8}$$

These states are called *mixed*, since they represent a statistical mixture of pure states. Such states on composite systems $\mathcal{H} = \mathcal{H}_A \otimes \mathcal{H}_B$ can still have entanglement. However, if there exists an unraveling of ρ such that all of its composite states are separable, then there is a completely separable representation for ρ, therefore ρ is not entangled. Thus, we can define the presence of entanglement in a mixed state as follows:

Definition 2. A mixed state $\rho \in \mathcal{P}(\mathcal{H}_1 \otimes \cdots \otimes \mathcal{H}_N)$ of a composite quantum system is called *separable* if and only if there exists a pure state decomposition

$$\rho = \sum_j p_j|\psi_j\rangle\langle\psi_j| \tag{2.9}$$

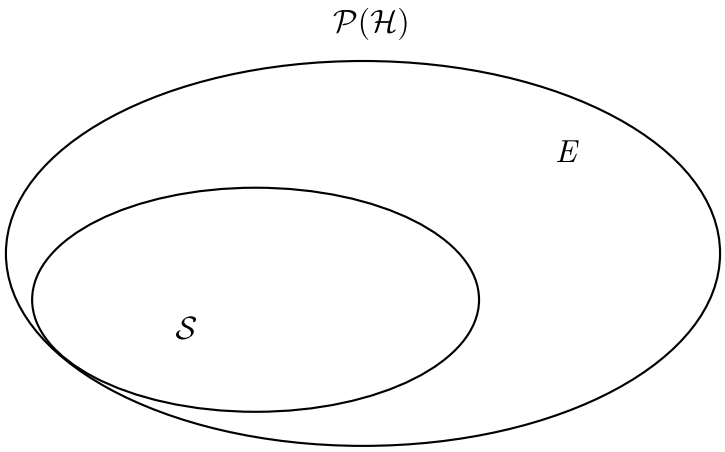

Figure 2.1: Illustration of the convexity of the space of all states of a quantum system, $\mathcal{P}(\mathcal{H})$, containing the convex subset of separable states $\mathcal{S}(\mathcal{H})$. States that are not separable are in the set of entangled states E. The points on the boundary of $\mathcal{P}(\mathcal{H})$ represent pure states.

with $|\psi_j\rangle \in \mathcal{H}_1 \otimes \cdots \otimes \mathcal{H}_N \; \forall j$, such that each $|\psi_j\rangle$ is separable according to eq. (2.4) in Definition 1. Otherwise, if every decomposition contains at least one pure state that is not separable, the state ρ is *entangled* [31].

We can gain some intuition from the geometric picture of the space of quantum states. Indeed, the above definition highlights an important property of the space of states, that of *convexity*. Primarily, the space of all possible quantum states of a system, represented by $\mathcal{P}(\mathcal{H})$, is a convex set. The mixture of any two density matrices is again a density matrix:

$$\forall \rho, \sigma \in \mathcal{P}(\mathcal{H}), \;\; \forall p \in [0,1] \quad p\rho + (1-p)\sigma \in \mathcal{P}(\mathcal{H}). \tag{2.10}$$

Additionally, since any mixture of separable states is also separable, the set of separable states forms a convex subset in the set of all possible states. The general structure of the space of states of a quantum system is represented in Figure 2.1.

2.1.3 Local equivalence

"Hilbert space is a big place,"[1] and it can be useful to define classes of states that are similar in some way to more easily handle the problem of describing entangled states in a quantum system. If we have some way to determine such similarity, it should be reasonable to conclude that if two states ρ_1 and ρ_2 are equivalent,

[1] Carlton Caves

e.g. have the same entanglement properties, then they can be used to perform the same task. The equivalence that we consider is that of local equivalence, which is discussed below. Indeed, the importance of local equivalence is something that is stressed in this thesis.

In order to create entangled states starting from product states, we need interactions between the subsystems. Without interactions, any purely local Hamiltonian H inducing an evolution of the composite system of A and B can be written as

$$H = H_A \otimes \mathbb{1}_B + \mathbb{1}_A \otimes H_B \tag{2.11}$$

where H_A and H_B are Hamiltonians of the subsystems A and B, and $\mathbb{1}$ is the identity operator each subsystem. Since $H_A \otimes \mathbb{1}_B$ and $\mathbb{1}_A \otimes H_B$ commute, the unitary evolution $U(t)$ that is determined by H acting on the composite system is a product

$$U(t) = e^{-iHt} = U_A(t) \otimes U_B(t), \tag{2.12}$$

where $U_A(t) = e^{-iH_A t}$ and $U_B(t) = e^{-iH_B t}$ are the unitary evolution operators on the subsystems A and B. The time evolution of any initial product state $|\psi(0)\rangle_{AB} = |a(0)\rangle \otimes |b(0)\rangle$ is given by

$$\begin{aligned} |\psi(t)\rangle_{AB} &= U(t)|\psi(0)\rangle_{AB} \\ &= (U_A(t)|a(0)\rangle) \otimes (U_B(t)|b(0)\rangle) \\ &= |a(t)\rangle \otimes |b(t)\rangle, \end{aligned} \tag{2.13}$$

which remains a product state.

Quite often in tasks that require entanglement between two subsystems, e.g. in quantum communication protocols, the particles in question are far apart from each other [11]. There can be no interaction between systems that are spatially separated, so entanglement cannot be created this way. The entangled state must first be prepared while the systems are interacting. Once the systems are separated, we expect that the interactions no longer exist, and therefore the entanglement properties can no longer change if they undergo purely local coherent dynamics. In fact, if our system does undergo some local coherent evolution given by $U_A \otimes U_B$, we can quite easily reclaim the original state by performing the inverse local operation $U_A^\dagger \otimes U_B^\dagger$.

Definition 3. Two states $\rho_1, \rho_2 \in \mathcal{H} = \mathcal{H}_1 \otimes \cdots \otimes \mathcal{H}_N$ are *locally equivalent*, or *LU-equivalent*, if they can be prepared from one another by purely local unitary operations, that is

$$\rho_2 = U_1 \otimes \cdots \otimes U_N \rho_1 U_1^\dagger \otimes \cdots \otimes U_N^\dagger \tag{2.14}$$

for some local unitaries $U_1, \ldots, U_N$. A function $f : \mathcal{P}(\mathcal{H}) \to \mathbb{R}$ is *locally invariant* (*LU-invariant*) if it maps all locally equivalent states to the same value. The set of all local unitaries on a composite Hilbert space is denoted as $\mathcal{U}_{\text{loc}}$.

2.2 Detecting entanglement

Determining whether or not a given state ρ is entangled is in general a very difficult problem. Even for bipartite systems this is an NP-hard task [32], i.e. the computational difficulty of the problem scales exponentially with the dimension of the system. There are some easily evaluable criteria available that can be used to determine if a state is entangled or not, the most common of which will be discussed below. The fulfillment of such separability criteria, however, is typically either a necessary *or* sufficient condition for detecting entanglement in a state. A single criterion is usually unable to universally detect all entangled states of a system.

Generally, a separability criterion takes the form of a function from the density matrices to the real numbers

$$f : \mathcal{P}(\mathcal{H}) \to \mathbb{R}, \tag{2.15}$$

such that for a state $\rho \in \mathcal{P}(\mathcal{H})$, a sufficient condition for ρ to be entangled is

$$f(\rho_s) < f(\rho) \quad \forall \rho_s \in \mathcal{S}(\mathcal{H}), \tag{2.16}$$

or equivalently, $\max_{\rho_S \in \mathcal{S}} f(\rho_s) < f(\rho)$. Ideally, f should be easily evaluable and able to detect a large number of entangled states.

For pure states, especially in bipartite systems, the question of separability is a rather simple task. This problem becomes much more difficult for mixed states with increasing numbers of particles. This section presents some separability criteria for bipartite systems. More examples can be found in [33].

2.2.1 Schmidt decomposition

For pure states of bipartite systems, the problem of characterizing entanglement has long been well understood and is relatively easy. One possible way to unambiguously determine whether a pure state of two qubits is entangled or not is a method provided by the *Schmidt decomposition* [11, 34]. Not only does this method yield a separability criterion that is easy to evaluate, it also reveals all of the entanglement properties of a given bipartite state.

Consider a bipartite system $\mathcal{H}_A \otimes \mathcal{H}_B$ whose subsystems have dimension n and m respectively. For given bases $\{|i_A\rangle\}$ and $\{|j_B\rangle\}$ of $\mathcal{H}_A$ and $\mathcal{H}_B$, any state $|\psi\rangle \in \mathcal{H}_A \otimes \mathcal{H}_B$ on the composite Hilbert space can be written as

$$|\psi\rangle = \sum_{i,j} C_{ij} |i_A\rangle |j_B\rangle. \tag{2.17}$$

We can find the singular value decomposition [30, 35] of the coefficient matrix C,

$$C = VSU^\dagger, \tag{2.18}$$

where V and U are $n \times n$ and $m \times m$ unitary matrices and S is diagonal, whose elements are the real and non-negative singular values of C. This implies that the state in question can be written as

$$|\psi\rangle = \sum_k s_k |k'_A\rangle |k'_B\rangle, \tag{2.19}$$

where s_k are the diagonal entries in S, and $\{|k'_A\rangle\}$ and $\{|k'_B\rangle\}$ are suitably chosen bases for subsystems A and B. The squares of the coefficients $s_k^2 = \lambda_k$ are known as the *Schmidt coefficients* of $|\psi\rangle$. If the singular values are taken to be decreasing, $s_1 \geq s_2 \geq \cdots$, then S is uniquely defined. Also important is that the Schmidt coefficients are invariant under local unitaries, since any local unitary can be absorbed into the U and V that factor the coefficient matrix C.

If only one of the Schmidt coefficients is non zero, the state $|\psi\rangle$ is clearly separable. If more than one is non-vanishing, the state is entangled.

2.2.2 Entanglement witnesses

The Schmidt decomposition provides an unambiguous criterion for the detection of entanglement in pure states of two qubits, but for mixed states the problem becomes much more difficult. To detect whether a mixed state ρ is entanged by the Schmidt criterion, we would have to check it for *all* possible decompositions into pure states.

One simple way to determine whether or not a state is entangled takes advantage of the geometric interpretation of the space of all states and, in particular, the convex nature of the subset of separable states. Every hermitian operator W on a Hilbert space $\mathcal{H}$ defines a hyperplane [30] in the space of density matrices $\mathcal{P}(\mathcal{H})$ with the solutions to the equation

$$\mathrm{Tr}\rho W = 0. \tag{2.20}$$

This hyperplane separates the space $\mathcal{P}(\mathcal{H})$ into two parts: states with negative expectation values $\mathrm{Tr}\rho W < 0$ and those with non-negative values $\mathrm{Tr}\rho W \geq 0$. Since the space of separables $\mathcal{S}(\mathcal{H})$ is convex, the Hahn-Banach theorem [36] ensures us that we can always find such a hyperplane that separates $\mathcal{S}(\mathcal{H})$ from a given entangled state $\rho_{\mathrm{ent}} \notin \mathcal{S}$ [37, 38]. The geometric picture in Fig. 2.2 presents this idea graphically, with an exemplary witness W that separates the state ρ_1 from the separables. Not all entangled states, however, are detected by W, as shown by the state ρ_2 in Fig. 2.2. Due to the convex nature of the separable states, for any entangled state ρ_{ent} there exists a witness that separates it from $\mathcal{S}$.

If we can find an operator W that separates a state ρ_{ent} from the separables $\mathcal{S}$, then we can conclude that the state is indeed entangled. Such an operator is called an *entanglement witness* [37].

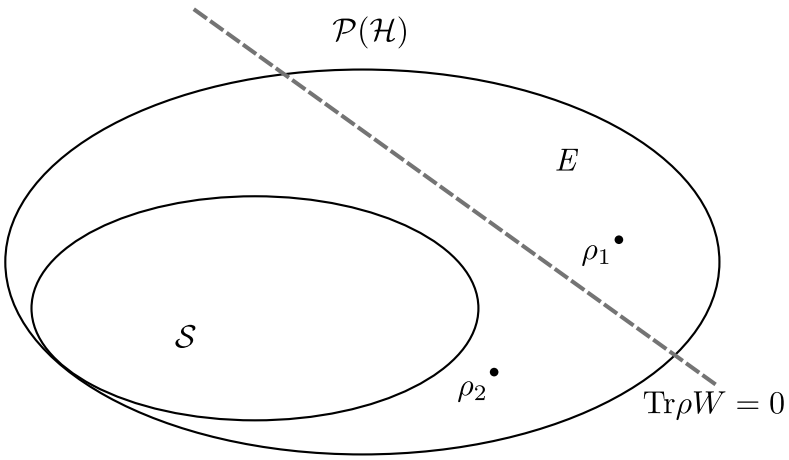

Figure 2.2: Geometric picture of an entanglement witness W detecting an entangled state ρ_1.

Definition 4. An entanglement witness W on a system $\mathcal{H} = \mathcal{H}_1 \otimes \cdots \otimes \mathcal{H}_N$ is a hermitian operator such that

i) W has at least one negative eigenvalue,

ii) and for all separables states $|\psi_{\text{sep}}\rangle \in \mathcal{S}(\mathcal{H})$, the expectation value of W is non-negative

$$\langle\psi_{\text{sep}}|W|\psi_{\text{sep}}\rangle \geq 0. \tag{2.21}$$

The witness W is said to *detect* or *witness* an entangled state ρ if its expectation value $\mathrm{Tr}\rho W$ is negative. A hermitian operator with only positive eigenvalues cannot distinguish entangled from non-entangled states with this criterion and thus cannot be a witness.

Consider the following example on a system of two qubits. The hermitian operator

$$W = \begin{pmatrix} 1 & 0 & 0 & 0 \\ 0 & 0 & 1 & 0 \\ 0 & 1 & 0 & 0 \\ 0 & 0 & 0 & 1 \end{pmatrix} \tag{2.22}$$

has an eigenvalue of -1 associated to the vector $\begin{pmatrix} 0, & 1, & -1, & 0 \end{pmatrix}$. All separable states have the form

$$|\psi_{\text{sep}}\rangle = \begin{pmatrix} a \\ b \end{pmatrix} \otimes \begin{pmatrix} c \\ d \end{pmatrix} = \begin{pmatrix} ac \\ ad \\ bc \\ bd \end{pmatrix}. \tag{2.23}$$

The expectation value of W for each separable state is positive, since

$$\begin{aligned}\langle\psi_{\text{sep}}|W|\psi_{\text{sep}}\rangle &= |a|^2|c|^2 + |b|^2|d|^2 - 2\text{Re}(a^*d^*bc) \\ &\geq |a|^2|c|^2 + |b|^2|d|^2 - 2|a||b||c||d| \\ &= (|a||c| - |b||d|)^2 \\ &\geq 0.\end{aligned} \tag{2.24}$$

The Bell state $|\phi^-\rangle = \frac{|01\rangle - |10\rangle}{\sqrt{2}}$ is witnessed by W since $\langle\phi^-|W|\phi^-\rangle = -1$, i.e. $|\phi^-\rangle$ is an eigenvector of W with -1 as its corresponding eigenvalue. Important to note, however, is that none of the *other* Bell states are detected by W, since they are the other eigenvectors of W with associated eigenvalue $+1$.

Entanglement witnesses are good for detecting entanglement since they are easy to evaluate, and they can even be determined through measurements on a real system [39]. That is, one can perform measurements corresponding to the observable W on a state such that the state is determined to be entangled if the result of the measurement is negative. The question of separability can thus be answered without performing a full quantum state tomography [16], which would require many measurements. There are, however, many drawbacks to the entanglement witness criteron. In particular, a single witness W cannot detect a large volume of entangled states. In the example above, the given witness was even optimal, in that the hyperplane associated with the equation $\text{Tr}\rho W = 0$ is tangent to the space of separables, but it still only detects one of the three Bell states. Additionally, for a given entangled state, it can be a difficult problem to *find* a witness that detects it [40]. Moreover, the witness criterion is not invariant under local unitary transformations on the state ρ. Since entanglement properties are locally invariant, we would like to have criteria that can detect entanglement irrespective of local unitary dynamics.

Later on, we consider criteria that employ witnesses of the form

$$W_\psi := \alpha_\psi \mathbb{1} - |\psi\rangle\langle\psi|, \tag{2.25}$$

with $|\psi\rangle$ chosen to be an entangled state and $\alpha_\psi > 0$ suitably chosen to ensure that W_ψ is a witness. To achieve invariance under local unitaries, we can optimize the value of $\text{Tr}(\rho W_\psi)$ over all states that are locally equivalent to $|\psi\rangle$.

2.2.3 Positive, but not completely positive, maps

Another method of constructing criteria for detecting entangled states is based on suitably chosen postive maps [41]. A *positive semi-definite matrix*, or just *positive* for short, has all non-negative eigenvalues, and a *positive map* is a linear map on the space of matrices $F : \mathbb{C}^{k\times k} \to \mathbb{C}^{k\times k}$ that maps positive matrices to positive

matrices. Given another space of matrices $\mathbb{C}^{m\times m}$, the positive map F induces another linear map $F\otimes\mathbb{1}:\mathbb{C}^{k\times k}\otimes\mathbb{C}^{m\times m}\to\mathbb{C}^{k\times k}\otimes\mathbb{C}^{m\times m}$. This extended map, however, is not necessarily positive. If the induced map $F\otimes\mathbb{1}$ is positive for all possible extensions, then F is called *completely positive*.

It is possible to construct separability criteria from linear maps that are positive but not completely positive [37]. Consider a positive map that acts on the states of a Hilbert space, $F:\mathcal{P}(\mathcal{H}_A)\to\mathcal{P}(\mathcal{H}_A)$, and extend it to a map on the states of the composite Hilbert space $\mathcal{H}_A\otimes\mathcal{H}_B$. The induced map $F\otimes\mathbb{1}$ applied to any *separable* state of the system will still yield a positive matrix. Indeed, any separable state can be written as a sum of product states $\rho_{\text{sep}}=\sum_i\rho_i^{(A)}\otimes\rho_i^{(B)}$, and $F\otimes\mathbb{1}$ applied to any product

$$(F\otimes\mathbb{1})\left(\sum_i\rho_i^{(A)}\otimes\rho_i^{(B)}\right)=\sum_i F(\rho_i^{(A)})\otimes\rho_i^{(B)} \tag{2.26}$$

is positive, since $F(\rho_A)$ is positive by the positivity of F, and $\rho_i^{(A)}$ and $\rho_i^{(B)}$ are positive by definition. This implies that if we apply an extension $F\otimes\mathbb{1}$ of a positive operator to a state ρ and obtain a *negative* matrix as a result, i.e. a matrix with at least one negative eigenvalue, then the initial state must have been entangled. Thus, we can devise separability criteria by applying extensions of non-completely positive maps to density matrices.

One particular criterion of this kind is based on the partial transpose operation Γ_A on density matrices that act on a Hilbert space $\mathcal{H}=\mathcal{H}_A\otimes\mathcal{H}_B$. For product states $\rho_A\otimes\rho_B$, this operation is defined by [42]

$$(\rho_A\otimes\rho_B)^{\Gamma_A}:=\rho_A^{\intercal}\otimes\rho_B, \tag{2.27}$$

which can be linearly extended to all other states. The transpose operator T acting on a single system is a positive map, since for any matrix ρ with non-negative eigenvalues, its transpose $T(\rho)=\rho^{\intercal}$ will have the same non-negative eigenvalues. It is not completely positive because the operation $\Gamma_A=T\otimes\mathbb{1}$ on the extended space $\mathcal{H}_A\otimes\mathcal{H}_B$ is no longer positive. For example, consider the state $\rho=|\psi^+\rangle\langle\psi^+|$ on the space $\mathcal{H}_A\otimes\mathcal{H}_B$. As a matrix, ρ is positive semi-definite, and the partial transpose of its matrix representation is

$$\rho^{\Gamma_A}=\frac{1}{2}\begin{pmatrix}1&0&0&1\\0&0&0&0\\0&0&0&0\\1&0&0&1\end{pmatrix}^{\Gamma_A}=\frac{1}{2}\begin{pmatrix}1&0&0&0\\0&0&1&0\\0&1&0&0\\0&0&0&1\end{pmatrix}, \tag{2.28}$$

which is the same matrix considered earlier in (2.22), up to a factor of $\frac{1}{2}$. It has a negative eigenvalue, so it is no longer positive. Thus, $|\psi^+\rangle$ is entangled.

Although all states with negative partial transpose must be entangled, states that remain positive under partial transposition (PPT) are not necessarily separable [42].

2.3 Quantifying entanglement

Separability criteria can provide a nice way to determine whether a state is entangled, but these indicators cannot in general give us idea as to how *much* a state is entangled. Entanglement can be used as a resource for various tasks, but some entangled states are more useful for certain tasks than others. Indeed, the initial idea to quantify entanglement came in connection to its usefulness in quantum communication. For example, quantum teleportation [9] is a process which involves a shared entangled state between two spatially separated parties. Through some local measurements and manipulations, as well as with some element of classical communication between the two parties, the state of another qubit may be transported from one party to the other. Although teleportation of a single qubit can still be performed probabilistically if an arbitrary entangled state is shared, it can only be reliably accomplished if the two parties involved share a maximally entangled quantum state [43], a concept that will be defined in Section 2.3.1. Furthermore, no teleporation is possible if the initial shared state is not entangled. In the following, we develop a background for classifying amount of entanglement based on characterization by local operations. This allows us to establish the axiomatic framework of entanglement measures. A more in depth discussion of entanglement measures can be found [44, 45].

2.3.1 Interconvertability of enangled states

Any attempt to quantify entanglement must first begin with a discussion of how it is used. The typical paradigm of multipartite quantum systems visualizes each particle as resting in separate laboratories that are spatially separated such that the particles cannot interact. However, as we have already seen, purely local dynamics are unable to create entanglement. If the state of the composite system is entangled, it is understood that the particles were initially in one place where they could interact, then distributed to their separate locations. Subsequently, the scientists in each of the labs may only perform local operations on their particle, and they may communicate classically to the other scientists the results of any local measurements that might be performed. The class of protocols that operate on such composite systems involving only local operations (LO) and classical communication (CC) are generally referred to as LOCC.

To accomplish tasks requiring entanglement, e.g. quantum communication

protocols, a system starts in an entangled state, and performing a specific LOCC protocol allows information to be securely transmitted between the labs. If a quantum task can be performed by a state $|\phi\rangle$, then it can be peformed by any state that is locally equivalent to a Bell state. However, as we will later see, it is impossible to deterministically *obtain* a Bell state from a less entangled state using only LOCC protocols. This gives us a natural hierarchy that we can use to quantify entanglement. If a state $|\psi'\rangle$ can be obtained from another entangled state $|\psi\rangle$, then any quantum communication protocol that can be performed with $|\psi\rangle$ can also be performed with $|\psi'\rangle$, and so one state must be more entangled than the other. Thus, to help us quantify quantum entanglement, we first need a formalism to characterize local quantum operations and LOCC protocols.

Before determining what a local quantum operation looks like, we first need to be able to mathematically describe any generalized quantum operation. The simplest types of operations in quantum mechanics are either unitary evolution, described by some unitary operator U, or projective measurements that collapse the system into one of the eigenstates of the observable that is being measured. However, interactions with an environment may prevent purely unitary dynamics from taking place in the system in question, and perfect projection measurements are not always possible. Thus, we need a more general formalism to account for evolutions that cannot be represented by simple unitaries and projections.

A generalized quantum operation on a system typically involves a sequence of three steps [45]:

(1) adding ancillary particles to the system,

(2) performing a unitary operation on the system and ancilla,

(3) measuring and discarding ancillae based on measurement outcomes.

A quantum circuit diagram of this process is depicted in Figure 2.3. Any evolution process of this kind can be described by a set of *Kraus operators* [11], i.e. a set of operators $\{K_i\}$ that satisfy $\sum_i K_i^\dagger K_i = \mathbb{1}$. Each operator K_i corresponds to one of the possible measurement outcomes in step (3) above. Consider a quantum system in the inital state ρ_{in}. The measurement outcome i occurs with probability $p_i = \mathrm{Tr}(K_i \rho_{in} K_i^\dagger)$, and the resulting state of the system based on this outcome is given by

$$\rho_i = \frac{K_i \rho_{in} K_i^\dagger}{\mathrm{Tr}(K_i \rho_{in} K_i^\dagger)}. \tag{2.29}$$

The condition $\sum_i K_i^\dagger K_i = \mathbb{1}$ is required such that the probabilites of all possible outcomes sum to unity.

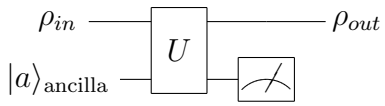

Figure 2.3: Quantum circuit diagram depicting the effect of a generalized quantum operation on a state ρ_{in}.

In some situations, such as when the system interacts with an environemnt, the measurement outcomes of the ancillae might not be accessible, and the ancilla particles are traced out. The resulting state of this process is given by

$$\rho_{out} = \sum_i K_i \rho_{in} K_i^\dagger. \tag{2.30}$$

While any generalized quantum operations can be written in the Kraus operator formalism, it can conversely be shown [46] that for any set of Kraus operators that satisfy $\sum_i K_i^\dagger K_i = \mathbb{1}$, there exists a process, composed of anicillae, unitary evolution, and measurements, that is represented by the operators $\{K_i\}$.

Now that we have a formalism for generalized quantum operations, those that can be classified as LOCC protocols can now be characterized. Considering an N-partite system, $\mathcal{H}_A \otimes \mathcal{H}_B \otimes \cdots \otimes \mathcal{H}_N$, a generalized *local operation* on the subsystem A can be defined by a set of Kraus operators $\{a_i\}$ on that subsystem's Hilbert space. If measurement result i is obtained, then the state of the system is

$$\rho_i = (a_i \otimes \mathbb{1} \otimes \cdots \otimes \mathbb{1}) \rho (a_i^\dagger \otimes \mathbb{1} \otimes \cdots \otimes \mathbb{1}). \tag{2.31}$$

This result ocurrs with probability $\text{Tr}\rho_i$. The scientist in lab A may communicate the results of this measurement to scientists in other labs who can then perform operations conditioned on the outcome of the first. For example, if the result i is obtained in the first measurement, then a scientist in lab B might perform the operation corresponding to the Kraus operators $\{b_{ij}\}$. If the outcome ij is obtained, the composite system is in the final state given by

$$\begin{aligned} \rho_{ij} &= (\mathbb{1} \otimes b_{ij} \otimes \mathbb{1} \otimes \cdots \otimes \mathbb{1}) \rho_i (\mathbb{1} \otimes b_{ij}^\dagger \otimes \mathbb{1} \otimes \cdots \otimes \mathbb{1}) \\ &= (a_i \otimes b_{ij} \otimes \mathbb{1} \otimes \cdots \otimes \mathbb{1}) \rho (a_i^\dagger \otimes b_{ij}^\dagger \otimes \mathbb{1} \otimes \cdots \otimes \mathbb{1}) \end{aligned} \tag{2.32}$$

with probability $\text{Tr}\rho_{ij}$. If this LOCC scheme is repeated many times with the same initial states and the possible resulting states are the probabilistic outcomes ij, the resulting state on average will be given by

$$\rho' = \sum_{ij} \rho_{ij}. \tag{2.33}$$

Continuing this kind of process for any finite number of successive local operations, where some sort of classical communication happens in between, this generates all possible LOCC protocols. That is, any LOCC protocol Λ is given by sets of local Kraus operators $\{K_{i_1,\dots i_k}\}_{i_k}$ that act on the same local system. This is written as

$$\Lambda(\rho) = \sum_{i_1,\dots,i_n} K_{i_1\cdots i_n} \cdots K_{i_1} \rho K_{i_1}^\dagger \cdots K_{i_1\cdots i_n}^\dagger \tag{2.34}$$

where $K_{i_1\dots i_k}$ is a local operation that acts on one subsytem for each i_k such that

$$\sum_{i_k} K_{i_1\dots i_k} K_{i_1\dots i_k}^\dagger = \mathbb{1} \tag{2.35}$$

for all i_j with $j < k$. We say that a state ρ' can be obtained *deterministically* from ρ via LOCC if there exists an LOCC protocol Λ such that

$$\rho' = \Lambda(\rho). \tag{2.36}$$

Now that we have a way of describing all possible protocols involving local operations, we can begin to determine a way to quantify entanglement. Clearly, a state that can be transformed into any other state deterministically via LOCC protocols is more entangled than any other state. We can use this to help us define a hierarchy. States that can be converted into any other state by LOCC are said to be *maximally entangled*. For systems of two particles, this observation helps to uniquely define a way to quantify entanglement, as discussed in the following sections. Whereas the existence of maximally entangled states in bipartite systems is easily confimed, the non-existence of such states in systems of more particles complicates any attempt to quantify entanglement in multipartite systems.

In the case of two qubits, maximally entangled states are those that are locally equivalent to the Bell state $|\psi^+\rangle = \frac{1}{\sqrt{2}}(|00\rangle + |11\rangle)$. To justify this statement, it suffices to show that for any bipartite pure state $|\phi\rangle$, we can find an LOCC protocol that takes $|\psi^+\rangle$ to $|\phi\rangle$ with certainty. Since the Schmidt decomposition ensures us that any state will be locally equivalent to a vector of the form

$$|\phi\rangle = \alpha|00\rangle + \beta|11\rangle, \tag{2.37}$$

we can limit ourselves to these states. To devise an LOCC scheme to transfer $|\psi^+\rangle$ into $|\phi\rangle$, let us first add an ancillary system A' in state $|0\rangle$ to system A, which results in the state

$$\frac{|0\rangle_{A'}|0\rangle_A|0\rangle_B + |0\rangle_{A'}|1\rangle_A|1\rangle_B}{\sqrt{2}}. \tag{2.38}$$

If a local unitary operation is performed on two-particle system $A'A$ that transfers the states

$$\begin{aligned} |00\rangle_{A'A} &\longmapsto \alpha|00\rangle_{A'A} + \beta|11\rangle_{A'A} \\ |01\rangle_{A'A} &\longmapsto \alpha|01\rangle_{A'A} + \alpha|10\rangle_{A'A}, \end{aligned} \tag{2.39}$$

then the full system is now in the state

$$\frac{|0\rangle_{A'}(\alpha|00\rangle_{AB} + \beta|11\rangle_{AB}) + |1\rangle_{A'}(\alpha|01\rangle_{AB} + \beta|10\rangle_{AB})}{\sqrt{2}}. \tag{2.40}$$

Finally, a local projective measurement on the acnillary system in the basis $\{|0\rangle_{A'}, |1\rangle_{A'}\}$ yields one of two outcomes. If the state of the ancillary system is found to be in $|0\rangle$, then no further operation is needed. If it is in $|1\rangle$, then a unitary flipping operation given by σ_x needs to be applied to system B. After removing the ancilla in both cases, the final state of the composite system AB is the desired state $|\phi\rangle$. Thus, performing this protocol allows us to produce any pure state from the initial state with certaity. Because an arbitrary mixed state can be written as a probabilistic mixture of pure states, it is possible to obtain any mixed state from $|\psi^+\rangle$ through LOCC protocols as well [45].

Now that we have seen a case where LOCC protocols can transform one state into another, the question arises: When is it possible to transform one state $|\psi\rangle$ into another $|\phi\rangle$? Although this question is rather difficult to answer in general, a complete solution has been developed using the mathematical framework of *majorization* [47] in the bipartite case. Consider two arbitrary pure states that can be written in corresponding Schmidt form

$$|\psi\rangle = \sum_{i=1}^{n} \sqrt{\lambda_i}|i_A\rangle|i_B\rangle, \qquad |\psi'\rangle = \sum_{i=1}^{n} \sqrt{\lambda'_i}|i'_A\rangle|i'_B\rangle. \tag{2.41}$$

We can take the Schmidt coefficients to be given in decreasing order, i.e. $\lambda_1 \geq \lambda_2 \geq \cdots \geq \lambda_n$ and $\lambda'_1 \geq \lambda'_2 \geq \cdots \geq \lambda'_n$. The question of whether two states can be converted into each other by LOCC is determined by the knowledge of their Schmidt coefficients. If the two states in question have the same Schmidt coefficients, the answer is simple, since any two pure states with equal Schmidt coefficients are straightforwardly equivalent via local unitary operations [45]. It turns out that there exists an LOCC protocol to deterministically transform the state $|\psi\rangle$ into $|\psi'\rangle$ if and only if the coefficients $\{\lambda_i\}$ are *majorized* by $\{\lambda'_i\}$, that is, if we have that

$$\sum_{i=1}^{k} \lambda_i \leq \sum_{i=1}^{k} \lambda'_i \tag{2.42}$$

for all integers k such that $1 \leq k \leq n$. This allows us to fully characterize which pure states of a bipartite system may be transformed into another by LOCC protocols.

2.3.2 Axiomatic approach to entanglement measures

Now that we have outlined methods for determining whether one state might be more entangled than another based on our formalism of LOCC protocols, we can finally approach the problem of quanifying entanglement. Before we analyze any specific examples of ways to do this, we first present an axiomatic approach to construct quantification schemes. In general, entanglement is quantified by entanglement *measures*, which are functions from the space of states to the real numbers that satisfy some specific postulates.

Definition 5. An entanglement *measure* is a function from the density matrices of a quantum system to the non-negative real numbers

$$E : \mathcal{P}(\mathcal{H}) \to \mathbb{R}_+ \tag{2.43}$$

that satisfies the following axioms:

M1. *Monotonicity under LOCC* - Entanglement cannot increase on average under local operations and classical communication protocols. That is, for any LOCC operation Λ, we require

$$E\left(\Lambda(\rho)\right) \leq E(\rho). \tag{2.44}$$

In particular, this implies that entanglement should remain invariant under local unitary transformations

$$E\left(U_1 \otimes \cdots \otimes U_n \rho U_1^\dagger 1 \otimes \cdots \otimes U_n^\dagger\right) = E(\rho), \tag{2.45}$$

since these are invertible local operations. Functionals on the density matrices that at least satisfy this axiom are called *entanglement monotones*.

M2. *Convexity* - The entanglement of a probabilistic mixture of states must not exceed their average entanglement. This means that we require

$$E\left(\sum_i p_i \rho_i\right) \leq \sum_i p_i E(\rho_i). \tag{2.46}$$

M3. *Vanishing for separables* - If the state $\rho_{\text{sep}} \in \mathcal{S}$ is separable, the measure should be zero:

$$E(\rho_{\text{sep}}) = 0. \tag{2.47}$$

The requirement M3 arises from the condition of invariance under local unitaries. All separable pure states are locally equivalent to each other, and invariance under local unitary operations implies that $E(\psi_{\text{sep}})$ should be the same constant value for all separable states. Since any entangled state can be converted into a separable one by LOCC, the monotonicity requirement M1 assures that if $E(\psi) > E(\psi_{\text{sep}})$ for some state $|\psi\rangle$, then that state must be entangled. Due to the equivalence of the concepts of "not separable" and "entangled," axiom M1 implies that $E(\psi_{\text{sep}})$ must be the minimum value for all pure states, which we can arbitrarily set to zero. Mixed separable states can be written as convex sums of pure separable states, so axiom M2 implies that the entanglement of a mixed separable state should be at most zero, which can be set to zero by definition.

2.4 Quantifying entanglement in two qubits

Now that we have laid out the the axioms for quantifying entanglement, let us now consider some examples in the simplest case of a pair of 2-dimensional quantum systems. As already discussed in Section 2.3.1, it is well known that there exist such maximally entangled states in bipartite systems. This implies that maximally entangled states should adopt the highest value of a measure.

The standard measure of entanglement for pure states of bipartite systems can be given by the *entropy of entanglement*. This measure is based on the von Neumann entropy [1] of the reduced states, and is defined as

$$E(\psi) := -\text{Tr}(\rho_A \log_2 \rho_A) = -\text{Tr}(\rho_B \log_2 \rho_B), \tag{2.48}$$

where ρ_A (resp. ρ_B) is obtained from $\rho = |\psi\rangle\langle\psi|$ by tracing out the subsystem B (resp. A). The entropy of entanglement has been shown to be monotonic and convex [45]. Furthermore, the reduced density matrix of any pure state is still pure, and the von Neumann entropy of a pure state is zero. At least for pure states, the definition of E in (2.48) satisfies our axioms for an entanglement measure.

However, the entropy of entanglement is not a suitable measure of entanglement for mixed quantum states, since the reduced density matrix of the maximally mixed state is again maximally mixed for example, with a von Neumann entropy of 1. A different way is needed to extend this measure to mixed states.

We have already determined that any state of two qubits may be obtained from the maximally entangled $|\psi^+\rangle$ by LOCC. However, not all of the initial entanglement is used up in such an operation. That is, if we want to prepare *two* copies of a state $|\phi\rangle$ from shared entangled states using only LOCC, it is possible that only *one* initial entangled state is needed, and the amount of initial entanglement is shared among the final two copies of $|\phi\rangle$.

In the case of mixed states, we would like to find an entanglement measure that answers the question: How many maximally entangled states are needed to prepare a given state by LOCC operations in the asymptotic limit? That is, in the limit of $m \to \infty$, how many copies of the maximally entangled state $|\psi^+\rangle$ are needed to create m copies of the desired state ρ? For a given number of copies m, there is a minimum number of copies n of $|\psi^+\rangle$ that are needed to obtain $\rho^{\otimes m}$ by LOCC

$$|\psi^+\rangle^{\otimes n} \xrightarrow{\text{LOCC}} \rho^{\otimes m}. \tag{2.49}$$

We can define the entanglement of a mixed state of two qubits to be the limit

$$\lim_{m\to\infty} \frac{n}{m}. \tag{2.50}$$

This value is given by the *entanglement of formation*, $E_f(\rho)$ [48], which is defined as the minimum average entanglement of an ensemble of pure states that represent ρ [33],

$$E_f(\rho) = \min_{\{p_i, |\psi_i\rangle\}} \sum_i p_i E(\psi_i). \tag{2.51}$$

The minimum is taken over all decompositions $\{p_i, |\psi_i\rangle\}$ such that $\rho = \sum_i p_i |\psi_i\rangle\langle\psi_i|$. This kind of extension of a quantity defined on pure states but applied to mixed states is called a *convex roof construction* [49].

2.4.1 Concurrence

In general, such convex roof constructions are difficult to evaluate, since they must be optimized over *all* decompositions of a given mixed state. Furthermore, a convex roof involves a minimization, so any numerical evaluation will overestimate the value of E. The *concurrence* of a quantum state was introduced [50] to simplify the computation of the entanglement of formation in two qubit systems. Importantly, the concurrence is also an entanglement measure, as it satisfies axioms M1-M3 in Section 2.3.2.

The concurrence of a pure quantum state is given by [33]

$$\mathcal{C}(\psi) = |\langle\psi^*|\sigma_y \otimes \sigma_y|\psi\rangle|, \tag{2.52}$$

where $\langle\psi^*|$ represents the transpose of $|\psi\rangle$ in the standard computational basis $\{|00\rangle, |01\rangle, |10\rangle, |11\rangle\}$. For a particular state

$$|\psi\rangle = \psi_{00}|00\rangle + \psi_{01}|01\rangle + \psi_{10}|10\rangle + \psi_{11}|11\rangle, \tag{2.53}$$

the concurrence evaluates to the simple expression $\mathcal{C}(\psi) = 2|\psi_{00}\psi_{11} - \psi_{01}\psi_{10}|$.

As above, the concurrence can be expanded to mixed states by the convex roof extension. Although this infimum may also appear impossible to evaluate, it was shown [50] that the infimum of this expression is given by

$$\mathcal{C}(\rho) = \max\{0, s_1 - s_2 - s_3 - s_4\} \tag{2.54}$$

where the s_i's are the singular values (with the convention $s_1 \geq s_i$) of the matrix $\sqrt{\sqrt{\rho}\tilde{\rho}\sqrt{\rho}}$ and $\tilde{\rho}$ is the spin-flipped state

$$\tilde{\rho} = \sigma_y \otimes \sigma_y \rho^* \sigma_y \otimes \sigma_y. \tag{2.55}$$

Wootters showed that the entanglement of formation of a state of two qubits is

$$E_f(\rho) = H(p, 1-p), \tag{2.56}$$

where $p = \frac{1-\sqrt{1-\mathcal{C}^2(\rho)}}{2}$ and H is the Shannon entropy defined as

$$H(p, 1-p) := p \log_2 p + (1-p) \log_2 (1-p). \tag{2.57}$$

Since the concurrence can easily be calculated for a given state, the above relation in (2.56) allows the entanglement of formation to also be evaluated [50].

Chapter 3

Multipartite entanglement

The problem of characterizing entanglement in systems of two particles has been thoroughly studied and understood. There is an established way to determine if one state is more entangled than another in systems of two qubits. Given any two pure states of two qubits, it is possible to transform one into the other with LOCC operations. However, in systems of many particles, the concept of entanglement becomes much more complicated. In systems with more than two particles, there is no such simple method to characterize entanglement due to the nonexistence of maximally entangled states [33]. That is, there exist states such that neither can be converted into the other via LOCC operations. In such cases, there is no straightforward way to quantitatively compare the entanglement in the two states. Nonetheless, we can still attept to quantify entanglement in multipartite systems.

Already in the case of tripartite systems, simple methods of characterizing entanglement are no longer applicable. In fact, there exist two different types of multipartite entanglement in systems of three qubits, which are described by the well known *Greenberger-Horne-Zeilinger* states [51], which have the form

$$|\mathrm{GHZ}\rangle = \frac{1}{\sqrt{2}}(|000\rangle + |111\rangle), \tag{3.1}$$

and the W-type states [52], which have the form

$$|\mathrm{W}\rangle = \frac{1}{\sqrt{3}}(|100\rangle + |010\rangle + |001\rangle). \tag{3.2}$$

To qualitatively compare the entanglement described by each of these states, we can trace out one particle of the system in each case. For the GHZ state, this leaves the remaining system in the maximally mixed state, which clearly is not entangled. However, performing the same operation on a W-state would leave the system in an entangled (albeit mixed) state. Furthermore, there is no LOCC

protocol that can convert a GHZ state to a W state or vice versa [53]. Whereas all 2-qubit states can be obtained from any maximally entangled state by LOCC transformations, the inequivalence of the W- and GHZ-types of entanglement in the three qubit case shows how manifestly more complicated the problem of characterizing entanglement is with larger numbers of particles. For some quantum tasks, certain types of entanglement may be more useful than others. Since entanglement measures assign a real numbered value to each state, it is possible to have different entanglement measures that say different types of entanglement are more or less entangled than the others. For example, for two states $|\phi\rangle$ and $|\psi\rangle$ of a many body system, two different measures E_1 and E_2 might yield the results $E_1(\phi) > E_1(\psi)$ and $E_2(\phi) < E_2(\psi)$.

Although assigning values to the various types of entanglement in multipartite systems is not a problem that can be definitively solved, we can still discern some type of hierarchy of entanglement in states of systems of many particles. Consider, for example, a state of a system of many particles in which the subsystems are only partially entangled. What if two of the subsystems are entangled with each other, but stay unentangled with the remaining particles of the full system? There clearly does exist entanglement in such a situation, and much work has been done in distinguishing between this type of situation and one in which all subsystems are entangled with each other [54]. In the latter case, we say that a pure state on a multipartite system is *genuinely* multipartite entangled, a concept that will be defined in more detail in Section 3.1.

While bipartite entanglement is understood quite well, there are still many open questions in the case of multipartite entanglement. This chapter provides a description of genuine multipartite entanglement and discusses methods of detecting and quantifying it.

3.1 Genuine multipartite entanglement and k-separability

In the simple case of bipartite systems, a particular pure state is either separable, such that it is a product of two states $|\Psi_{12}\rangle = |\phi_1\rangle \otimes |\varphi_2\rangle$, or it is entangled. In systems of multiple particles, there exist multiple ways in which the composite system can be separated into two subsystems, called *bipartitions*. An N-partite system $\mathcal{H} = \mathcal{H}_1 \otimes \cdots \otimes \mathcal{H}_N$ (with $N > 2$) will have many different ways in which we can group the individual $\mathcal{H}_i$'s. In total, an N-partite system has $2^{N-1} - 1$ inequivalent bipartitions [55]. For example, the bipartitions of a 3-partite system $\{1, 2, 3\}$ are

$$\{1|2,3\}, \quad \{2|1,3\}, \quad \text{and} \quad \{3|1,2\}. \tag{3.3}$$

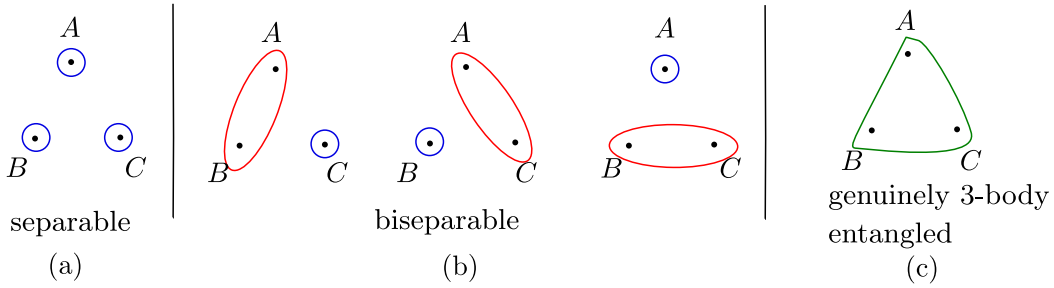

Figure 3.1: Different classes of entanglement for pure states in tripartite systems. (a) States that are completely separable have no entanglement among the individual subsystems. (b) Some states exhibit entanglement between only two of the three subsystems, while the remaining system remains unentangled with the first two. Such states are biseparable, since there exits a bipartition under which the state can be expressed as a product. (c) States that are not biseparable are genuinely multipartite entangled.

It is possible for a state of three qubits to be separable among one of these bipartitions but impossible to express as a fully separable product, e.g. if a state of the form $|\psi_{12}\rangle \otimes |\phi\rangle$ where $|\psi_{12}\rangle$ is an entangled state of two qubits and $|\phi\rangle$ is a single qubit state vector. Figure 3.1 depicts the various degrees of entanglement and separability in the case of three qubit pure states.

Consider a system of N-particles with corresponding Hilbert space $\mathcal{H} = \mathcal{H}_1 \otimes \cdots \otimes \mathcal{H}_N$. We first introduce an arbitrary indexing of the labels such that the Hilbert space is equivalent to

$$\mathcal{H} = \mathcal{H}_{j_1} \otimes \mathcal{H}_{j_2} \otimes \cdots \otimes \mathcal{H}_{j_N}, \tag{3.4}$$

where $j_i \in \{1, 2, \ldots, N\}$ is a discrete labelling of the N individual particles. Now a particular bipartition of $\mathcal{H}$ can be written as $\mathcal{H}_A \otimes \mathcal{H}_B$ with $\mathcal{H}_A = \mathcal{H}_{j_1} \otimes \cdots \otimes \mathcal{H}_{j_k}$ and $\mathcal{H}_B = \mathcal{H}_{j_{k+1}} \otimes \cdots \otimes \mathcal{H}_{j_N}$. In this case, for the biseparation defined by $\{A|B\}$, we have

$$A = \{j_1, \ldots, j_k\} \quad \text{and} \quad B = \{j_{k+1}, \ldots, j_N\} \quad \text{with} \quad A \cup B = \{1, \ldots, N\}. \tag{3.5}$$

A state $|\psi\rangle \in \mathcal{H}$ is separable according to this bipartition if it can be written as $|\psi_A\rangle \otimes |\psi_B\rangle$ with $|\psi_A\rangle \in \mathcal{H}_A$ and $|\psi_B\rangle \in \mathcal{H}_B$. We can now define the idea of genuine multipartite entanglement a bit more rigorously.

Definition 6. An N-partite pure state $|\psi\rangle \in \mathcal{H} = \mathcal{H}_1 \otimes \cdots \otimes \mathcal{H}_N$ is called *biseparable* if it can be written as a product $|\psi\rangle = |\psi_A\rangle \otimes |\psi_B\rangle$, where

$$\begin{aligned} |\psi_A\rangle \in \mathcal{H}_A &= \mathcal{H}_{j_1} \otimes \cdots \otimes \mathcal{H}_{j_m} \\ \text{and } |\psi_B\rangle \in \mathcal{H}_B &= \mathcal{H}_{j_{m+1}} \otimes \cdots \otimes \mathcal{H}_{j_N} \end{aligned} \tag{3.6}$$

under some bipartition $\{A|B\}$ of the composite Hilbert space $\mathcal{H}$. In the case of mixed states, we say that an N-partite mixed state ρ is biseparable if it can be expressed as a mixture of biseparable pure states

$$\rho = \sum_i p_i |\psi_i\rangle\langle\psi_i|, \ |\psi_i\rangle \text{ biseparable } \forall i. \tag{3.7}$$

A state is called *genuinely multipartite entangled* (or *gme*) if it is not biseparable.

For pure states, the question of biseparability is simply a matter of finding a particular bipartition of the Hilbert space under which the state is separable. This question become manifeslty more difficult in the case of mixed states. Even if a mixed state is not biseparable under any biseparation, this does not necessarily mean that it is not biseparable. For example, consider the tripartite system $\mathcal{H} = \mathcal{H}_A \otimes \mathcal{H}_B \otimes \mathcal{H}_C$ and the state

$$\rho = \sum_j p_j \rho_j^{(AB)} \otimes \rho_j^{(C)} + \sum_j q_j \rho_j^{(AC)} \otimes \rho_j^{(B)} + \sum_j r_j \rho_j^{(BC)} \otimes \rho_j^{(A)}, \tag{3.8}$$

which is a sum of biseparable states where $\rho_j^{(AB)}$, $\rho_j^{(AC)}$, and $\rho_j^{(BC)}$ are entangled. Even though there is no single biseparation with respect to which the full state ρ is separable, it is still considered biseparable. Thus, the individual pure states that compose a biseparable mixed state can be biseparable under different partitions. In fact, biseparable mixed states are generally not separable with respect to any particular bipartition. This greatly complicates the problem of identifying genuine multipartite entanglement in a state.

3.1.1 k-separability

The concepts of genuine multipartite entanglement and biseparability can be generalized to other degrees of separability in systems of many particles. The ability to distinguish genuinely entangled states is important if we desire a high degree of entanglement for a particular quantum task. We would also like to be able to differentiate between different degrees of separability. A fully separable state $|\psi_1\rangle \otimes \cdots \otimes |\psi_N\rangle$ would certainly be less desirable than a state which has at least some degree of entanglement, such as $|\psi_{1,2}\rangle \otimes |\psi_{3,4}\rangle \otimes \cdots$. This state is still separable without being fully separable. We can extend this concept of biseparability to the idea of k-separability, which is defined in the following.

Before we can define the notion of k-separability, we first need a mathematical description of a k-partition of a composite Hilbert space. In general, a k-partition of the N-partite Hilbert space $\mathcal{H} = \mathcal{H}_1 \otimes \cdots \otimes \mathcal{H}_N$ is given by k nonempty sets $\{A_1|A_2|\cdots|A_k\}$ of indices $A_s = \{j_1^s, \ldots, j_{m_s}^s\} \subset \{1, \ldots, N\}$, such that

$$A_1 \cup \cdots \cup A_N = \{1, \ldots, N\} \quad \text{and} \quad A_i \cap A_j = \emptyset. \tag{3.9}$$

The composite Hilbert space can be written as a product $\mathcal{H}_{A_1} \otimes \cdots \otimes \mathcal{H}_{A_k}$ of the groups of subsystems.

Definition 7. An N-partite pure state $|\psi\rangle$ is *separable under the partition*

$$\{A_1|\cdots|A_k\} \tag{3.10}$$

if it can be written as a product

$$|\psi\rangle = |\psi_{A_1}\rangle \otimes \cdots \otimes |\psi_{A_k}\rangle \tag{3.11}$$

of k states $|\psi_{A_s}\rangle \in \mathcal{H}_{A_s}$. A state $|\psi\rangle$ is *k-separable* if it is separable under some k-partition. For mixed states, a state ρ is k-separable if it can be written as a mixture of k-separable pure states

$$\rho = \sum_i p_i |\psi_i\rangle\langle\psi_i|.$$

The states that are N-separable are the same as the fully separable states in Definition 2. The set of k-separable states is denoted by $\mathcal{S}_k$.

To determine k-separability in pure states, as in the case of genuine multipartite entanglement above, it is sufficient to identify a k-partition of the Hilbert space under which the state is k-separable. Detecting k-separability in a given mixed state, however, is again complicated by the fact that its components are not generally separable by the same partitions. We also note that states that are k-separable are also k'-separable for all $k' \leq k$, as illustrated in Figure 3.2. Since k-separable mixed states are convex combinations of k-separable pure states, the individual sets $\mathcal{S}_k$ of all k-separable states are convex.

While the importance of k-partite entanglement has been recognized [56, 57], work on its characterization is only beginning [58–60]. In this thesis, however, we are mostly interested in genuine N-body entanglement.

3.2 Quantifying multipartite entanglement

In Chapter 5, we will need to create highly entangled states in many-body quantum systems, so we need a way to identify these states. While there are no *maximally* entangled states that can be converted into *all* other states via LOCC, there certainly exist some states in systems of more than two particles that are more entangled than others. For example, if $|\psi_1\rangle$ and $|\psi_2\rangle$ are two states such that $|\psi_1\rangle$ can be converted into $|\psi_2\rangle$ via LOCC but not vice versa, then $|\psi_1\rangle$ should be considered more entangled than $|\psi_2\rangle$, i.e. $E(\psi_1) > E(\psi_2)$.

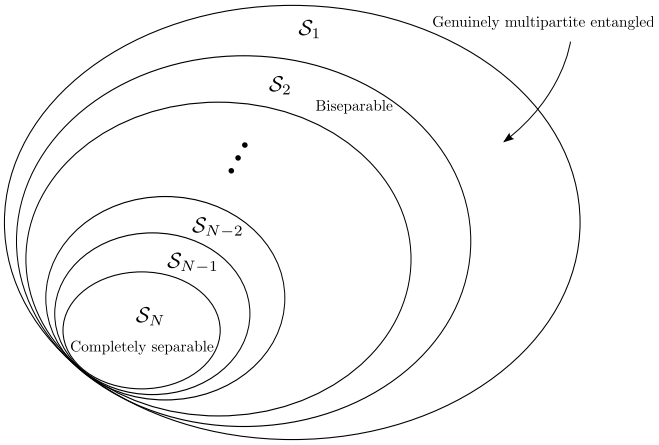

Figure 3.2: An illustration of the convex nature and the geometry of the sets $\mathcal{S}_k$, i.e. the sets of all k-separable states. Each set is convex and embedded within the superceding set: $\mathcal{S}_N \subset \cdots \subset \mathcal{S}_2 \subset \mathcal{S}_1 = \mathcal{P}(\mathcal{H})$.

Although entanglement in multipartite systems has now been defined and classified, we still need ways to detect and quantify it. Because genuinely multipartite entangled states are of particular interest here, a way to characterize it is desired. We want a functional on the density matrices $\tau : \mathcal{P}(\mathcal{H}) \to \mathbb{R}$ that detects genuine multipartite entanglement. It should evaluate to $\tau(\rho_{\text{bisep}}) \leq 0$ for all biseparable states, such that a positive value $\tau(\rho_{\text{ent}}) > 0$ implies that the state is genuinely N-body entangled. Determining separability in pure states of multipartite systems is only a matter of finding a partition under which the state is separable. This question, however, becomes much more difficult for mixed states, so any criteria should be easy to evaluate for mixed states as well as pure states.

In this section, we outline a few methods to detect and quantify various degrees of entanglement in systems of many particles. At the end, a particular detection criterion is introduced that we will use to quantify genuine multipartite entanglement for the remainder of this thesis.

3.2.1 Generalized concurrence

The concurrence of a two qubit pure state $|\psi\rangle$ on the Hilbert space $\mathcal{H} = \mathcal{H}_A \otimes \mathcal{H}_B$ can be given by [33]

$$\mathcal{C}(\psi) = \sqrt{2 - 2\text{Tr}(\rho_A^2)}, \tag{3.12}$$

in terms of the reduced density matrix $\rho_A = \text{Tr}_B(|\psi\rangle\langle\psi|)$. In higher dimensional systems, i.e. $\dim \mathcal{H}_A, \dim \mathcal{H}_B > 2$, the concept of concurrence is straightforwardly generalized since there is still a unique way to determine the reduced density

matrices. In a system of many particles $\mathcal{H} = \mathcal{H}_1 \otimes \cdots \otimes \mathcal{H}_N$, we can always choose a bipartition $\{A|B\}$ of $\mathcal{H}$, and take the concurrence along this bipartition $\mathcal{C}_A(\psi) = \sqrt{2 - 2\mathrm{Tr}(\rho_A^2)}$, which detects entanglement in $|\psi\rangle$ if and only if some part of subsystem A is entangled with part of subsystem B. In N-partite systems, there are $2^{N-1} - 1$ different bipartitions along which we can evaluate such a concurrence, so there is no straightforward way to generalize this to systems of many particles.

One possible generalization of this to an N-partite system [61] is given by

$$\mathcal{C}_N(\psi) = 2^{1-(N/2)} \sqrt{\sum_i \mathcal{C}_{A_i}^2(\psi)} \tag{3.13}$$

where i indexes the bipartition $\{A_i|B_i\}$ of the composite space $\mathcal{H} = \mathcal{H}_{A_i} \otimes \mathcal{H}_{B_i}$, and the sum is taken over all possible bipartitions. Apart from the complicated convex roof extension, this definition does not easily extend to mixed states. However, there is another equivalent formulation based on expectation values of projection operators that provides a way to determine a lower bound for the convex roof.

For pure states, the concurrence can also be written as an expectation value of an hermitian operator [62]. Consider a system of two qubits and expand it to the *two-fold* Hilbert space $\mathcal{H} \otimes \mathcal{H}$, such that it now represents a four-partite system. We can define a projection operator $\mathcal{A} = |\chi\rangle\langle\chi|$ acting on this space, where $|\chi\rangle$ is the state

$$|\chi\rangle = |0011\rangle - |0110\rangle - |1001\rangle + |1100\rangle. \tag{3.14}$$

The concurrence of a two-qubit pure state $|\psi\rangle$ can be written as the expectation value

$$\mathcal{C}^2(\psi) = \langle\psi| \otimes \langle\psi|\mathcal{A}|\psi\rangle \otimes |\psi\rangle \tag{3.15}$$

of the two-fold copy $|\psi\rangle \otimes |\psi\rangle$. If we label the subsystems of the composite Hilbert space $\mathcal{H} = \mathcal{H}_1 \otimes \mathcal{H}_2$, the two-fold product Hilbert space takes the form $\mathcal{H}_1 \otimes \mathcal{H}_2 \otimes \mathcal{H}_1 \otimes \mathcal{H}_2$. The operator $\mathcal{A}$ can also be expressed as a combination of projection operators $\mathcal{A} = 4P_-^{(1)} \otimes P_-^{(2)}$, where $P_-^{(i)}$ represents the projection operator onto the antisymmetric subspace of the product Hilbert space $\mathcal{H}_i \otimes \mathcal{H}_i$ [62].

Expanding to multipartite systems [63], we can generalize this by defining a hermitian operator $\mathcal{A}$ as be the sum of all possible tensor products of the $P_\pm^{(i)}$'s, where $P_+^{(i)}$ is the projector onto the symmetric subspace of $\mathcal{H}_i \otimes \mathcal{H}_i$, such that the concurrence is given by the expectation value $\mathcal{C}^2(\psi) = \langle\psi| \otimes \langle\psi|\mathcal{A}|\psi\rangle \otimes |\psi\rangle$. Each combination of tensors of permutation operators defines one type of concurrence. For a generalized concurrence we set $\mathcal{A}$ as a weighted sum

$$\begin{aligned} \mathcal{A} =& c_N^{(12)} P_-^{(1)} \otimes P_-^{(2)} \otimes P_+^{(3)} \otimes \cdots \otimes P_+^{(N)} \\ &+ c_N^{(13)} P_-^{(1)} \otimes P_+^{(2)} \otimes P_-^{(3)} \otimes \cdots \otimes P_+^{(N)} \\ &+ \cdots \end{aligned} \tag{3.16}$$

where each summand includes an even number of $P_-^{(i)}$'s. We consider only the case when all of the coefficients c in this equation are equal. In this case the concurrence reduces exactly to that of $\mathcal{C}_N$ given above in (3.13) [64].

In particular, this construction allows us to deduce a lower bound on $\mathcal{C}_N(\rho)$ for mixed states [63] given by the expectation value

$$\tau_{\mathcal{C}}(\rho) := \mathrm{Tr}(\rho \otimes \rho \mathbf{V}) \leq \mathcal{C}_N(\rho), \tag{3.17}$$

where $\mathbf{V}$ is given by

$$\mathbf{V} = 4(\mathbf{P}_+ - P_+^{(1)} \otimes \cdots \otimes P_+^{(N)} - (1 - 2^{1-N})\mathbf{P}_-), \tag{3.18}$$

and $\mathbf{P}_\pm$ are the projectors on the the symmetric and antisymmetric subspaces of the duplicate total Hilbert space $\mathcal{H} \otimes \mathcal{H}$.

The lower bound given in (3.17) is exact for pure states [65]. Additionally, the quantity $\tau_{\mathcal{C}}$ is invariant under local unitaries since the two-fold tensor product of local unitaries will be invariant under the permutations given by swapping any of the duplicated systems. Even more importantly, this lower bound is easy to evaluate analytically without any sort of required optimization. However, $\tau_{\mathcal{C}}$ is not intended to detect when states are *genuinely* multipartite entangled, which is the primary theme in this thesis.

3.2.2 Geometric measure

Considering the geometry of the space of quantum states, one natural way of defining entanglement is the geometric distance to the subspace of separable states. Given an N-partite pure state $|\Psi\rangle$, we define the geometric measure of entanglement to be [66]

$$E_{\mathrm{G}}(|\psi\rangle) := 1 - \max_{|\Phi\rangle \in \mathcal{S}} |\langle \Phi | \psi \rangle|^2 . \tag{3.19}$$

The maximum is taken with respect to all pure states that are fully separable, i.e.

$$|\Psi\rangle = |\phi_1\rangle \otimes \cdots \otimes |\phi_N\rangle \in \mathcal{H}_1 \otimes \cdots \otimes \mathcal{H}_N. \tag{3.20}$$

This measure is intrinsically geometric, since it coincides with the distance between a given pure state and the set of fully separable pure states with respect to the Hilbert-Schmidt norm. This definition can be extended to mixed states via a convex roof construction, but its evaluation is difficult since this measure requires an optimization even for pure states.

This notion of a geometric measure can be extended to the definition of measures that detect k-partite entanglement in N-partite systems [60]. We can similarly define the distance from a state $|\psi\rangle$ to the set of k-separable pure states by

maximizing the overlap with any k-separable pure state in $\mathcal{S}_k$. Thus, we can define the family of geometric measures

$$E_{\mathrm{G},k}(|\psi\rangle) = 1 - \max_{|\Phi\rangle \in \mathcal{S}_k} |\langle \Phi|\psi\rangle|^2 . \tag{3.21}$$

Because $\mathcal{S}_k \subset \mathcal{S}_{k-1}$ from Definition 7 in Section 3.1.1, i.e. all k-separable state are also $(k-1)$-separable, $E_{\mathrm{G},k}(|\psi_{k'}\rangle) = 0$ for any fully k'-separable state with $k \leq k'$.

In particular, for N-partite systems, the measure $E_{G,2}(|\psi\rangle)$ defines the distance from a state to the set of biseparable states, and so it is non-vanishing only for those states that are genuinely multipartite entanged. Geometric measures of entanglement have been extensively studied [60, 67, 68].

3.2.3 gme-Concurrence

Another useful measure of genuine multipartite entanglement is given by a particular generalization of the concurrence called the *genuine multipartite entanglement concurrence*, or gme-concurrence [69, 70]. The concurrence of a pure state of a bipartite system is a function of the mixedness of the reduced density matrix of one of its subspaces. In a multipartite system, there are multiple ways to separate the composite Hilbert space such that we can evaluate its concurrence. If we are interested purely in *genuine* multipartite entanglement, then we can conclude that a pure state $|\psi\rangle$ is biseparable if and only if there exists at least one bipartition such that the concurrence is zero. Thus, by taking the minimum over all of these concurrences, we obtain a quantity that vanishes for biseparable pure states and is strictly greater than zero for genuinely multipartite entangled pure states.

This generalization of the concurrence that detects genuine multipartite entanglement is defined as

$$\begin{aligned} C_{gme}(\psi) :=& \min_{\{A\}} \sqrt{1 - \mathrm{Tr}\rho_A^2} \\ =& \min_{\{A\}} \mathcal{C}_A(\psi), \end{aligned} \tag{3.22}$$

where the minimization is taken over all bipartitions $\{A|B\}$ of the composite Hilbert space $\mathcal{H} = \mathcal{H}_1 \otimes \cdots \otimes \mathcal{H}_N = \mathcal{H}_A \otimes \mathcal{H}_B$ [69]. As stated above, this is equivalent to the minimum of the bipartite concurrences over all possible bipartitions. If $|\psi\rangle$ is separable among some bipartition $\{A|B\}$, then the reduced density matrix ρ_A will be pure, and the concurrence along this separation is exactly zero. Therefore, this quantity indeed vanishes for pure states that are not genuinely multipartite entangled. The gme-concurrence can also be generalized to mixed states via the convex roof construction

$$C_{gme}(\rho) = \min_{\{p_i, |\psi_i\rangle\}} \sum_i p_i C_{gme}(\psi_i). \tag{3.23}$$

Although this generalization is well-defined, it is not generally computable since it involves a discrete optimization for the pure states as well as an optimization for mixed states to determine the convex roof. This makes it more difficult to evaluate than other types of convex roofs.

3.2.4 Maximal overlap functionals

Another possible way to determine entanglement properties of a given state ρ is to calculate how much overlap it has with a particular entangled state $|\psi\rangle$. For a pure state $|\phi\rangle$, this overlap is given by $|\langle\phi|\psi\rangle|^2$. This can be generalized to mixed states by $\langle\psi|\rho|\psi\rangle = \mathrm{Tr}(\rho P_\psi)$, where $P_\psi = |\psi\rangle\langle\psi|$ is the projector on the the state $|\psi\rangle$. If we are not interested in local effects, we can instead determine how close the state ρ is to *any* state that is locally equivalent to the test state $|\psi\rangle$. We therefore define the *maximal overlap functional* of a state ρ with given state $|\psi\rangle$ as

$$\tau_\psi(\rho) := \max_{U\in\mathcal{U}_{\mathrm{loc}}} \mathrm{Tr}(\rho U P_\psi U^\dagger), \tag{3.24}$$

where the maximum is taken over all local unitaries. To determine whether or not a state ρ is highly entangled, an appropriate choice of test states $|\psi\rangle$ that are also highly entangled is needed. In particular, this quantity is a detector of genuine multipartite entanglement if there is a quantity α_ψ such that $\tau_\psi(\rho_{\mathrm{bisep}}) \leq \alpha_\psi$ for all biseparable states ρ_{bisep} of the system.

For a given state $|\psi\rangle$, the quantity τ_ψ displays some important properties. In particular, it is convex:

$$\begin{aligned}\tau_\psi(p\rho + (1-p)\sigma) &= \max_{U\in\mathcal{U}_{\mathrm{loc}}} \left\{p\mathrm{Tr}(\rho U P_\psi U^\dagger) + (1-p)\mathrm{Tr}(\sigma U P_\psi U^\dagger)\right\} \\ &\leq p \max_{U\in\mathcal{U}_{\mathrm{loc}}} \mathrm{Tr}(\rho U P_\psi U^\dagger) + (1-p)\max_{V\in\mathcal{U}_{\mathrm{loc}}} \mathrm{Tr}(\sigma V P_\psi V^\dagger) \\ &= p\tau_\psi(\rho) + (1-p)\tau_\psi(\sigma).\end{aligned} \tag{3.25}$$

It is also invariant under local unitaries. For biseparable states, there is an explicit solution to the optimization for the the maximal overlap of $|\psi\rangle$ [71]

$$\alpha_\psi := \max_{|\phi\rangle\in\mathcal{S}_2} |\langle\phi|\psi\rangle|^2. \tag{3.26}$$

For a given bipartition $\{A|B\}$, we first optimize only over the states $|\phi\rangle \in \mathcal{S}_{\{A|B\}}$ that are separable according to this partition. For the subsystems A and B, we can choose an orthonormal product basis $|ij\rangle$ for this partition such that

$$|\phi\rangle = \sum_{i,j} a_i b_j |ij\rangle \qquad \text{and} \qquad |\psi\rangle = \sum_{i,j} c_{ij}|ij\rangle. \tag{3.27}$$

Denoting the coefficient matrix by $C = (c_{ij})$ and the normalized coefficients of the product vectors by $\vec{a} = (a_i)$ and $\vec{b} = (b_j)$, we have

$$\begin{aligned} \max_{|\phi\rangle \in \mathcal{S}_{\{A|B\}}} |\langle \phi | \psi \rangle| &= \max_{a_i, b_j} \left| \sum_{ij} a_i^* b_j^* c_{ij} \right| \\ &= \max_{\vec{a}, \vec{b}} |\langle \vec{a} | C | \vec{b}^* \rangle| = \max_k \{ s_k(C) \}, \end{aligned} \tag{3.28}$$

where $s_k(C)$ are the singular values of C. To determine the maximal overlap of $|\psi\rangle$ with *all* biseparable states, we simply take the maximum singular value of C over all biseparations [71].

For a suitably chosen $|\psi\rangle \in \mathcal{H}$, the maximal overlap function can be used as a quantity to detect genuine multipartite entanglement. Above, we showed that we can determine the maximal overlap that any pure biseparable state can have with $|\psi\rangle$. Due to its convexity, the maximal overlap satisfies $\tau_\psi(\rho_{\text{bisep}}) \leq \alpha_\psi$ for any *mixed* biseparable state ρ_{bisep} as well. Thus, if $\tau_\psi(\rho) > \alpha_\psi$ for a given state ρ, then that state is genuinely multipartite entangled. If we want τ_ψ to detect many genuinely entangled states, then $|\psi\rangle$ should be chosen to be highly entangled, e.g. $|\text{W}\rangle$ or $|\text{GHZ}\rangle$.

For systems of three qubits, analyzing the maximal overlap function for W- and GHZ-type states has been determined [71]. The maximal overlaps of each of these states with a biseparable states are

$$\alpha_{\text{W}} = \tfrac{2}{3} \qquad \text{and} \qquad \alpha_{\text{GHZ}} = \tfrac{3}{4}. \tag{3.29}$$

However, the maximum overlap of a W with a GHZ state is $\frac{3}{4}$. Thus, τ_{W} can detect genuine multipartite entanglement in GHZ-like states, but not the other way around.

3.2.5 A quantity for detecting genuine multipartite entanglement

It is of interest to find an easily computable method to determine whether or not a state is biseparable so that we can identitfy states that are genuinely multipartite entangled. The lower bound $\tau_{\mathcal{C}}$ of the generalized concurrence $\mathcal{C}_N$, discussed in Section 3.2.1, can be evaluated analytically for any state, but it does not differentiate between different levels of k-separability. Although the gme-concurrence $\mathcal{C}_{gme}$ certainly detects genuine multipartite entanglement, its convex-roof generalization to mixed states makes it difficult to evaluate. Geometric measures of entanglement can be constructed to quantify genuine multipartite entanglement, but even for pure states their evaluation requires an optimization. The space of

bipartite pure states, however, can be easily parametrized, and maximization procedures over this space can be efficiently performed. On the other hand, although algorithms for evaluating convex roof constructions exist [72], evaluation of convex roof measures requires a minimization process rather than a maximization such that a numerical value always overestimates the actual value. Furthermore, the number of parameters required for optimizing convex roofs increases exponentially with systems of higher dimension.

Maximal overlap functionals can also be used to identify genuine N-body entanglement. The space of all local unitary matrices admits a simple and unconstrained parametrization. Furthermore, the number of parameters needed to describe an arbitrary local unitary increases only linearly with the number of particles. In contrast to minimizations required for evaluating convex roofs, evaluation of τ_ψ involves a maximization, so numerical evaluations never overestimate the value. This makes them possible candidates for quantifying genuine multipartite entanglement for our needs.

More recently, another method has been developed that can create stronger detection critera, i.e. ones that can detect more genuinely multipartite entangled states than optimal witness operators can. Huber et al [55] introduced a general framework to construct detection critera that identify genuinely multipartite entanglement in mixed quantum states of arbitrary-dimensional systems. Here, we introduce a particular criterion that can be derived from this framework. We will analyze its characteristics in the following section, since this is the criterion that we will focus on in this thesis.

The criteria presented by Huber et al are based on formulating nonlinear functions of the matrix elements of a state ρ. The evaluation of these detection critera makes use of the two-fold product of the state in question $\rho \otimes \rho$ that acts on the product space $\mathcal{H} \otimes \mathcal{H}$, similar to the derivation of the generalized concurrence in Secion 3.2.1. Additionally, these criteria employ the fully separable states of $2N$ qubits $|\Phi\rangle \in \mathcal{H} \otimes \mathcal{H}$, i.e. $|\Phi\rangle = |\Phi_1\rangle \otimes |\Phi_2\rangle$ such that

$$\begin{aligned} |\Phi_1\rangle &= |\phi_1\rangle \otimes |\phi_2\rangle \otimes \cdots \otimes |\phi_N\rangle \\ |\Phi_2\rangle &= |\psi_1\rangle \otimes |\psi_2\rangle \otimes \cdots \otimes |\psi_N\rangle. \end{aligned} \tag{3.30}$$

The detection criterion is defined in terms of some permutation operators on the product space $\mathcal{H} \otimes \mathcal{H}$ that we must first explicitly define.

Given a state $|\Phi\rangle = |\Phi_1\rangle \otimes |\Phi_2\rangle$ in the two-fold Hilbert space $\mathcal{H} \otimes \mathcal{H}$, the *global permutation operator* Π permutes the elements of the two copies of the system, i.e.

$$\Pi(|\Phi_1\rangle \otimes |\Phi_2\rangle) = |\Phi_2\rangle \otimes |\Phi_1\rangle. \tag{3.31}$$

For a particular bipartition of the composite space, $\mathcal{H} = \mathcal{H}_{A_i} \otimes \mathcal{H}_{B_i}$, we can also define an operator $\mathcal{P}_i$ that permutes the copies of $\mathcal{H}_{A_i}$ while leaving the elements

of $\mathcal{H}_{B_i} \otimes \mathcal{H}_{B_i}$ untouched. The simplest example of this is in the bipartite case, with the Hilbert space $\mathcal{H} = \mathcal{H}_1 \otimes \mathcal{H}_2$. Given a product state in $\mathcal{H} \otimes \mathcal{H}$, permuting the copies of the first subsystem $\mathcal{H}_1$ yields

$$\mathcal{P}_1 \left(|\phi_1 \phi_2\rangle \otimes |\psi_1 \psi_2\rangle \right) = |\psi_1 \phi_2\rangle \otimes |\phi_1 \psi_2\rangle. \tag{3.32}$$

A criterion to detect genuine multipartite entanglement (gme) can be constructed with these definitions of the permutation operators Π and $\mathcal{P}_i$. Indeed, for every fully separable state $|\Phi\rangle$ of the two-fold system, any biseparable state ρ satisfies the inequality

$$\sqrt{\langle \Phi | \rho^{\otimes 2} \Pi | \Phi \rangle} - \sum_i \sqrt{\langle \Phi | \mathcal{P}_i^\dagger \rho^{\otimes 2} \mathcal{P}_i | \Phi \rangle} \leq 0, \tag{3.33}$$

where the sum runs over all inequivalent bipartitions [55]. In particular, if there exists a fully separable vector $|\Phi\rangle \in \mathcal{H} \otimes \mathcal{H}$ such that this inequality is violated, then the state ρ must be genuinely multipartite entangled.

We now prove the inequality in (3.33) for biseparables states. The left-hand side of the inequality in (3.33) is convex [55], so if we can show that the inequality holds for all pure biseparable states, then it is satisfied by all mixed biseparable states as well. Indeed, consider a biseparable pure state $\rho = |\psi_{\text{bisep}}\rangle\langle\psi_{\text{bisep}}|$, where $|\psi_{\text{bisep}}\rangle$ is separable under some bipartition $\{A_j | B_j\}$ labled j,

$$|\psi_{\text{bisep}}\rangle = |\psi_{A_j}\rangle \otimes |\psi_{B_j}\rangle. \tag{3.34}$$

Any duplicated state $|\psi\rangle \otimes |\psi\rangle$ is invariant under the global permuation Π, under which the copies of $|\psi\rangle$ are swapped. Similarly, the product of the biseparable state $|\psi_{\text{bisep}}\rangle \otimes |\psi_{\text{bisep}}\rangle$ will be invariant under the exchange of the two copies of $\mathcal{H}_{A_j}$, since

$$\begin{aligned} \mathcal{P}_j \left(|\psi_{A_j}\rangle \otimes |\psi_{B_j}\rangle \otimes |\psi_{A_j}\rangle \otimes |\psi_{B_j}\rangle \right) &= |\psi_{A_j}\rangle \otimes |\psi_{B_j}\rangle \otimes |\psi_{A_j}\rangle \otimes |\psi_{B_j}\rangle \\ &= |\psi_{\text{bisep}}\rangle \otimes |\psi_{\text{bisep}}\rangle. \end{aligned} \tag{3.35}$$

Therefore, the j^{th} term of the sum in (3.33) exactly cancels out the positive term on the left. The inequality is satisfied, since the remaining terms of the left-hand side are negative.

The inequality in (3.33) only detects when a state is genuinely multipartite entangled. This can be turned into a quantification of genuine multipartite entanglement by evaluating how much it violates the inequality. Thus, we define the genuine multipartite (gme) detection quantity

$$\tau_{gme}(\rho, |\Phi\rangle) := 2\sqrt{\langle \Phi | \rho^{\otimes 2} \Pi | \Phi \rangle} - 2 \sum_i \sqrt{\langle \Phi | \mathcal{P}_i^\dagger \rho^{\otimes 2} \mathcal{P}_i | \Phi \rangle}, \tag{3.36}$$

which is just the left-hand side of (3.33) multiplied by a factor of two. In 3.3.1, we show that this factor ensures that the maximum value of τ_{gme} is unity. Maximizing this quantitiy over all choices $|\Phi\rangle$ of fully separables states, we define

$$\tau_{gme}(\rho) := \max_{\{|\Phi\rangle\}} \tau_{gme}(\rho, |\Phi\rangle). \tag{3.37}$$

Already, we see that τ_{gme} has some nice properties. It is convex [55], and it is non-positive when evaluated on all biseparable states. Although it is unknown if the maximized value of $\tau_{gme}(\rho)$ satisfies the requirement of monotonicity, it is at least invariant under local unitaries. Indeed, for any local unitary $U = U_1 \otimes \cdots \otimes U_N$, the permutation operators Π and $\mathcal{P}_i$ commute with $U \otimes U$. Thus, for any fully separable vector $|\Phi\rangle$ of $2N$ particles,

$$|\langle\Phi|(U \otimes U)(\rho \otimes \rho)(U^\dagger \otimes U^\dagger)\Pi|\Phi\rangle| = |\langle\Phi'|(\rho \otimes \rho)\Pi|\Phi'\rangle|, \tag{3.38}$$

where $|\Phi'\rangle = U^\dagger \otimes U^\dagger|\Phi\rangle$ is still fully separable, and

$$\sqrt{\langle\Phi|\mathcal{P}_i^\dagger(U \otimes U)(\rho \otimes \rho)(U^\dagger \otimes U^\dagger)\mathcal{P}_i|\Phi\rangle} = \sqrt{\langle\Phi'|\mathcal{P}_i^\dagger(\rho \otimes \rho)\mathcal{P}_i|\Phi'\rangle}. \tag{3.39}$$

Therefore, if the maximum of $\tau_{gme}(\rho)$ is obtained from the choice $|\Phi\rangle$, the maximum of $\tau_{gme}(U\rho U^\dagger)$ is obtained with $|\Phi'\rangle$ such that

$$\tau_{gme}(\rho, |\Phi\rangle) = \tau_{gme}(U\rho U^\dagger, |\Phi'\rangle), \tag{3.40}$$

so the optimal values are the same.

The evaluation of τ_{gme} involves an optimization over all fully separable states $|\Phi\rangle$. Similar to the maximal overlap functionals, the nubmer of parameters needed to specify an arbitrary fully separable state of $2N$ qubits only increases linearly with the number of subsystems. This allows it to be more easily evaluated than convex roof constructions. Since it was shown [55] that τ_{gme} can detect *more* states than typical witness critera [16], this makes the gme-detection quantity a good candidate for quantifying genuine multipartite entanglement.

3.3 Characterizing the gme-detection quantity

The gme-detection quantity τ_{gme} quantifies the violation of the inequality (3.33) for an arbitrary genuine multipartite entanglement state. Here, we will first explore some of its properties and characteristics, since we will make extensive use of this quantity later on. As we have already noted, τ_{gme} has some nice properties that make it a good candidate for quantifying genuine multipartite entanglement that are summarized here:

- it is convex and invariant under local unitaries,
- it is non-positive for all biseparable states, $\tau_{gme}(\rho_{\text{bisep}}) \leq 0$,
- it detects a large volume of genuinely multipartite entangled states,
- its optimization is relatively easy to evaluate, since its parameter space grows only linearly with the number of particles,
- it is maximized instead of minimized, so it never overestimates the amount of entanglement in a state.

The gme-detection quantity τ_{gme} is of manifold importance in this thesis. We will use this functional when we develop schemes to control entanglement dynamics. In this section, we first present a way of reducing the parameter space that simplifies the evaluation of τ_{gme} without losing too much information. The genuine multipartite detection quantity will then be characterized for systems of two and three qubits.

3.3.1 Orthogonal parameterization

Evaluating our gme-detection quantity for a particular state requires an optimization, which makes it in practice more computationaly expensive to employ than functionals that can be analytically evaluated. Such optimizations, however, are common in the theory of entangled states, and in this case the maximization is easier than performing a convex roof optimization. Although the optimization space of fully separable pure states of $2N$ qubits is already relatively straightforward, the parametrization space can be limited to a subset of fully separable states of $2N$ qubits. This can further reduce the computational complexity needed to evaluate τ_{gme}. Maximizing $|\Phi\rangle$ over a subset of the fully separable states simply yields a lower bound on the fully optimized quantity.

In particular, the size of the parameter space can be reduced by half if only fully separable states $|\Phi\rangle$ of the form

$$|\Phi\rangle = |\phi_1\phi_2\cdots\phi_N\rangle \otimes |\phi_1^\perp\phi_2^\perp\cdots\phi_N^\perp\rangle \tag{3.41}$$

are considered, where we require the two states of each copied Hilbert space to be orthogonal, i.e. $\langle\phi_i^\perp|\phi_i\rangle = 0$. Since we are dealing with systems of qubits, the corresponding Hilbert space of each subsystem is only two dimensional. Thus, the vectors $|\phi\rangle$ and $|\phi^\perp\rangle$ can be jointly parametrized from the continuous, real variables $\{\theta, \varphi\}$ by

$$|\phi\rangle = \cos\theta|0\rangle - \sin\theta e^{-i\varphi}|1\rangle \quad \text{and} \quad |\phi^\perp\rangle = \sin\theta e^{i\varphi}|0\rangle + \cos\theta|1\rangle. \tag{3.42}$$

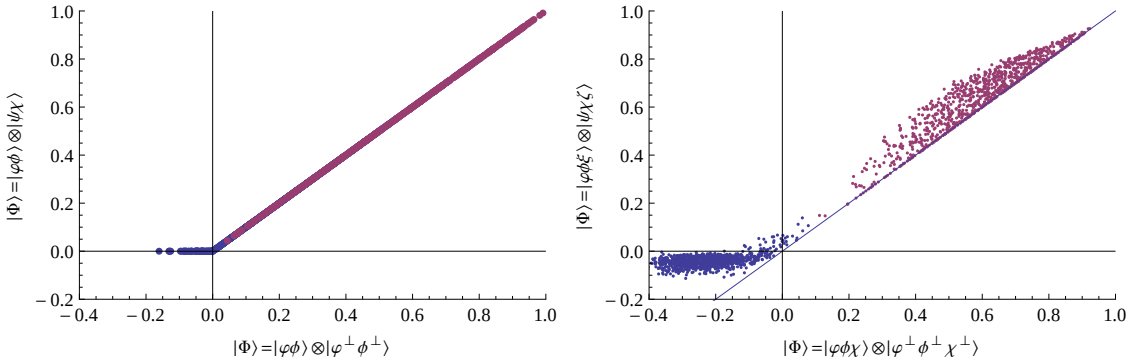

(a) (b)

Figure 3.3: Comparison of parametrizations for maximizing τ. In each plot, 1000 random pure states (purple) and 1000 random mixed states (blue) were generated using the method given by Miszczak [73], for systems of two qubits (a) and three qubits (b). The x-axis shows the value obtained when the vectors $|\Phi_1\rangle$ and $|\Phi_2\rangle$ are parameterized to be orthogonal, and the y-axis shows the optimal value obtained when the vectors are freely parametrized. For states of two qubits, the parametrization spaces yield the exact same results, with comparable results in the three qubit case.

Since we are now only considering just a *subset* of all of the fully separable product states, evaluating the maximum over this parametrization only yields a lower bound on τ_{gme}. As we shall see, the results from maximizing over this subset are not far from the actual maximum.

In the simple case of two qubits, numerical results show that maximizing over the parametrization of the orthogonal subset $|\Phi\rangle = |\phi\varphi\rangle \otimes |\phi^{\perp}\varphi^{\perp}\rangle$ always yields the same maximum as optimizing over the entire space, as long as τ_{gme} is positive. A comparison of the numerical results in Figure 3.3a shows that this is the case for a collection of randomly generated states of two qubits. If a state ρ is *not* entangled, τ_{gme} optimizing over all possible product vectors will yield zero for all states, but might be negative when optimizing over the orthogonal subset.

For random states of three qubits, a comparison of optimizing τ_{gme} over the two different parameter spaces is shown in Figure 3.3b. The results from the two optimizations here do not agree for all states as they do in the the two qubit case. Indeed, optimizing over the subspace of states of the form

$$|\Phi\rangle = |\Psi\rangle \otimes |\Psi^{\perp}\rangle = |\phi\varphi\chi\rangle \otimes |\phi^{\perp}\varphi^{\perp}\chi^{\perp}\rangle \tag{3.43}$$

yields a lower bound for the maximum over the entire space of fully separable states. However, for states with a values of τ_{gme} that are close to unity, optimizations over the two parameter spaces seem to coincide, as seen in Figure 3.3. That

is, when the state has a high degree of genuine multipartite entanglement, it does not matter over which parameter space the maximization is performed. Since we are interested in creating states that maximize τ_{gme}, we can reduce the number of parameters and simplify numerics by optimizing over the subspace of separable states of the form in eq. (3.43) instead of the space of all fully separable states.

Restriction to the orthogonal parameterization also allows us to more easily determine the maximum value that τ_{gme} can take. Consider a pure state $|\psi\rangle$ and any orthogonal states $|\Psi\rangle$ and $|\Psi^{\perp}\rangle$ of N particles. These vectors can be augmented to form an orthonormal basis of the whole space, in which we can expand the vector $|\psi\rangle$. If $|\psi\rangle$ is required to be normalized, then the maximum value of the possible product of overlaps of ψ with $|\Psi\rangle$ and $|\Psi^{\perp}\rangle$ is

$$|\langle\Psi|\psi\rangle\langle\Psi^{\perp}|\psi\rangle| \leq \frac{1}{2}. \tag{3.44}$$

If only the fully separable states of the orthogonal parametrization are considered, i.e. $|\Phi\rangle = |\Psi\rangle \otimes |\Psi^{\perp}\rangle$, then this also represents the maximum value of τ_{gme}. Thus, the factor of two introduced in (3.36) ensures that the maximum value of τ_{gme} for any state is unity. In fact, this maximum can always be attained by the GHZ states. For a GHZ state of N-qubits, $|\psi\rangle = \frac{|0\cdots0\rangle+|1\cdots1\rangle}{\sqrt{2}}$, the choice $|\Phi\rangle = |0\cdots0\rangle \otimes |1\cdots1\rangle$ yields

$$\begin{aligned}\tau_{gme}(\psi, |\Phi\rangle) &= 2|\underbrace{\langle 0\cdots0|\psi\rangle}_{\frac{1}{\sqrt{2}}}\underbrace{\langle\psi|1\cdots1\rangle}_{\frac{1}{\sqrt{2}}}| - 2\sum_i |\underbrace{\langle\{i\}|\psi\rangle}_{0}\underbrace{\langle\{2^N-i-1\}|\psi\rangle}_{0}| \\ &= 1,\end{aligned} \tag{3.45}$$

where $\{k\}$ is the binary representation of the integer $0 \leq k \leq 2^N - 1$ in N bits.

3.3.2 Two qubit gme-detection

Although the quantity τ_{gme} was constructed to be able to identify states that are genuinely multipartite entangled in systems of many particles, we can still apply it to systems of two qubits to help us better understand how the detection works. In bipartite systems, there exists only one possible biseparation, so the quantity τ_{gme} takes the relatively simple form

$$\tau_{gme}(\rho, |\phi\varphi\phi^{\perp}\varphi^{\perp}\rangle) = 2|\langle\phi\varphi|\rho|\phi^{\perp}\varphi^{\perp}\rangle| - 2\sqrt{\langle\phi\varphi^{\perp}|\rho|\phi\varphi^{\perp}\rangle\langle\phi^{\perp}\varphi|\rho|\phi^{\perp}\varphi\rangle}, \tag{3.46}$$

corresponding to the choice $|\Phi\rangle = |\phi\varphi\phi^{\perp}\varphi^{\perp}\rangle$. Since entanglement in two qubit systems is already well understood, we can compare this quantity to the established methods of quantifying entanglement in bipartite systems, e.g. the concurrence.

In the two qubit case, we show that the multipartite entanglement detection quantity $\tau_{gme}(\rho, |\Phi\rangle)$ supplies a lower bound for the concurrence $\mathcal{C}(\rho)$. In fact, for two qubit pure states, we show that the maximum

$$\tau_{gme}(\rho) := \max_{\{|\Phi\rangle\}} \tau_{gme}(\rho, |\Phi\rangle) \tag{3.47}$$

is equivalent to the two qubit concurrence. Additionally, we have found that, numerically, the maximum value of τ_{gme} over all choices $|\Phi\rangle$ coincides with the value of the concurrence for mixed states as well. The fact that our multipartite entanglement detection quantity matches the concurrence ensures us that it correctly identifies and quantifies entanglement in two-qubit systems.

We now show that τ_{gme} provides a lower bound for the concurrence in the case of a two qubit system. The concurrence of a mixed state is defined by the convex roof $\inf_{\{p_i,|\psi_i\rangle\}} \sum_i p_i |\psi_i\rangle\langle\psi_i|$. We proceed by showing this for all possible decompositions $\{p_i, |\psi_i\rangle\}$ of $\rho = \sum_i p_i |\psi\rangle\langle\psi|$. For the choice, $|\Phi\rangle = |0011\rangle$, we have

$$\begin{aligned} |\langle 00|\rho|11\rangle| &= |\sum_i p_i \langle 00|\psi_i\rangle\langle\psi_i|11\rangle| \\ &= |\sum_i p_i \psi^i_{00}\psi^{i*}_{11}| \leq \sum_i p_i |\psi^i_{00}\psi^i_{11}|, \end{aligned} \tag{3.48}$$

which holds due the triangle inequality. Similarly, we have

$$\begin{aligned} \langle 01|\rho|01\rangle\langle 10|\rho|10\rangle &= (\sum_i p_i \langle 01|\psi_i\rangle\langle\psi_i|01\rangle)(\sum_i p_i \langle 10|\psi_i\rangle\langle\psi_i|10\rangle) \\ &= (\sum_i p_i |\psi^i_{01}|^2)(\sum_i p_i |\psi^i_{10}|^2) \\ &\geq (\sum_i p_i |\psi^i_{10}\psi^i_{01}|)^2, \end{aligned} \tag{3.49}$$

by the Cauchy-Schwartz inequality. Combining the inequalities in (3.48) and (3.49), we obtain

$$\begin{aligned} \tau_{gme}(\rho, |0011\rangle) &= 2|\langle 00|\rho|11\rangle| - 2\sqrt{\langle 01|\rho|01\rangle\langle 10|\rho|10\rangle} \\ &\leq 2\sum_i p_i \left(|\psi^i_{00}\psi^i_{11}| - |\psi^i_{10}\psi^i_{01}|\right) \\ &\leq \sum_i p_i \underbrace{2|\psi^i_{00}\psi^i_{11} - \psi^i_{10}\psi^i_{01}|}_{\mathcal{C}(\psi_i)}. \end{aligned} \tag{3.50}$$

Since this inequality holds for all decompositions $\{p_i, |\psi_i\rangle\}$, it must also hold for

the infimum

$$\begin{aligned}\tau(\rho, |0011\rangle) &\leq \inf_{\{p_i, |\psi_i\rangle\}} \sum_i p_i \mathcal{C}(\psi_i) \\ &= \mathcal{C}(\rho),\end{aligned} \tag{3.51}$$

so $\tau_{gme}(\rho, |0011\rangle)$ is bounded above by the concurrence.

Any other choice of fully separable pure state using the orthogonal parametrization $|\Phi\rangle = |\phi\varphi\phi^{\perp}\varphi^{\perp}\rangle$ will be locally equivalent to $|0011\rangle$, and we can write it as

$$\begin{aligned}|\Phi\rangle &= (U_1 \otimes U_2|00\rangle) \otimes (U_1 \otimes U_2|11\rangle) \\ &= (U \otimes U)|0011\rangle\end{aligned} \tag{3.52}$$

for some unitary matrices U_1 and U_2, with $U = U_1 \otimes U_2$. Furthermore, for any local unitary operation U and corresponding choice of fully separable states $|\Phi\rangle = (U \otimes U)|0011\rangle$, we have that

$$\begin{aligned}\tau_{gme}(\rho, |\Phi\rangle) &= |\langle 00|U^{\dagger}\rho U|11\rangle| - \sqrt{\langle 01|U^{\dagger}\rho U|01\rangle\langle 01|U^{\dagger}\rho U|01\rangle} \\ &= \tau_{gme}(U^{\dagger}\rho U, |0011\rangle) \\ &\leq \mathcal{C}(U^{\dagger}\rho U).\end{aligned} \tag{3.53}$$

The concurrence is invariant under local unitaries, i.e. $\mathcal{C}(\rho) = \mathcal{C}(U^{\dagger}\rho U)$, so $\tau_{gme}(\rho, (U \otimes U)|0011\rangle)$ is also bounded above by the concurrence of ρ. Therefore, the quantity $\tau_{gme}(\rho, |\Phi\rangle)$ is a lower bound of $\mathcal{C}(\rho)$ for every vector $|\Phi\rangle = |\phi\varphi\phi^{\perp}\varphi^{\perp}\rangle$.

In fact, in the case of two qubit *pure* states, the maximum value of $\tau_{gme}(\rho)$ is equivalent to the concurrence. Since every two-qubit pure state is locally equivalent to a state of the form $|\psi\rangle = \sqrt{\lambda_1}|00\rangle + \sqrt{\lambda_2}|11\rangle$, we can evaluate τ_{gme} by choosing $|\Phi\rangle = |0011\rangle$. Thus $\tau_{gme}(\rho, |\Phi\rangle)$ evaluates to

$$\begin{aligned}\tau_{gme}(|\psi\rangle\langle\psi|, |0011\rangle) &= |\langle 00|\psi\rangle\langle\psi|11\rangle| - \sqrt{\langle 01|\psi\rangle\langle\psi|01\rangle\langle 10|\psi\rangle\langle\psi|10\rangle} \\ &= \sqrt{\lambda_1\lambda_2} \\ &= \mathcal{C}(\psi).\end{aligned} \tag{3.54}$$

Since τ_{gme} is also bounded above by the concurrence, we have $\tau_{gme}(\psi) = \mathcal{C}(\psi)$ for pure states.

While we have shown that our gme-detection quantity is analytically equivalent to the concurrence in the case of pure states, numerically it appears that τ_{gme} coincides with $\mathcal{C}$ for any state of two qubits (see Figure 3.3a). Although it is not yet known whether this is true for all states, there are at least some classes of states for which we can prove this analytically.

For example, consider the class of Bell diagonal states of the form

$$\rho_{\mathrm{BD}} = \sum_{i=1}^{4} s_i |\psi_i\rangle\langle\psi_i| \tag{3.55}$$

where the coefficients s_i are decreasing, i.e. $s_1 \geq s_2 \geq s_3 \geq s_4$, and the states $|\psi_i\rangle$ are the Bell states

$$\begin{aligned} |\psi_{1/2}\rangle &= |\psi^{+/-}\rangle = \tfrac{1}{\sqrt{2}}(|00\rangle \pm |11\rangle) \\ |\psi_{3/4}\rangle &= |\phi^{+/-}\rangle = \tfrac{1}{\sqrt{2}}(|01\rangle \pm |10\rangle). \end{aligned} \tag{3.56}$$

A state ρ is considered to be Bell diagonal if it is locally equivalent to a state of the form given in (3.55), or equivalently, if it is Bell diagonal in some local basis. The concurrence of such a state is simple to compute. In the computational basis, the Bell states all have real entries and are all eigenvectors of $\sigma_y \otimes \sigma_y$ with eigenvalues ± 1. Using the Wootters formula [50] from Chapter 2 we have

$$\sqrt{\sqrt{\rho_{\mathrm{BD}}}\sigma_y \otimes \sigma_y \rho^*_{\mathrm{BD}} \sigma_y \otimes \sigma_y \sqrt{\rho_{\mathrm{BD}}}} = \rho_{\mathrm{BD}}, \tag{3.57}$$

so $\mathcal{C}(\rho_{\mathrm{BD}}) = \max\{0, s_1 - s_2 - s_3 - s_4\}$.

To determine τ_{gme} of a Bell diagonal state, we choose $|\Phi\rangle = |0011\rangle$, and $\tau_{gme}(\rho_{\mathrm{BD}}, |0011\rangle)$ evaluates to

$$\begin{aligned} \tau_{gme}(\rho_{\mathrm{BD}}, |0011\rangle) &= 2|\langle 00|\rho_{\mathrm{BD}}|11\rangle| - 2\sqrt{\langle 01|\rho_{\mathrm{BD}}|01\rangle\langle 10|\rho_{\mathrm{BD}}|10\rangle} \\ &= s_1 - s_2 - s_3 - s_4. \end{aligned} \tag{3.58}$$

Since it is possible for $\tau_{gme}(\rho)$ to take on negative values, we may redefine it to be the maximum $\tau'_{gme}(\rho) := \max\{0, \tau_{gme}(\rho)\}$, similar to the Wootters formula for the concurrence, such that $\tau'_{gme}(\rho_{\mathrm{BD}}) = \mathcal{C}(\rho_{\mathrm{BD}})$.

3.3.3 Evaluating τ_{gme} for systems of three qubits

In systems of two qubits, the gme-detection quantity has a nice interpretation since it appears to be equivalent to the concurrence, at least for pure states. However, we are more interested in what τ_{gme} reveals about entangled states of multipartite systems.

Since the evaluation of $\tau_{gme}(\rho)$ is numerically not too complicated, we can analyze its value on large swaths of the entire state space for N-partite systems as long as N is not too large. Consider the example states of three qubits,

$$\rho_{\alpha\beta} = \tfrac{1-\alpha-\beta}{8}\mathbb{1} + \alpha\rho_{\mathrm{GHZ}} + \beta\rho_{\mathrm{W}}, \tag{3.59}$$

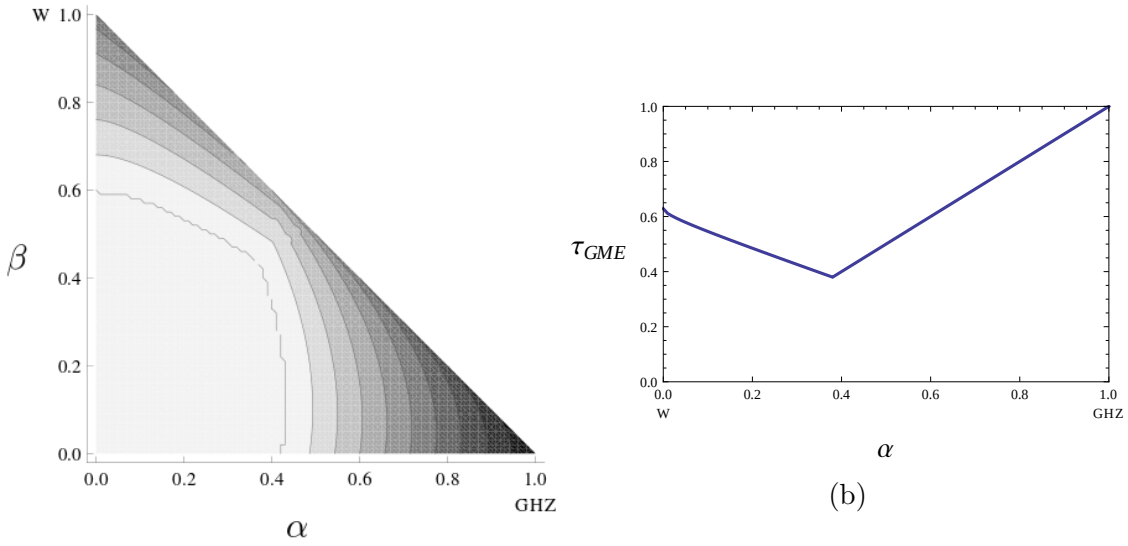

Figure 3.4: (a) Evaluation of the optimal value of τ_{gme} for particular tripartite states of the form $\rho_{\alpha\beta} = \frac{1-\alpha-\beta}{8}\mathbb{1} + \alpha\rho_{\text{GHZ}} + \beta\rho_{\text{W}}$. (b) The value for states of the form $\alpha\rho_{\text{GHZ}} + (1-\alpha)\rho_{\text{W}}$.

which are mixtures of the GHZ state and the W state that have been dampened by isotropic noise. A plot illustrating the the values of $\tau_{gme}(\rho)$ for these types of states is given in Figure 3.4a. Most notably, we see that when evaluated for the GHZ-state, $\tau_{gme}(\rho_{\text{GHZ}}) = 1$, while for a W-state we have $\tau_{gme}(\rho_{\text{W}}) = 0.6285$. The values of τ_{gme} for mixtures of just the GHZ and W states (i.e. the upper edge of the triangular plot in Fig. 3.4a) are plotted in Figure 3.4b.

It was shown by Ma et al [69] that our gme-detection quantity $\tau_{gme}(\rho)$ provides a lower bound for $\mathcal{C}_{gme}(\rho)$ as defined in Section 3.2.3, even for mixed states. The proof of this is based on the similar proof presented in section 2.4.1, which shows this fact in the case of two qubits.

Although τ_{gme} is not an entanglement measure itself, it supplies a lower bound for $\mathcal{C}_{gme}(\rho)$, which is a measure of genuine multipartite entanglement. Even though evaluating this quantity still requires an optimization, its optimization space is quite easy to parametrize. Generating states such that τ_{gme} is close to unity means that those states will have a high value of gme-concurrence as well. In Chapter 6, we use τ_{gme} as the quantity of interest and design control that maximizes it.

Chapter 4

Quantum optimal control theory

The dynamics of quantum systems and entanglement therein are becoming better and better understood [62, 74], and the presence of entanglement in quantum systems has been identified as a useful resource for many important tasks [33]. The problem now is the experimental implementation of such tasks. As our ability to engineer quantum systems improves, the important ability to control them such that they exhibit desired properties has been thrust into the forefront of research.

Dynamics of a closed quantum system are given by solutions to the Schrödinger or von Neumann equations, which are governed by some Hamiltonian H. If these dynamics can be manipulated, the tools of *optimal control theory* [75] can help determine optimal ways of controlling the system such that specific desired properties may be targeted. One of the central problems is that quantum systems are very sensitive to environmental effects, which often destroy the main features of quantum mechanics. If the objective is to transfer an initial state to a final one, decoherence can be avoided by determining control that transfers the state in the least amount of time.

In general, there are two ways to implementat on control on a system: closed-loop and open-loop feedback control [76]. Closed-loop feedback methods involve making adjustments according to measurements of the response of the system and are manipulated appropriately. This is useful in a system where the dynamics are unpredictable due to imperfect control or external effects of the environment. Such control schemes are useful for implementing quantum error correction codes [77]. Open-loop feedback control does not rely on physically measuring the response of a system during the application of control. As a result, the response of a system to a control application must be well-known, or a range of possible responses must be accounted for. The advantage here in using open-loop feedback control is that undesirable effects on the system due to measurements made during the application of the control and issues with measurement precision is avoided. In this case, a control scheme must be completely determined prior to the experiment

in which the control is applied, such that it is used and not modified during the experiment [25].

In this chapter, we present the fundamentals of quantum control theory needed to help us formulate our control scheme to maximize entanglement later on.

4.1 Dynamics of control

Before discussing the optimal aspects of quantum control, we first need to understand how control effects the dynamics of the system in question. A *control system* [25] is a system of ordinary differential equations with one or more varying functions of time $u(t)$, called the *controls*, such that a general control system has the form

$$\dot{x} = f(t, x, u). \tag{4.1}$$

Here, x represents a complete description the state of the system, and f is a function that dictates the dynamics of the system.

The relevant equation describing coherent dynamics of our states in quantum control systems is the Schrödinger equation. In this case, the dynamics of the system are given by the unitary time evolution

$$|\psi(t)\rangle = U(t)|\psi_0\rangle, \qquad \frac{d}{dt}U(t) = -i[H(u(t))]U(t), \qquad U(0) = \mathbb{1}, \tag{4.2}$$

where H is a matrix function of the controls u. In the examples that we will consider, the full Hamiltonian takes the form

$$H(u) = H_\mathrm{s} + \sum_k u_k H_c^{(k)} = H_\mathrm{s} + H_\mathrm{c}(t), \tag{4.3}$$

where H_s is the *drift* Hamiltonian that represents the uncontrolled dynamics of the system [75]. Each $H_c^{(k)}$ represents an interaction whose strength can by controlled by the corresponding control function u_k.

In the early applications of quantum control of molecular dynamics, the control Hamiltonian employed had the form

$$H_\mathrm{c}(t) = -u(t)\hat{\mu}, \tag{4.4}$$

where $\hat{\mu}$ is the dipole operator and $u(t)$ is the control function which represented the amplitude of the applied electromagnetic field over time [25,78]. The objective in such systems is to maximize the amount of a desired product in a chemical reaction. In other examples, such as in controlling the dynamics of a single spin, the dynamics can be manipulated through interactions with a controllable, classical magnetic field $\vec{B}$. In this case, the control Hamiltonian takes the form

$$H_\mathrm{c}(t) = \gamma(B_x(t)\sigma_x + B_y(t)\sigma_y + B_z(t)\sigma_z) \tag{4.5}$$

where B_x, B_y, and B_z are the orthogonal components of the magnetic field [25]. In typical experimental implementations of quantum control in many-body systems, the dynamics of the system are governed by electromagnetic interactions between particles. In this case, the system may be controlled by applying external electromagnet radiation, and the control Hamiltonian H_c arises from timed sequences of multiple laser pulses [22].

No quantum system can be completely protected from its environment. For open-loop control schemes, it is critical that we know how the environment interacts with the system. Depending on the character of the coupling of the system with the environment, there are many dynamical models for quantum systems undergoing enviromentally induced decoherence [74]. If the environment is not initially coupled to the system, the evolution of the system's reduced density matrix from time $t = 0$ to t can be described by a completely positive, trace-preserving map $\rho(t) = \Phi(\rho_0)$, with $\rho_0 = \rho(0)$. Just like our description of generalized quantum operations in Section 2.3.1, any map of this form can be expressed using Kraus operators in operator-sum representation

$$\rho(t) = \Phi(\rho_0) = \sum_j K_j(t)\rho_0 K_j^\dagger(t), \tag{4.6}$$

where K_j are the Kraus operators [74].

Along with some additional assumptions [74], a quantum master equation can be derived from this representation of interactions of a system with its environment. For Markovian environments, dynamics of an open quantum system can be described using the Lindblad-type master equation

$$\frac{d}{dt}\rho(t) = -i[H_s + H_c(t), \rho(t)] + \sum_i \gamma_i \left(L_i\rho(t)L_i^\dagger - \tfrac{1}{2}L_iL_i^\dagger\rho(t) - \tfrac{1}{2}\rho(t)L_iL_i^\dagger \right), \tag{4.7}$$

where γ_i are nonnegative numbers that denote the strength of the coupling to the environment and L_i are the Lindblad operators that represent the non-unitary effect of coupling to the environment.

4.2 Objective functionals

The question of whether the desired final state may be achieved given a set of controllable interactions $H_c^{(k)}$ and a system Hamiltonian H_s has been addressed elsewhere [25, 76]. Given a particular objective, there may exist many different control functions yielding trajectories of the state that end in the desired result. Optimal control theory can help answer the question of which of these trajectories is most ideal.

The determination of optimal control functions is performed by defining an appropriate *objective functional* that we would like to maximize. For a particular choice of control function u that yields a trajectory of the state of the system $\rho(t)$, the general class of objective functionals can be written as

$$J[u] = \mathcal{F}(\rho(T)) - \int_0^T F(t, \rho(t), u(t))dt. \tag{4.8}$$

The first term in (4.8) is the *target functional* that we would like to maximize. The latter term represents the *cost functional* of the control function that we would like to minimize. For example, we might penalize control fields with large amplitudes in order to minimize the energy required to reach the desired final state [79]. The general problem of optimal quantum control theory is to identify the structure of controls that enable us to attain the quantum objective in the best possible way, i.e. determination of the the control functions u that maximize the objective

$$J_{\text{opt}} = \max_u J[u]. \tag{4.9}$$

In many cases, there are no constraints or cost funcitons associated with the objective functional. The general objective functional (4.8) reduces to a Mayer-type [25] functional of the form

$$J[u] = \mathcal{F}(\rho(T), T). \tag{4.10}$$

Objective functionals of this type are used to minimize the time it takes to drive the system into a desired state. Alternatively, we set a time $T > 0$ over which we apply control and only consider control functions on the interval $[0, T]$. In this case, the only figure of merit is the value of the target functional $\mathcal{F}$ at the end of the control at time T.

In typical implementations of quantum control, such as in NMR [22], the objective is to bring the quantum system as close as possible to a particular target state $|\psi_{\text{tar}}\rangle$. The target functional that is to be maximized in this case is the overlap of the state ρ with the target state

$$\mathcal{F}(\rho(T)) = \langle\psi_{\text{tar}}|\rho(T)|\psi_{\text{tar}}\rangle. \tag{4.11}$$

In experimental realizations of quantum computers, the objective is not necessarily to produce particular states, but to create high fidelity unitary gates [24] that can be implemented in quantum computational algorithms.

In this thesis, the objective is to create a state that is the maximum of a particular functional. Because we are interested in generating highly entangled states, we use an entanglement measure as a target functional in the development of our control scheme in the next chapter.

4.3 Control strategies

Control of molecular and atomic systems can be achieved through appropriately shaped laser pulses. The strength of the electromagnetic fields emitted can have, in theory, an arbitrary profile in time. The shape of this profile can be modified using pulse shaping techniques. The goal of quantum control is to determine the optimal pulse shapes for controlling the dynamics of the system such that the final state meets a desired criteria. In principle, there is no restriction to the light shapes that can be obtained with pulse shaping techniques except that the electromagnetic field is limited by the Heisenberg uncertainty principle. In application, the shapes of laser pulses are limited by current technology [79]. Realization of quantum control has only been made possible with the development of intense femtosecond laser pulses and pulse shapers that can manipulate quantum coherences in ultrafast atomic and molecular dynamics [80].

There are numerous strategies available to implement quantum optimal control. Due to the complex nature of quantum systems, an exact solution is usually not accessible, and numerical techniques must be employed to approximate a solution. When there are many control variables, optimization procedures can be quite numerically expensive. As a result, it is often advantageous to use simpler methods to construct an approximate solution to the problem rather than perform full optimizations.

In this section, we first describe a general class of optimal control methods that rely on iterative methods. They determine optimal control functions that drive a system into states that maximize some predetermined target functional $\tau(\rho)$ after a given time T. The scheme starts with choosing an initial control function $u(t)$ and propagating the initial state ρ_i forward in time. With given control functions, the dynamics of the system are completely defined, and the final state at some later time T can be determined. The control functions can then be slightly modified, which leads to an increase on the value of the functional at the final time T. After many iterations, this converges to an optimal pulse shape. We also present a method based on the Lyapunov formalism. Using this type of method, a control field is chosen at each instant in time such that it yields the greatest increase in the target functional. Only one forward-propagation is necessary to derive control fields from this method.

4.3.1 Gradient-based maximization techniques

Typically, the control Hamiltonian is broken down into different controllable parts, $H_c^{(k)}$, such that the tunable parameters are the amplitudes of each of the compo-

nents of

$$H_{\mathrm{c}}(t) = \sum_k u_k(t) H_{\mathrm{c}}^{(k)}. \tag{4.12}$$

The time-independent Hamiltonians $H_{\mathrm{c}}^{(k)}$ describe the coupling of the system to various external control fields, and the $u_k(t)$ are the amplitudes of each of these corresponding fields. Since the control fields are usually applied to a system through a time-modulated laser, the problem statement can be reformulated as "shaping" the laser pulses to yield optimal results.

Unitary evolution of a system that is induced by the full Hamiltonian is given by $\rho(t) = U_{\mathrm{c}}(t)\rho_i U_{\mathrm{c}}^{\dagger}(t)$, where ρ_i is the initial state of the system and $U_{\mathrm{c}}(t)$ is defined by

$$\dot{U}_{\mathrm{c}}(t) = \left(H_{\mathrm{s}} + \sum_i u_k(t) H_{\mathrm{c}}^{(k)} \right) U_{\mathrm{c}}(t). \tag{4.13}$$

The time over which the control is applied is usually fixed at $T > 0$. The goal is to determine the optimal control pulses in the time interval $[0, T]$ such that the final state $\rho_f = U_{\mathrm{c}}(T)\rho_i U_{\mathrm{c}}^{\dagger}(T)$ is achieved.

Rather than trying to determine the optimal time-varying control amplitudes over all possible functions, these amplitudes are expanded as a combination of chosen basis functions $g_j(t)$ that are defined on the time interval $[0, T]$. Determing the optimal field strengths $u_k(t)$ that lead to optimal control of the quantum system is now reduced to finding the optimal choice in the space of functions that is spanned by the basis $\{g_j\}$:

$$u_k(t) = \sum_j a_{kj} g_j(t). \tag{4.14}$$

Determining the choice of parameters a_{kj} that yield the optimal control pulse is a task which may be determined numerically. The quantity to be optimized is the target functional of the final state of the system ρ_f,

$$\tau(T) = \tau\left(U_{\mathrm{c}}(T)\rho_i U_{\mathrm{c}}^{\dagger}(T) \right). \tag{4.15}$$

The unitary evolution operator $U_{\mathrm{c}}(T)$ is dependent on each of the amplitudes a_{ij}, and thus $\tau(T)$ is as well. The target functional is therefore purley a function of the real parameters a_{kj}.

One commonly used control strategy is the GRAPE algorithm [26], which was originally motivated by applications in nuclear magnetic resonance (NMR) spectroscopy. An acronym for GRadient Ascent Pulse Engineering, the GRAPE algorithm describes an adaptation of a classical optimal control method for using tunable radio frequency pulses to perturb the alignment of nuclear spins in desirable ways. Although the inspiration and primary application of this method was

for NMR experiments, the approach can be expanded to deal with any type of closed quantum system.

The GRAPE algorithm describes a gradient-based maximization technique. It determines optimal control pulses where the target functional is the overlap with some target state ρ_{tar} and the control amplitudes are expanded in the basis of piecewise constant functions

$$g_j(t) = \begin{cases} 1, & t \in [t_{j-1}, t_j) \\ 0, & \text{otherwise.} \end{cases} \tag{4.16}$$

The time interval over which control is applied is segmented into n subintervals, during which the control is constant. Thus, during each subinterval the constant unitary evolution operator is given as

$$U_j(t) = \exp\left(-i\left[H_{\text{s}} + \sum_k a_{kj} H_{\text{c}}^{(k)}\right] t\right). \tag{4.17}$$

An initial guess for the coefficients is chosen, and the system is propagated forward in time to acquire the final state $\rho(T)$ from these dynamics. The final value of the target functional at the final time $\tau(T)$ is a function of the choice of the individual coefficients a_{kj}. The gradient of the final value of the functional with respect to each of the variables a_{kj} can be calculated. Based on the gradient, these parameters may be slightly adjusted to yield an increase in the final value of the target functional at time T. This procedure then converges to an optimal choice of control parameters through multiple iterations of this technique.

The downside of the standard gradient ascent methods is that determination of optimal pulses requires decomposition of the control over the time interval into many piecewise constant segments. Without any extra constraints on the values of the individual amplitudes a_{kj} of each segment, this method can yield pulses with many high frequency components [81]. Additionally, this often requires optimization over thousands of parameters, depending on the number of subintervals and controllable amplitudes [82].

Instead of segmenting the time interval into many piecewise constant sections, we can instead consider a set of basis functions that are smooth on the time interval $[0, T]$. One such choice would be to expand the amplitudes as sums of periodic functions with periodicity T [83]. In this case, an initial pulse is generated by selecting random amplitudes a_{kj} for each basis function. Through gradient ascent methods, these amplitudes can be modified to yield an increase in the target functional of the final state until a maximum value is reached. Since the basis functions are chosen to be smooth, the resulting optimal pulse will not only be a smooth funciton of time, but the frequency components of the pulse will be limited

to the frequencies of the basis functions. Compared to other methods, the number of parameters needed is relatively small, allowing for optimization techniques that make use of second-order approximations. Additionally, it is much simpler to give a physical interpretation of the optimal smooth control pulses that are acquired from this method rather than the high-frequency and chaotic pulses created by GRAPE.

4.3.2 Lyapunov control

With the exception of the simplest of quantum systems, exact solutions to the optimal control problem are not accessible and numerical techniques must be used to approximate a solution. For the most part, the optimal control methods mentioned above involve an iterative approach that converges to an optimal value. However, optimization is not always required or necessary in quantum control. We can alternatively design control such that the value of the target function increases a maximal amount during all times of the propagation. Although this leads to a gradual increase of the target functional, the resulting control from such schemes are generally not optimal. This is the basis of Lyapunov control [25].

In its early days, quantum control often manifested itself as problems of determining optimal population transfer [84]. Given a quantum system whose initial state $|\psi_i\rangle$ was an eigenstate of the system Hamiltonian H_s, an optimal control pulse needed to be designed to transfer the system into a final state $|\psi_f\rangle$ that was also an eigenstate of H_s.

The target functional of a Lyapunov control scheme, called a *Lyapunov function*, generally takes the form

$$V(\rho) = \mathrm{Tr}(A\rho), \tag{4.18}$$

where A is a Hermitian matrix. Usually, this is the projection operator on to the desired target state. The problem of Lyapunov control is that of finding control functions $u_i(t)$ such that the solution of

$$\dot{\rho} = -i[H_\mathrm{s} + \sum_i u_k(t) H_\mathrm{c}^{(k)}, \rho] \tag{4.19}$$

converges to an optimal value, i.e. the target state $|\psi_f\rangle\langle\psi_f|$. We wish to establish a choice for the control fields $u_k(t)$ that achieves this target. The time derivative

of the target functional V is

$$\begin{aligned}\dot{V} &= \mathrm{Tr}(A\dot{\rho}) \\ &= -i\left(\mathrm{Tr}(A[H_\mathrm{s},\rho] + \sum_k u_k(t)\mathrm{Tr}(A[H_\mathrm{c}^{(k)},\rho])\right) \\ &= -i\mathrm{Tr}(\rho[A,H_\mathrm{s}] - i\sum_k u_k(t)\mathrm{Tr}(\rho[A,H_\mathrm{c}^{(k)}]),\end{aligned} \tag{4.20}$$

using identity $\mathrm{Tr}(A[B,C]) = \mathrm{Tr}(B[C,A])$. The operator A is usually chosen such that it has the same eigenvectors as the system Hamiltonian H_s. Since the state that maximzes V will be an eigenvector of A [25], this ensures that the objective state will also be an eigenstate of H_s. Assuming that A commutes with H_s, the expression for $\dot{V}$ reduces to

$$\begin{aligned}\dot{V} &= -i\sum_k u_k(t)\mathrm{Tr}(\rho[A,H_\mathrm{c}^{(k)}]) \\ &= \vec{u}(t)\cdot\vec{Y},\end{aligned} \tag{4.21}$$

which is an inner product between the control vector and the vector $\vec{Y}$, with $Y_k = -i\mathrm{Tr}(\rho[A,H_\mathrm{c}^{(k)}])$. For the control field to have the optimal effect on the system, we choose the control vector to be $\vec{u} = c\cdot\vec{Y}$ with $c > 0$ to maximize $\dot{V}$.

Lyapunov-based controls are feedback-based, i.e. the control is a function of the state at any given point in time. In quantum systems, the state is not available for measurement, so the dynamics must be simulated. For a given input state $\rho(0) = \rho_0$, one simultaneously evaluates the evolution of the state and calculates the optimal control vector $\vec{u}(t)$ based on the value of the state $\rho(t)$ over a given period of time. From the simulation, a control function is acquired which may be applied to a real system.

This method of judiciously choosing the control fields during propagation of the system can be applied to other systems and target functionals as well. In fact, we make use of this idea in our control scheme that is presented in the next chapter. Although Lyapunov-like schemes are not optimal in that they do not determine the most effective pulse shape for ideal state transfer, such control gives useful pulse shapes that lead to an increase of the target functional and are easily computed.

Chapter 5

Optimal control of entanglement

As discussed in Chapter 4, the most common type of target functional used in quantum control is defined as the overlap with a predetermined target state $|\psi_{\text{tar}}\rangle$. However, we are interested in finding optimal control to generate highly entangled states. If we choose, for example, a highly entangled multipartite target state, then controlling the system such that the final state has the greatest overlap with the target state $\langle\psi_{\text{tar}}|\rho_f|\psi_{\text{tar}}\rangle$ will certainly yield a high degree of entanglement.

Choosing a particular target state that has desired entanglement properties is certainly one possible strategy, but there is a manifold of states that exhibit equivalent entanglement properties, namely those that can be converted into each other by local unitary transformations.

In all experimental implementations of quantum entanglement, interaction with the environment inevitably leads to decoherence and therefore a decay of entanglement. Because entanglement depends non-linearly on the coherences, some locally equivalent states will exhibit a more rapid decay of entanglement due to decoherence than others. The identification of those states which are most robust against environment interactions is a non-trivial question, and investigation into this problem has already begun [61, 85]. Chosing the overlap with a single particular state as the target functional is limiting and excludes one from obtaining a locally equivalent state that might be more desirable, e.g. more robust against decoherence.

Additionally, due to the interactions of the system, some locally equivalent states may be more easily obtained than others. If the overlap with a target state is the target functional, one would have to consider these criteria before selecting which of the locally equivalent states would be the most ideal target. We can eliminate these problems by choosing a functional that is invariant under local unitaries, and we can tailor control such that the most robust and easily obtained states are targeted.

If entanglement is chosen as the quantity that we want to maximize, the above

arguments illustrate that targeting specific states is rather unnecessary. We want to generate states with a high degree of genuine multipartite entanglement, especially ones that are most robust against decoherence effects from the environment. Therefore, we propose a control scheme that employs an *entanglement measure* as a target functional. Our aim is to apply the principles of optimal quantum control, introduced in Chapter 4, to determine optimal external control fields that will generate states that maximize a particular quantification of entanglement. The derived control fields will optimally exploit the interactions of the system and, at the same time, minimize the effects of decoherence to create states that are highly entangled.

The problem with most current ways of quantifying entanglement is that they cannot be straightforwardly evaluated, as we have seen in Chapter 3. Successfully implementing a Lyapunov-like control scheme, however, requires us not only to be able to repeatedly evaulate the target functional, but also to compute its time derivatives. If the target functional is not analytic and its evaluation requires an optimization over a parameter space, determining its time derivatives may seem like an impossible task.

In this chapter, we present an innovative method for determining optimal control of entanglement measures and tackle the problem of their derivatives and optimization. Because all entanglement measures are invariant under local unitaries, we first show how optimal control can be computed in the general case of locally invariant functionals based on the evaluation of their time derivatives. Applying this scheme to functionals that can be analytically evaluated is straightforward. In fact, a specific version of our control scheme has been studied in the case when the target functional is $\tau_{\mathcal{C}}$ [27], the lower bound of the generalized concurrence introduced in 3.2.1. However, since most measures of entanglement require an optimization procedure, we also present a method to calculate time derivatives of functionals that must be optimized over some parameter space. Finally, we show how our control scheme can be used to calculate control for specific examples of entanglement quantifiers as target functionals.

5.1 Optimal control of entanglement

The framework of Lyapunov control was designed as a method for determining optimal control of population transfers, but can be extended to control that optimizes other functionals as well. If the relationship between the first time derivative of the target functional and the control Hamiltonian is linear, the Lyapunov method delivers a direct way to determine optimal control. In this section, we develop a similar method of deriving optimal control fields based on maximizing the time derivatives of the target functional. Since we are interested in the generation of

highly entangled states, it is natural to choose an entanglement measure as a target functional. In particular, all entanglement measures are invariant under local unitaries, so we first adopt an approach to derive control on LU-invariant functionals in general. To implement control with targets that require an optimization, we also establish a way to determine the time derivatives of functionals that involve an optimization over a real, unconstrained parameter space.

In many experimental setups, it is challenging or even impossible to engineer or manipulate interactions between particles. In general, we therfore assume that control of the system is limited to producing only single particle dynamics, but no interactions between different subsystems. That is, we limit our control to Hamiltonians of the form

$$H_{\mathrm{c}} = \sum_{n=1}^{N} \sum_{\xi} k_{\xi}^{(n)} \sigma_{\xi}^{(n)} \tag{5.1}$$

where $\sigma_{\xi}^{(n)} = \mathbb{1} \otimes \cdots \otimes \sigma_{\xi} \otimes \cdots \otimes \mathbb{1}$ represent the Pauli matrices ($\xi = x, y, z$) acting on the n^{th} Hilbert space of the composite system. Any Hamiltonian that can only induce single particle dynamics can be written as a linear combination of the individual local Pauli matrices $\sigma_{\xi}^{(n)}$. Thus, we can consider Hamiltonians of the form

$$H_{\mathrm{c}} = \sum_{\lambda} k_{\lambda} \sigma_{\lambda}, \tag{5.2}$$

where the σ_{λ} are linear combinations of the local Pauli matrices corresponding to the tunable aspects of the system, and k_{λ} are the amplitudes of each of these controls.

In this section, we first show how we can extend the Lyapunov method of quantum control to situations where the target functional is invariant under local unitaries. Similar to the Lyapunov control introduced in 4.3.2, this is performed by determining the control fields that maximize the time derivatives of the target functional at all times. Finally, we show how this method can be used to derive control fields that can maximize entanglement in a system.

5.1.1 Local control of LU-invariant functionals

The functions of interest that we optimize in this work are all invariant under local unitaries. In the following, we show that the first time derivatives of such functions are independent of local control, so we must resort to higher-order derivatives. Physically, this has the interpretation that it is impossible to create entanglement with purely local effects. Although application of control may give rise to entanglement, since it helps to exploit the intrinsic interactions of the system, local control alone cannot create entanglement. As a result of this, the second time derivative

of LU-invariant functionals is linearly dependent on control. This allows us to extend the Lyapunov-style control scheme to entanglement measures.

Consider a functional $\mathcal{F}$ on the density matrices that is invariant under local unitaries

$$\mathcal{F}(\rho) = \mathcal{F}(U_1 \otimes \cdots \otimes U_N \rho U_1^\dagger \otimes \cdots \otimes U_N^\dagger), \tag{5.3}$$

where the U_i's act only on a single qubit. The state undergoes time evolution according to

$$\dot{\rho} = -i[H_\mathrm{s} + H_\mathrm{c}, \rho] + \mathcal{D}(\rho),$$

where H_c is an external, time-varying control Hamiltonian that induces only single particle dynamics, but not interactions between subsystems. H_s is an interaction Hamiltonian, and $\mathcal{D}$ represents an incoherent part of the evolution.

Our strategy to maximize $\mathcal{F}$ is to optimize the increase of $\mathcal{F}$ at all times. By choosing the control fields that maximize the time derivatives, we cause the value of the target functional to increase most rapidly, an effect that can be seen directly by analyzing the Taylor expansion of $\mathcal{F}$

$$\mathcal{F}(t_0 + t) \;=\; \mathcal{F}(t_0) \;+\; t\frac{d\mathcal{F}}{dt}\bigg|_{t_0} \;+\; \frac{1}{2}t^2\frac{d^2\mathcal{F}}{d^2t}\bigg|_{t_0} \;+\; \mathcal{O}(t^3). \tag{5.4}$$

The state ρ can be expressed as a generalized Bloch vector $\vec{R}$. If we are considering a system of N qubits, then we have $R_\alpha = \mathrm{Tr}(\rho\sigma_\alpha)$, where the σ_α's are the 4^N generalized tensor products of the Pauli matrices, $\{\sigma_x, \sigma_y, \sigma_z, \mathbb{1}\}$. Because $\mathcal{F}$ is a functional of density matrices, we can expand it as a function of the elements of the generalized Bloch vector, $\mathcal{F}(\rho) = \mathcal{F}(\vec{R})$. The total time derivative of $\mathcal{F}$ is

$$\dot{\mathcal{F}} = \sum_\alpha \frac{\partial \mathcal{F}}{\partial R_\alpha}\dot{R}_\alpha. \tag{5.5}$$

Inserting the expressions for each $\dot{R}_\alpha$, we obtain

$$\begin{aligned}\dot{\mathcal{F}} = \sum_\alpha \frac{\partial \mathcal{F}}{\partial R_\alpha}\dot{R}_\alpha &= \sum_i \frac{\partial \mathcal{F}}{\partial R_\alpha}\mathrm{Tr}(\sigma_\alpha(-i[H_\mathrm{s} + H_\mathrm{c}, \rho] + \mathcal{D}(\rho))) \\ &= -i\sum_\alpha \frac{\partial \mathcal{F}}{\partial R_\alpha}\mathrm{Tr}(\sigma_\alpha[H_\mathrm{c}, \rho]) + \dot{\mathcal{F}}_0,\end{aligned} \tag{5.6}$$

where $\dot{\mathcal{F}}_0$ contains the parts of $\dot{\mathcal{F}}$ that do not depend on control, i.e.

$$\dot{\mathcal{F}}_0 = \sum_\alpha \frac{\partial \mathcal{F}}{\partial R_\alpha}\mathrm{Tr}\left\{\sigma_\alpha(-i[H_\mathrm{s}, \rho] + \mathcal{D}(\rho))\right\}. \tag{5.7}$$

Time-local optimal control, such as in the Lyapunov scheme, can be determined by taking the derivative of $\dot{\mathcal{F}}$ with respect to the local control amplitudes k_λ. Since

$\dot{\mathcal{F}}_0$ is independent of H_c, it does not depend on the amplitudes, so the derivatives of $\dot{\mathcal{F}}_0$ with respect to the amplitudes k_λ all vanish. Note, however, that the first term in (5.6) is equivalent to

$$\frac{d}{dt}\mathcal{F}(e^{-iH_c t}\rho e^{iH_c t}), \tag{5.8}$$

where $e^{-iH_c t}$ is a local unitary due to the fact that H_c is a local Hamiltonian. It is important here that we are only interested in locally invariant functionals, which implies that $\mathcal{F}(e^{-iH_c t}\rho e^{iH_c t}) = \mathcal{F}(\rho)$, where ρ is the state at time $t = t_0$. However, this expression is not time-dependent, so the time derivative of $\mathcal{F}(\rho_{t_0})$ vanishes as well. The only term of $\dot{\mathcal{F}}$ that is non-vanishing is $\dot{\mathcal{F}}_0$, i.e. the increase of $\mathcal{F}$ in the absence of control. Therefore, $\dot{\mathcal{F}}$ is independent of the local control amplitudes, i.e.

$$\frac{\partial}{\partial k_\lambda}\dot{\mathcal{F}} = 0. \tag{5.9}$$

Straightforward application of the Lyapunov scheme is therefore no longer possible.

Although the first time derivative of a locally invariant functional is independent of local control, the second time derivative is not, as we will show here. Consequently, we can resort to finding optimal control amplitudes by maximizing the curvature of the target functional $\ddot{\mathcal{F}}$. This is given as

$$\ddot{\mathcal{F}} = \sum_\alpha \frac{\partial \mathcal{F}}{\partial R_\alpha}\ddot{R}_\alpha + \sum_{\alpha,\beta}\frac{\partial^2 \mathcal{F}}{\partial R_\alpha \partial R_\beta}\dot{R}_\alpha \dot{R}_\beta, \tag{5.10}$$

where the derivatives of the elements of the generalized Bloch vector are again given by $\dot{R}_\alpha = \mathrm{Tr}(\sigma_\alpha \dot{\rho})$ and $\ddot{R}_\alpha = \mathrm{Tr}(\sigma_\alpha \ddot{\rho})$. Rather than writing out the entire expression for $\ddot{\mathcal{F}}$ after inserting the expressions for $\dot{R}_\alpha$ and $\ddot{R}_\alpha$, we instead can group the terms into three types. As above, the terms that have no dependence on H_c are grouped into $\ddot{\mathcal{F}}_0$. Furthermore, the terms that depend only on H_c, and not on H_s or $\mathcal{D}$, are grouped into $\ddot{\mathcal{F}}_c$. All that remains will be the cross-terms that depend both on the control and the system, which we group into $\ddot{\mathcal{F}}_I$. Thus, the second time derivative of $\mathcal{F}$ has the simplified expression

$$\ddot{\mathcal{F}} = \ddot{\mathcal{F}}_I + \ddot{\mathcal{F}}_0 + \ddot{\mathcal{F}}_c. \tag{5.11}$$

Determining time-optimal control is now a matter of calculating the derivatives of each of these terms with respect to k_λ.

In particular, $\ddot{\mathcal{F}}_0$ is independent of the control amplitudes, so this part of the derivative vanishes. Expanding the terms in $\ddot{\mathcal{F}}_c$ yields

$$\begin{aligned}\ddot{\mathcal{F}}_c = \sum_\alpha \frac{\partial \mathcal{F}}{\partial R_\alpha}\mathrm{Tr}\left\{\sigma_\alpha\left(-[H_c,[H_c,\rho]] - i[\dot{H}_c,\rho]\right)\right\} \\ - \sum_{\alpha,\beta}\frac{\partial^2 \mathcal{F}}{\partial R_\alpha \partial R_\beta}\mathrm{Tr}(\sigma_\alpha[H_c,\rho])\mathrm{Tr}(\sigma_\beta[H_c,\rho]).\end{aligned} \tag{5.12}$$

Similar to the expression for the first time derivative, this is equivalent to

$$\ddot{\mathcal{F}}_c = \frac{d^2}{dt^2}\mathcal{F}(e^{-iH_c t}\rho e^{iH_c t}). \tag{5.13}$$

Just as before, this term vanishes since $\mathcal{F}$ is invariant under local unitaries.

The only remaining term in the derivative of $\ddot{\mathcal{F}}$ with respect to the control amplitudes k_λ is the term that contains the interplay of H_c with H_s and $\mathcal{D}$. Writing $\ddot{\mathcal{F}}_I$ out explicitly, we have

$$\begin{aligned}\ddot{\mathcal{F}}_I = \sum_\alpha \frac{\partial \mathcal{F}}{\partial R_\alpha}\mathrm{Tr}\Big\{\sigma_\alpha\Big(- [H_\mathrm{c},([H_\mathrm{s},\rho] + i\mathcal{D}(\rho))] - [H_\mathrm{s},[H_\mathrm{c},\rho]] - i\mathcal{D}([H_\mathrm{c},\rho])\Big)\Big\} \\ + \sum_{\alpha,\beta}\frac{\partial^2\mathcal{F}}{\partial R_\alpha \partial R_\beta}\Big\{ - i\mathrm{Tr}(\sigma_\alpha[H_\mathrm{c},\rho])\mathrm{Tr}\Big(\sigma_\beta(\mathcal{D}(\rho) - i[H_\mathrm{s},\rho])\Big) \\ - i\mathrm{Tr}\Big(\sigma_\alpha(\mathcal{D}(\rho) - i[H_\mathrm{s},\rho])\Big)\mathrm{Tr}(\sigma_\beta[H_\mathrm{c},\rho])\Big\}.\end{aligned} \tag{5.14}$$

Namely, the control Hamiltonian H_c apears linearly in this expression. Thus, $\ddot{\mathcal{F}}$ is indeed linearly dependent on the control. We can exploit this linear relationship to determine the optimal control that maximizes the curvature of the target functional.

Since $\ddot{\mathcal{F}}_I$ is the only term of $\ddot{\mathcal{F}}$ that depends on control, the derivative of $\ddot{\mathcal{F}}$ with respect to the control amplitide k_λ is equivalent to

$$\frac{\partial \ddot{\mathcal{F}}}{\partial k_\lambda} = \frac{\partial \ddot{\mathcal{F}}_I}{\partial k_\lambda}. \tag{5.15}$$

The control Hamiltonian $H_\mathrm{c} = \sum_\lambda k_\lambda \sigma_\lambda$ is linear with respect to each individual amplitude, so the derivative of $\ddot{\mathcal{F}}_I$ with respect to one control aplitude k_λ can simply be determined by replacing each instance of "H_c" in (5.14) with "σ_λ".

However, if the functional $\mathcal{F}$ is not a straightforward function of the density matrix, the derivatives of $\mathcal{F}$ with respect to the Bloch vector elements R_α are not accessible. In this case, the expression in eq. (5.14) cannot be determined. For the functionals that we use, it is much easier to evaluate $\ddot{\mathcal{F}}$ if the dynamics $\dot{\rho}$ are given. In general, the dynamics depend on the control Hamiltonian, which is exactly what needs to be determined. The components of the optimal control Hamiltonian are derived by evaluating the derivatives in (5.15). To do this, we first note that $\ddot{\mathcal{F}}_I$ can be decomposed as

$$\ddot{\mathcal{F}}_I = \ddot{\mathcal{F}} - \ddot{\mathcal{F}}_c - \ddot{\mathcal{F}}_0, \tag{5.16}$$

where each term on the right-hand side represents the second time derivative of the target functional for given dynamics of $\dot{\rho}$. The $\mathcal{F}_c$ term vanishes, since the

value of the functional cannot change under purely local dynamics generated by H_c. As in the previous paragraph, we can determine the derivitive of the right-hand side of equation (5.16) with respect to the control amplitude k_λ by replacing each instance of "H_c" with "σ_λ". That is, to evaluate the derivative of $\ddot{\mathcal{F}}_I$ with respect to the control amplitude k_λ, we set the dynamics of the system to be

$$\begin{aligned} \dot{\rho}_{\lambda,s} &= -i[H_s + \sigma_\lambda, \rho] + \mathcal{D}(\rho) && \text{for evaluation of } \ddot{\mathcal{F}} \text{ and} \\ \dot{\rho}_s &= -i[H_s, \rho] + \mathcal{D}(\rho) && \text{for evaluation of } \ddot{\mathcal{F}}_0. \end{aligned} \tag{5.17}$$

Thus, we must evaluate $\ddot{\mathcal{F}}_0$ once, then $\ddot{\mathcal{F}}$ for each control element σ_λ of the tunable control Hamiltonian to determine all of the derivatives $\dfrac{\partial \ddot{\mathcal{F}}_I}{\partial k_\lambda}$.

5.1.2 Determining optimal control

The Lyapunov control scheme outlined in Section 4.3.2 relies on the fact that the time derivative of the target functional $\dot{\mathcal{F}}$ is linearly dependent on the control. Although the first time derivatives of LU-invariant functions are independent of local control, we have just shown that their second derivative is linearly dependent on local effects. We can use this result to apply a Lyapunov-like scheme to derive optimal control fields.

If the control Hamiltonian consists of orthogonal components

$$H_c(t) = \sum_\alpha k_\lambda(t)\sigma_\alpha, \tag{5.18}$$

our Lyapunov-based control scheme dictates that the optimal control vector $\vec{k}$ should be parallel to the gradient of $\ddot{\mathcal{F}}$ with respect to the control elements, *i.e.* $\vec{k}||\vec{Y}$, where the elements of $\vec{Y}$ are

$$Y_\lambda = \frac{\partial \ddot{\mathcal{F}}}{\partial k_\lambda}. \tag{5.19}$$

Here, we consider the control elements as addressing individual spins in the system, such that the control vector $\vec{k}^{(n)}$ determines the control on the n^{th} spin. For each spin, we obtain the vector

$$\vec{X}^{(n)}(\rho, H_{\text{sys}}, \mathcal{D}) = \left(\frac{\partial \ddot{\mathcal{F}}}{\partial k_1^{(n)}}, \frac{\partial \ddot{\mathcal{F}}}{\partial k_2^{(n)}}, \frac{\partial \ddot{\mathcal{F}}}{\partial k_3^{(n)}} \right), \tag{5.20}$$

representing the control applied by the Pauli operatos $(\sigma_1, \sigma_2, \sigma_3)$ on each qubit. The expansion of the coefficient k_λ of the control Hamiltonian represents the amplitude of one of the three control fields ($\xi = 1, 2, 3$) applied to the n^{th} spin. The

total amplitude of the control fields applied on the n^{th} spin is given by

$$||\vec{k}^{(n)}|| = \sqrt{|k_1^{(n)}|^2 + |k_2^{(n)}|^2 + |k_3^{(n)}|^2}. \tag{5.21}$$

In a realistic experimental implementation of such control fields, the total amplitude of the control field addressed at the individual spins will be limited by some maximal field strength, *i.e.*

$$k_{\max} \geq ||\vec{k}^{(n)}||. \tag{5.22}$$

Therefore, maximization of $\ddot{\mathcal{F}}$ will be achieved by choosing the control vector $\vec{k}^{(n)}$ to be parallel to $\vec{X}^{(n)}$, such that the amplitude of the control field is maximal, i.e. $||\vec{k}^{(n)}|| = k_{\max}$.

5.1.3 Application to analytical functionals

If the functional in question can be evaluated analytically, its time derivatives can be determined without any further problems. One possible choice of such a target functional is the generalization of the concurrence discussed in 3.2.1, where a lower bound on mixed states can be given by

$$\tau_{\mathcal{C}}(\rho) = \mathrm{Tr}(\rho \otimes \rho V). \tag{5.23}$$

Control of entanglement dynamics using this as the target functional has been previously studied [27, 86, 87]. This functional is invariant under local unitaries. Thus, from the previous sections, we know that its first time derivative will be independent of local control and that evaluating its second time derivative yields a way to calculate the optimal control by determining the derivatives of $\ddot{\tau}_{\mathcal{C}}$ with respect to the control elements $\frac{\partial \ddot{\tau}_{\mathcal{C}}}{\partial k_\lambda}$.

If the dynamics of the system are given by $\dot{\rho}(t) = -i[H_{\text{sys}} + H_{\text{c}}(t), \rho(t)] + \mathcal{D}(\rho(t))$, the second time derivative of $\tau_{\mathcal{C}}$ is given by

$$\ddot{\tau}_{\mathcal{C}} = 2\mathrm{Tr}\left(\left(\ddot{\rho} \otimes \rho + \dot{\rho} \otimes \dot{\rho}\right) V\right). \tag{5.24}$$

This will have terms that are linear and quadratic in the control H_{c}, as well as components that are independent of control. From the analysis in 5.1.1, we only need to consider the parts of $\ddot{\tau}_{\mathcal{C}}$ that are linear with respect to the control elements. Simplifying this way, we arrive at

$$\begin{aligned} &\frac{\partial \ddot{\tau}_{\mathcal{C}}}{\partial k_\lambda} = \\ &\quad -\mathrm{Tr}\Big(\Big[\big([H_{\text{sys}}, [\sigma_\lambda, \rho]] + [\sigma_\lambda, [H_{\text{sys}}, \rho]] + i[\sigma_\lambda, \mathcal{D}(\rho)] + i\mathcal{D}([\sigma_\lambda, \rho])\big) \otimes \rho \\ &\qquad + \big(i[H_{\text{sys}}, \rho] + \mathcal{D}(\rho)\big) \otimes [\sigma_\lambda, \rho] + [\sigma_\lambda, \rho] \otimes \big(i[H_{\text{sys}}, \rho] + \mathcal{D}(\rho)\big)\Big] V\Big) \end{aligned} \tag{5.25}$$

as our expression for $\frac{\partial \ddot{\tau}_{\mathcal{C}}}{\partial k_\lambda}$ [27]. This allows us to analytically determine the optimal strength of the control fields for generating states that maximize $\tau_{\mathcal{C}}$.

5.2 Control of optimization functionals

As stated earlier, we want to implement optimal control that maximizes functionals which quantify entanglement. Although the analytical nature of $\tau_{\mathcal{C}}$ makes it a natural candidate for a target functional, this functional cannot identify genuine multipartite entanglement, so we must employ other target functionals. Most methods of quantifying entanglement cannot be straightforwardly evaluated and require and optimization. However, we still need to calculate the time derivatives of these optimization functionals, a task that is not straightforward.

In this section, we present a method that can be used to determine time derivatives of such functionals, as long as the parameterization in question is continuous and free of constraints. In Chapter 3 we introduced several functionals that satisfy this requirement, such as the maximum overlap funcitonals τ_{ψ} and the genuine multipartite entanglement detection quantity τ_{gme} introduced in 3.2.5.

The functionals of interest here involve maximizations over locally equivalent states. To fully evaluate these functionals as the state ρ evolves, a new optimization must be performed continuously. However, we can greatly simplify this problem by intelligently keeping track of the optimal choice of parameters needed to evaluate these functionals. The final goal is to be able to determine the optimal control on a system such that our target functional is maximized, using the means presented in the previous section for controlling LU-invariant functionals. Along the way, however, the target functional must be evaluated at each step, i.e. we must continuously re-optimize the parameters needed to evaluate $\mathcal{F}$. Here, all of our parameters are real numbers. If the target functional $\mathcal{F}$ is smooth and the value of the functional $\mathcal{F}(\rho)$ changes smoothly as the state ρ evolves, then we assume that the optimal choice of real parameters will smoothly change as well. This fact is useful in re-optimizing the functional as the state changes, and helps us evaluate the derivatives needed for determining the optimal control.

This implies that we need to perform two optimizations simultaneously: the determination of optimal external control on the system and the determination of parameter adjustment that ensures that we are correctly evaluating the target functional. Thus, while we calculate what control fields to use, the entanglement meausres that we employ as target functionals will be optimized "on-the-fly"[1].

In this section, we first present a method of determing time derivatives of optimization functionals, assuming their parameterizations fulfill some basic requirements. Once this is done, we can use the methods of the previous section to determine optimal control, provided that the functional is locally invariant. In the following sections, we show some examples of our contol scheme applied to some

[1] "on-the-fly" is an idiomatic English expression meaning: done as one goes, or during another activity.

specific measures of entanglment.

5.2.1 Time derivatives of optimization functionals

The type of functionals that are of primary interest here are functionals on the density matrices that involve optimization over some set of real parameters φ_i, e.g.

$$\mathcal{F}(\rho) = \max_{\{\varphi_i\}} \tau(\rho, \{\varphi_i\}). \tag{5.26}$$

Thus, we can define the dynamics of the optimized functional $\mathcal{F}$ by

$$\mathcal{F}(t) = \tau(\rho(t), \vec{\varphi}(t)), \tag{5.27}$$

where $\vec{\varphi}(t)$ is chosen such that it is optimal for all times. Whereas $\rho(t)$ represents the state evolution of the *real* system, the real variables $\vec{\varphi} \in \mathbb{R}^m$ correspond to a "state" of what we will call the *fictitious system*. Although the real numbers in $\vec{\varphi}$ represent the choice of parameters that optimizes the functional, they do not necessarily have any physical interpretation. Our control problem now consists of optimally controlling the dynamics of the real system as well as the fictitious system simultaneously. That is, as the state $\rho(t)$ evolves, we also need to determine how the optimal choice $\vec{\varphi}(t)$ evolves.

We cannot simply take derivatives of such functions in order to determine their dynamics as in the analysis in 5.1.3. For our optimal control scheme, however, we need to calculate the second time derivatives to determine how we should apply control to the real system and to optimize our target functional.

If the functional $\tau(\rho, \vec{\varphi})$ is smooth in both the ρ and $\vec{\varphi}$ variables, it is reasonable to assume that if $\rho(t)$ changes smoothly, at least for small changes, then the optimal choice $\vec{\varphi}(t)$ should also change smoothly. That is, if $\vec{\varphi}(t)$ is optimal for $\rho(t)$, then at least for small times δt the optimal choice of parameters for $\rho(t + \delta t)$ should also only change by a small amount $\vec{\varphi}(t + \delta t) = \vec{\varphi}(t) + \delta\vec{\varphi}$.

In light of the previous observations, the problem of keeping track of the optimal parameters for a given evolution of the real system is simplified if we consider the following assumptions:

(i) At all times t, the choice of parameters $\vec{\varphi}(t)$ is optimal (or at leasts rests on a local maximum)

(ii) For smooth evolution of $\rho(t)$, the parameters $\vec{\varphi}(t)$ also evolve smoothly.

Assumption (i) assures that the derivatives of $\tau(\rho, \vec{\varphi})$ with respect to the parameter variables all vanish. Namely, the gradient is zero if the choice of variables is at a local maximum. That is,

$$\left.\frac{\partial\tau(\rho(t), \vec{\varphi})}{\partial\varphi_i}\right|_{\vec{\varphi}=\vec{\varphi}(t)} = 0, \tag{5.28}$$

which is useful in the following calculations. Assumption (ii), as the arguments above show, is not only reasonable, but also greatly simplifies the problem.

Considering these assumptions, we can attempt to calculate the derivatives that are required for our control scheme. The first time derivative of the functional in question is given by

$$\begin{aligned} \dot{\mathcal{F}} = \dot{\tau} &= \frac{\partial \tau}{\partial \rho}\dot{\rho} + \sum_i \underbrace{\frac{\partial \tau}{\partial \varphi_i}}_{=0} \dot{\varphi}_i \\ &= \frac{\partial \tau}{\partial \rho}\dot{\rho}, \end{aligned} \tag{5.29}$$

where $\dfrac{\partial \tau}{\partial \rho}\dot{\rho}$ is a short-hand notation for $\displaystyle\sum \frac{\partial \tau}{\partial R_\alpha}\dot{R}_\alpha$, and the R_α's are the expansion of the state ρ is some orthogonal basis, i.e. the generalized Bloch vector elements. Additionally, the derivatives of τ with respect to the parameter variables all vanish based on the assumption above. Although it appears from (5.29) that the first time derivative of τ is independent of $\dot{\vec{\varphi}}$, we can still use this expression to determine the optimal change in $\vec{\varphi}$.

To understand how the optimal choice of the parameters $\vec{\varphi}(t)$ evolves, we consider propagating τ an infinitessimally small step forward in time. Consider the Taylor expansion of τ around $t = 0$,

$$\begin{aligned} \tau(\delta t) &= \tau_0 + \delta t \ \dot{\tau}_0 \\ &= \tau_0 + \delta t \ \frac{\partial \tau}{\partial \rho}\dot{\rho}. \end{aligned} \tag{5.30}$$

To find the optimal choice of parameters $\vec{\varphi}$ at this new time, we can approximate the functional $\tau(\rho, \vec{\varphi})$ to second order in $\vec{\varphi}$. That is, we calculate the gradient $\vec{h}$ and the Hessian Ω as

$$h_i = \frac{\partial \tau(\delta t)}{\partial \varphi_i} \quad \text{and} \quad \Omega_{ij} = \frac{\partial^2 \tau(\delta t)}{\partial \varphi_i \partial \varphi_j}. \tag{5.31}$$

Assuming that, after a small change in the density matrix $\rho(\delta t) \approx \rho + \dot{\rho}\ \delta t$, the optimal choice of variables changes very little, $\vec{\varphi}(0)$ should be close to the maximum supplied by the new optimal choice $\vec{\varphi}(\delta t)$ and the curvature of $\tau(\rho + \dot{\rho}\ dt, \vec{\varphi})$ should be nonpositive in all directions of the parameter space. We then approximate the optimal choice of parameters $\vec{\varphi}(\delta t) = \vec{\varphi}(0) + \vec{\varphi}'$ by finding the solution to

$$\Omega \vec{\varphi}' = -\vec{h}. \tag{5.32}$$

This is exactly solvable as long as the Hessian Ω is invertible. The gradient of $\tau(\delta t)$ with respect to the parameters is

$$\begin{aligned} h_i &= \frac{\partial \tau(\delta t)}{\partial \varphi_i} \\ &= \underbrace{\frac{\partial \tau_0}{\partial \varphi_i}}_{=0} + \delta t \frac{\partial^2 \tau_0}{\partial \varphi_i \partial \rho} \dot{\rho}. \end{aligned} \tag{5.33}$$

So the elements of the gradient are $h_i = \delta t \cdot g_i$, with $g_i = \dfrac{\partial^2 \tau_0}{\partial \varphi_i \partial \rho} \dot{\rho}$.

The elements of the Hessian matrix of $\tau(\delta t)$ with respect to the parameters $\vec{\varphi}$ are given by

$$\Omega_{ij} = \frac{\partial^2 \tau_0}{\partial \varphi_i \partial \varphi_j}. \tag{5.34}$$

Incidentally, Ω is also the Hessian of the functional $\tau(\rho, \vec{\varphi})$ at time $t = 0$ with respect to the parameter variables.

The optimal choice of parameters at time δt can be approximated by $\vec{\varphi}(\delta t) = \vec{\varphi}(0) + \delta \vec{\varphi}$, where $\delta \vec{\varphi}$ is acquired by solving the linear equation $\Omega \delta \vec{\varphi} = -\vec{g}\ \delta t$, or equivalently

$$\Omega \dot{\vec{\varphi}} = -\vec{g}, \tag{5.35}$$

where $\vec{\varphi}(\delta t) = \vec{\varphi}(0) + \dot{\vec{\varphi}}\ \delta t$.

With the calculations outlined above, we can now determine how the optimal choice of parameters evolves for small time intervals by solving the differential equation (5.35). This method now allows us to calculate the time derivatives of the non-analytic functions in which we are interested.

5.2.2 Calculating control of optimization functionals

To determine what control field should be applied to the system, the time derivative $\ddot{\tau}$ must be calculated given the dynamics of the state $\rho(t)$. Assuming that the optimal choice of parameters $\vec{\varphi}(t)$ changes smoothly in time, the second time derivative of $\tau(\rho(t), \vec{\varphi}(t))$ is

$$\begin{aligned} \ddot{\tau} &= \frac{d}{dt}\left(\frac{\partial \tau}{\partial \rho} \dot{\rho} + \sum_i \frac{\partial \tau}{\partial \varphi_i} \dot{\varphi}_i \right) \\ &= \frac{\partial^2 \tau}{\partial^2 \rho} \dot{\rho}^2 + \frac{\partial \tau}{\partial \rho} \ddot{\rho} + 2 \sum_i \underbrace{\frac{\partial^2 \tau}{\partial \varphi_i \partial \rho}}_{g_i} \dot{\rho}\, \dot{\varphi}_i + \sum_{ij} \underbrace{\frac{\partial^2 \tau}{\partial \varphi_i \partial \varphi_j}}_{\Omega_{ij}} \dot{\varphi}_i \dot{\varphi}_j + \sum_i \underbrace{\frac{\partial \tau}{\partial \varphi_i}}_{=0} \ddot{\varphi}_i \\ &= \frac{\partial^2 \tau}{\partial^2 \rho} \dot{\rho}^2 + \frac{\partial \tau}{\partial \rho} \ddot{\rho} + 2 \dot{\vec{\varphi}}^\top \vec{g} + \dot{\vec{\varphi}}^\top \Omega \dot{\vec{\varphi}}. \end{aligned} \tag{5.36}$$

With (5.35), we simplify this to

$$\ddot{\tau} = \frac{\partial^2 \tau}{\partial^2 \rho}\dot{\rho}^2 + \frac{\partial \tau}{\partial \rho}\ddot{\rho} + \dot{\vec{\varphi}}^\top \vec{g}. \tag{5.37}$$

Thus, for a given dynamics of $\rho(t)$, we can calculate how the optimal choice of parameters $\vec{\varphi}$ evolves by solving for $\dot{\vec{\varphi}}$ in (5.35) and use (5.37) to determine $\ddot{\tau}$.

Up to this point, we have assumed that the dynamics of $\rho(t)$ are already known. However, our goal is to determine the optimal control H_c on the real system, so the dynamics are not yet known. To find the optimal real control that should be applied, we exploit the linear dependence of $\ddot{\mathcal{F}}$ on the control H_c that was pointed out in section 5.1.1. As long as the target functional is LU-invariant, the second time derivative of the functional is linear with respect to the local control.

Since we are able to calculate $\ddot{\tau}$ if the dynamics of the system $\dot{\rho}$ are specified, we can make use of (5.16) in Section 5.1.1 to calculate the optimal amplitude k_λ of the corresponding part of the control Hamiltonian σ_λ. That is, for each σ_λ, we need to calculate

$$\ddot{\tau}_{\lambda,s} = \ddot{\tau}|_{\dot{\rho}=-i[H_\mathrm{s}+\sigma_\lambda,\rho]+\mathcal{D}(\rho)}\,, \tag{5.38}$$

as already shown in (5.17). To determine the optimal control, we first calculate the second time derivative of the functional when no external control is applied,

$$\ddot{\tau}_s = \ddot{\tau}|_{\dot{\rho}=-i[H_\mathrm{s},\rho]+\mathcal{D}(\rho)}\,, \tag{5.39}$$

and again with control σ_λ to determine $\ddot{\tau}_{\lambda,s}$.

Just as in the Lyapunov control scheme, we set the real optimal control vector $\vec{k}$ to be parallel to $\vec{Y}$, whose elements are given by

$$Y_\lambda = \ddot{\tau}_{\lambda,s} - \ddot{\tau}_s. \tag{5.40}$$

This maximizes the second time derivative of the functional at all times, yielding the greatest increase over time.

5.3 Parameterizing the fictitious system

Although our control scheme is based on the determination of the optimal control that should be applied to the real system, we must also consider how to optimally address the dynamics of the parameters $\vec{\varphi}$ as the state of the system changes. This is what we call *fictitious* control. For this purpose, we need in particular to ensure that we are efficiently parameterizing our fictitious system. If there are directions in the parameter space along which the functional does not change, the Hessian will have a zero eigenvector associated with these directions and will no longer be

invertible. This leads to problems in trying to solve the linear equation in (5.32). Therefore, it is advantageous to determine a parameterization with the minimal number of necessary variables.

Here, we recall a few of the entanglement quantification schemes introduced in Chapter 3. These are the quantities that we will use as target functionals in the next section. We also outline ideal ways of parameterizing the space of variables needed to evaluate each function.

5.3.1 Parameterizing orbits for maximal overlap

Recall that the maximum overlap functional of a state with a given target state $|\psi\rangle$ is given as

$$\tau_\psi(\rho) = \max_{U \in \mathcal{U}_{\text{loc}}} \text{Tr}(\rho U P_\psi U^\dagger), \tag{5.41}$$

where $P_\psi = |\psi\rangle\langle\psi|$ is the projection operator on to the target state. To fully maximize this functional, an optimization must be performed over the space of all local unitaries. Because a state $|\phi\rangle$ is locally equivalent to $|\psi\rangle$ if and only if there is a local unitary U such that $|\phi\rangle = U|\psi\rangle$, the optimization is equivalent to maximizing over all states that are locally equivalent to $|\psi\rangle$. The set of all such states is called the *orbit* of $|\psi\rangle$ under local unitaries, which we denote by $\mathcal{O}(\psi)$ [90]. Surprisingly, the number of parameters needed to describe an arbitrary local unitary is not the same as the number needed to characterize the orbit of $|\psi\rangle$ for most states. To reduce the number of parameters, we can determine ideal ways to parameterize these orbits. Determining the minimum number of necessary parameters is equivalent to calculating the dimension of its orbit [88]. Methods to understand aspects of the local unitary orbits and their dimensions have already been developed [89–91].

First, we consider the space of all possible local unitaries on a system of N qubits. An arbitrary local unitary is a tensor product of N unitaries acting on each subsystem, i.e.

$$U = U_1 \otimes \cdots \otimes U_N. \tag{5.42}$$

An arbitrary unitary operation on a two-dimensional system requires four parameters to fully describe it. The standard parameterization of these unitaries is

$$U_j'(\theta, \phi, \varphi, \xi) = e^{i\xi} \begin{pmatrix} \cos\theta e^{i\phi} & \sin\theta e^{i\varphi} \\ -\sin\theta e^{-i\varphi} & \cos\theta e^{-i\phi} \end{pmatrix}.$$

At least one of these parameters is redundant since the target functional is invariant under any changes of global phase. Eliminating this extra phase parameter, we are left with

$$U_j(\theta, \phi, \varphi) = \begin{pmatrix} \cos\theta e^{i\phi} & \sin\theta e^{i\varphi} \\ -\sin\theta e^{-i\varphi} & \cos\theta e^{-i\phi} \end{pmatrix} \tag{5.43}$$

to parameterize an arbitrary unitary matrix on each individual subsystem. However, it is also possible to generate an arbitrary unitary on a two dimensional system by taking a general Hamiltonian as a linear combination of Pauli matrices

$$H = h_x\sigma_x + h_y\sigma_y + h_z\sigma_z. \tag{5.44}$$

The corresponding unitary operation is

$$U = e^{iH}. \tag{5.45}$$

Expanding this to arbitrary unitaries on an N-qubit system, we can parameterize all local Hamiltonians as

$$H = \sum_{n=1}^{N} \sum_{\xi_n=x,y,z} h_{\xi_n}^{(n)} \sigma_{\xi_n}^{(n)}, \tag{5.46}$$

where $\sigma_{\xi_n}^{(n)} = \mathbb{1} \otimes \cdots \otimes \sigma_{\xi_n} \otimes \cdots \otimes \mathbb{1}$ is the Pauli operator σ_{ξ_n} acting on the n^{th} qubit of the system. The $3N$ real numbers $h_{\xi_n}^{(n)}$ parameterize the set of all local unitaries[2], since any local unitary (up to a global phase) can be given by $U = e^{iH}$.

To determine the dimension of the orbit of a particular state $|\psi\rangle$, we can determine the dimension of the space of local unitaries that leave the state unchanged [88],

$$U|\psi\rangle = |\psi\rangle. \tag{5.47}$$

If the dimension of this subspace is m, then the dimension of $\mathcal{O}(\psi)$ is $3N-m$, since $3N$ is the number of parameters needed to describe an arbitrary local unitary. It has been shown [88] that finding m is equivalent to determining the number of linearly independent local Hamiltonians whose nullspace contains the state $|\psi\rangle$. That is, we need to determine which local Hamiltonians have the state $|\psi\rangle$ as an eigenvector with an eigenvalue of zero, i.e.

$$H|\psi\rangle = 0. \tag{5.48}$$

In the following sections, we determine which parameters are unecessary by solving (5.48) for particular states $|\psi\rangle$ of interest.

LU-orbit of two-qubit entangled states

As seen in Chapter 2, all maximally two-qubit entangled states $|\phi\rangle = U_1 \otimes U_2|\psi^-\rangle$ are locally equivalent to the singlet state

$$|\psi^-\rangle = \frac{|01\rangle - |10\rangle}{\sqrt{2}}. \tag{5.49}$$

[2]More formally [88], this is given by the statement that the Lie algebra of the of the group of local unitaries is generated by the local Pauli operators $\sigma_{\xi}^{(n)}$.

To determine how many parameters are unnecessary in the description of this orbit, we need to find the local unitaries that leave the state $|\psi^-\rangle$ unchanged up to a global phase factor. Consider an arbitrary local Hamiltonian

$$H_{\text{loc}} = \sum_{\xi} h_{\xi}^{(1)} \sigma_{\xi} \otimes \mathbb{1} + \sum_{\xi} h_{\xi}^{(2)} \mathbb{1} \otimes \sigma_{\xi}. \tag{5.50}$$

Since all local unitaries can be described as e^{iH}, where H is any arbitrary Hamiltonian, determining which unitaries leave the state $|\psi^-\rangle$ unchanged is equivalent to determining which Hamiltonians H_{loc} have $|\psi^-\rangle$ as an eigenvector.

Applying an arbitrary local Hamiltonian to $|\psi^-\rangle$ yields

$$\begin{aligned} H_{\text{loc}}|\psi^-\rangle =& \frac{1}{\sqrt{2}}\Big[\big(\sum_{\xi} h_{\xi}^{(1)} \sigma_{\xi} \otimes \mathbb{1}\big) + \big(\sum_{\xi} h_{\xi}^{(2)} \mathbb{1} \otimes \sigma_{\xi}\big)\Big](|01\rangle - |10\rangle) \\ =& \frac{1}{\sqrt{2}}\Big[(h_x^{(1)} - h_x^{(2)})(|00\rangle - |11\rangle) + i(h_y^{(1)} - h_y^{(2)})(|00\rangle + |11\rangle) \\ & + (h_z^{(1)} - h_z^{(2)})(|10\rangle + |10\rangle)\Big], \end{aligned} \tag{5.51}$$

which is a superposition of all of the other Bell states introduced in eq. (3.56). The Bell states are mutually orthogonal. Therefore, $|\psi^-\rangle$ can only be an eigenvector of H_{loc} if all scalar factors $h_{\xi}^{(1)} - h_{\xi}^{(2)}$ vanish. This expression vanishes if and only if

$$h_{\xi}^{(1)} = h_{\xi}^{(2)} \tag{5.52}$$

for all $\xi = x, y, z$. This implies that we only need three parameters to fully parameterize the orbit of maximally entangled two-qubit states. Indeed, for an arbitrary $|\phi\rangle = U_1 \otimes U_2|\psi^-\rangle$, we can parameterize it up to global phase as

$$|\phi\rangle = U \otimes \mathbb{1}|\psi^-\rangle, \tag{5.53}$$

with the local unitary U parameterized in the standard method presented by (5.43).

Alternatively, this can be shown by noting that the singlet state is invariant under transformations of the form $V \otimes V$, i.e. it is a Werner state [31]. We can rewrite any state that is locally equivalent to the singlet, $|\phi\rangle = U \otimes V|\psi^-\rangle$, as

$$\begin{aligned} |\phi\rangle &= (UV^\dagger \otimes \mathbb{1})(V \otimes V)|\psi^-\rangle \\ &= (UV^\dagger \otimes \mathbb{1})|\psi^-\rangle = (U' \otimes \mathbb{1})|\psi^-\rangle, \end{aligned} \tag{5.54}$$

where $U' = UV^\dagger$ is another unitary.

LU-Orbit of the GHZ states

Before we determine how to parameterize the orbit of GHZ states, we introduce some useful notation. For a system of N-qubits, the composite Hilbert space is spanned by 2^N orthonormal vectors. For each integer $p \in \{0, \ldots, 2^N - 1\}$, we define the state $|p\rangle$ as the binary representation of p with N bits, for example

$$\begin{aligned} |0\rangle &:= |0 \cdots 00\rangle \\ |1\rangle &:= |0 \cdots 01\rangle \\ &\vdots \\ |2^N - 1\rangle &:= |1 \cdots 11\rangle. \end{aligned} \tag{5.55}$$

Additionally, we can define $|\bar{p}\rangle$ as $|2^N - p - 1\rangle$, i.e. the state where all of the bits of $|p\rangle$ are swapped $0 \leftrightarrow 1$. This notation greatly simplifies some of the following tasks.

For a system of N qubits, the generalized GHZ state can be written as

$$\begin{aligned} |\mathrm{GHZ}\rangle &= \tfrac{1}{\sqrt{2}} \left(|0 \cdots 0\rangle + |1 \cdots 1\rangle \right) \\ &= \tfrac{1}{\sqrt{2}} \left(|0\rangle + |\bar{0}\rangle \right) \end{aligned} \tag{5.56}$$

using the shorthand notation. We can determine the number of unnecessary parameters by finding the local Hamiltonians H_{loc} that have $|\mathrm{GHZ}\rangle$ as an eigenvector. Consider the following relations:

$$\begin{aligned} \sigma_x^{(n)}|0\rangle &= |2^{n-1}\rangle & \sigma_x^{(n)}|\bar{0}\rangle &= |\overline{2^{n-1}}\rangle \\ \sigma_y^{(n)}|0\rangle &= i|2^{n-1}\rangle & \sigma_y^{(n)}|\bar{0}\rangle &= -i|\overline{2^{n-1}}\rangle \\ \sigma_z^{(n)}|0\rangle &= |0\rangle & \sigma_z^{(n)}|\bar{0}\rangle &= -|\bar{0}\rangle. \end{aligned} \tag{5.57}$$

Note that the $\sigma_x^{(n)}$ and $\sigma_y^{(n)}$ parts of the local Hamiltonian map $|\mathrm{GHZ}\rangle$ to a vector that is orthogonal to it. Additionally, each $\sigma_x^{(n)}$ and $\sigma_y^{(n)}$ map $|\mathrm{GHZ}\rangle$ to vectors that are mutually orthogonal to each other. That is,

$$\begin{aligned} \langle \mathrm{GHZ}|\sigma_x^{(n)}\sigma_x^{(m)}|\mathrm{GHZ}\rangle = \langle \mathrm{GHZ}|\sigma_y^{(n)}\sigma_y^{(m)}|\mathrm{GHZ}\rangle = \delta_{mn} \\ \text{and} \qquad \langle \mathrm{GHZ}|\sigma_x^{(n)}\sigma_y^{(m)}|\mathrm{GHZ}\rangle = 0. \end{aligned} \tag{5.58}$$

Thus, $|\mathrm{GHZ}\rangle$ can only be an eigenvector of H_{loc} if $h_x^{(n)} = h_y^{(n)} = 0$ for all n.

Considering only the $\sigma_z^{(n)}$ parts of the local Hamiltonian, we are left with

$$\sum_{n=1}^{N} h_z^{(n)} \sigma_z^{(n)} \left(|0\rangle + |\bar{0}\rangle \right) = \sum_{n=1}^{N} h_z^{(n)} \left(|0\rangle - |\bar{0}\rangle \right), \tag{5.59}$$

which is also orthogonal to the initial state. Therefore, $|GHZ\rangle$ is an eigenvector of H_{loc}, if and only if this expression vanishes, which occurs when $\sum_n h_z^{(n)} = 0$. The subspace defined by the solutions to

$$h_x^{(n)} = h_y^{(n)} = 0 \quad \forall n \qquad \text{and} \qquad \sum_{n=1}^{N} h_z^{(n)} = 0 \tag{5.60}$$

has dimension $N-1$. Therefore, the orbit of GHZ states has dimension $3N - (N-1) = 2N+1$, meaning that $2N+1$ parameters are required to describe an arbitrary locally equivalent GHZ state.

Subsequently (see Appendix A), it can be shown that any arbitrary state in this orbit can be parameterized by

$$V_1 \otimes U_2 \otimes \cdots \otimes U_N |GHZ\rangle, \tag{5.61}$$

where V_1 requires three parameters and each U_j with $j \geq 2$ requires only two parameters, i.e.

$$V_1 = \begin{pmatrix} \cos\theta_1 e^{i\phi_1} & \sin\theta_1 e^{i\varphi_1} \\ -\sin\theta_1 e^{-i\varphi_1} & \cos\theta_1 e^{-i\phi_1} \end{pmatrix}, \quad U_j = \begin{pmatrix} \cos\theta_j & \sin\theta_j e^{i\varphi_j} \\ -\sin\theta_j e^{-i\varphi_j} & \cos\theta_j \end{pmatrix}. \tag{5.62}$$

W-states of 3-qubits

Using the same methods, we can also determine the dimension of the orbit of a W state in a system of N qubits. With the notation introduced earlier, the generalized W state $|\mathrm{W}\rangle$ can be written as

$$\begin{aligned} |\mathrm{W}\rangle &= \frac{1}{\sqrt{N}} \left(|0\cdots01\rangle + |0\cdots10\rangle + \cdots + |10\cdots0\rangle \right) \\ &= \frac{1}{\sqrt{N}} \sum_{n=1}^{N} |2^{n-1}\rangle. \end{aligned} \tag{5.63}$$

We note the relations

$$\begin{aligned} \sigma_x^{(n)} |2^{m-1}\rangle &= \begin{cases} |0\rangle, & n = m \\ |2^{m-1} + 2^{n-1}\rangle, & n \neq m \end{cases} \\ \sigma_y^{(n)} |2^{m-1}\rangle &= \begin{cases} -i|0\rangle, & n = m \\ i|2^{m-1} + 2^{n-1}\rangle, & n \neq m \end{cases} \\ \sigma_z^{(n)} |2^{m-1}\rangle &= \begin{cases} -|2^{m-1}\rangle, & n = m \\ |2^{m-1}\rangle, & n \neq m. \end{cases} \end{aligned} \tag{5.64}$$

Similar to the GHZ case, the $\sigma_x^{(n)}$ and $\sigma_y^{(n)}$ parts of the local Hamiltonian map the W state to vectors that are orthogonal to the initial state. In particular, $|0\rangle$ is orthogonal to $|\mathrm{W}\rangle$, so $|\mathrm{W}\rangle$ can be an eigenvector of H_{loc} only if $\langle 0|H_{\mathrm{loc}}|\mathrm{W}\rangle = 0$, i.e

$$\sum_{n=1}^{N} h_x^{(n)} + i h_y^{(n)} = 0. \tag{5.65}$$

Similarly, $|2^{m-1} + 2^{n-1}\rangle$ is orthogonal to $|\mathrm{W}\rangle$ for all $n \neq m$, so $|\mathrm{W}\rangle$ can only be an eigenvector of H_{loc} if $\langle 2^{m-1} + 2^{n-1}|H_{\mathrm{loc}}|\mathrm{W}\rangle = 0$, i.e.

$$h_x^{(m)} + h_x^{(n)} + i(h_y^{(m)} + i h_y^{(n)}) = 0. \tag{5.66}$$

Since the coefficients $h_\xi^{(n)}$ must be real, equations (5.65) and (5.67) reduce to

$$h_x^{(n)} = 0 \qquad \text{and} \qquad h_y^{(n)} = 0 \qquad \text{for all } n \tag{5.67}$$

in systems of $n \geq 3$ qubits. To determine the parameters $h_z^{(n)}$, only the $\sigma_z^{(n)}$ terms must be considered. Now, applying the σ_z parts of H_{loc} to $|\mathrm{W}\rangle$ yields

$$\frac{1}{\sqrt{N}} \sum_{n=1}^{N} \sum_{m=1}^{N} h_z^{(n)} \sigma_z^{(n)} |2^{m-1}\rangle. \tag{5.68}$$

The result is a constant multiple of the initial vector $|\mathrm{W}\rangle$ if and only if $h_z^{(1)} = h_z^{(2)} = \cdots = h_z^{(N)}$. Thus, the space of solutions to the linear equations

$$h_x^{(n)} = h_y^{(n)} = 0 \quad \forall n \qquad \text{and} \qquad h_z^{(1)} = \cdots = h_z^{(N)} \tag{5.69}$$

is one dimensional. The orbit of W states has dimension $3N - 1$, which is the number of parameters needed to describe an arbitrary locally equivalent W state.

Subsequently (see Appendix A), it can be shown that any arbitrary state in this orbit can be parameterized by

$$V_1 \otimes \cdots \otimes V_{N-1} \otimes U_N |W\rangle, \tag{5.70}$$

where the V_j's require three parameters each and U_N requires only two parameters, just as in (5.62).

5.3.2 Parameterizing separable states

The canonical way to parameterize the orbit of separable states in a system of N qubits is

$$|\Psi\rangle = (\cos\theta_1|0\rangle + \sin\theta_1 e^{-i\phi_1}|1\rangle) \otimes \cdots \otimes (\cos\theta_N|0\rangle + \sin\theta_N e^{-i\phi_N}|1\rangle), \tag{5.71}$$

which requires the $2N$ variables $\{\theta_j, \phi_j\}$.

To evaluate τ_{gme}, we use the orthogonal parameterization of the fully separable pure states of $2N$ qubits, as introduced in Section 3.3.1. Each vector in this subset of fully separable pure states is given by

$$|\Phi\rangle = |\Psi\rangle \otimes |\Psi^{\perp}\rangle, \tag{5.72}$$

where $|\Psi\rangle$ is parameterized as above in (5.71), and each subsystem of $|\Psi^{\perp}\rangle$ is orthogonal to the corresponding subsytem in $|\Psi\rangle$. This requires the same number of variables to parameterize as the fully separable states of N qubits above.

Chapter 6

Application of optimal control

Equipped with the methods of determining optimal control sequences described in Chapter 5, we are now ready to implement this approach in composite quantum systems. We will target highly entangled states that maximize the functionals described in Chapter 3.

Before using these methods to determine optimal control, however, we will first demonstrate that the approach derived in Chapter 5 correctly determines the evolution of the optimal choice of parameters $\vec{\varphi}(t)$ for evaluating a particular functional, given the dynamics of the state $\rho(t)$. To establish this, we consider the simplest quantum system of a single qubit undergoing unitary evolution. A very simple functional is chosen as the figure of merit, which requires an optimization over a parameter space. We demonstrate that the value of the optimal parameters can be correctly determined as the state evolves over time. After this has been established, an example with a single qubit system is constructed where control can be applied to counteract decoherence from environmental effects. We demonstrate that our scheme accomplishes optimal control in driving the qubit into a state that minimizes these decoherence effects. Once it is determined that our "on-the-fly" methods successfully realize optimal control of simple systems systems and simultaneously determine the exact dynamics of the optimal parameters in the fictitious space, we move on to more complicated functionals in systems of more particles.

The effectiveness of our approach will be demonstrated in the case of multipartite systems, where we use the maximal overlap functionals τ_ψ and the gme-detection quantity τ_{gme} as target functionals. For the system Hamiltonians, only systems with dipole-dipole interactions given by Ising-type Hamiltonians of the form

$$H_{\text{sys}} = \sum_{\substack{i,j=1 \\ i<j}}^{N} J_{ij}\sigma_z^{(i)} \otimes \sigma_z^{(j)} \tag{6.1}$$

were considered, where the coupling constants J_{ij} are fixed [92]. These Hamiltonians can model systems of NV-centers in diamond [93], where the coupling constants are determined by the fixed distances between the respective points. Application of local control on systems of NV-centers can be achieved with shaped laser pulses on the individual spins [94]. Using these types of interactions, we will show how optimal local control can be determined to maximize entanglement measures.

We will first show how our local control scheme can be applied to generate highly entangled states by optimally exploiting existing interactions within a system. Then we demonstrate how we can determine states that are most robust against decoherence effects.

6.1 Single qubit case

To demonstrate the effectiveness of the methods in Chapter 5, we first consider the simplest quantum system, that of a single qubit. We choose an uncomplicated functional τ on the space of states that requires an optimization over a small number of parameters, and show that we can keep track of the parameters that maximize $\tau(\rho)$ as ρ changes. Once we understand the evolution of the parameters in the case when the dynamics of ρ are coherent, we consider incoherent dynamics that must be controlled. Different states of a qubit are not equally affected by environmental effects. However, coherent control can be applied to the qubit that drives the system into states that are least affected by incoherent effects. This is the simplest application of our control scheme that must first be understood before moving on to more complicated systems and target functionals.

The target functional that we consider in this case is the "maximal overlap" of the state ρ with any pure state,

$$\tau(\rho) = \max_{|\phi\rangle} \langle\phi|\rho|\phi\rangle. \tag{6.2}$$

This system consists of only one particle, and any pure state can be reached by any other pure state with a unitary operator, so the pure states are all locally equivalent in this sense. The value of $\tau(\rho)$ is equivalent to the maximum eigenvalue of ρ, which can be obtained analytically from the matrix ρ. For our purposes, we must demonstrate that the methods outlined in Chapter 5 can keep track of the parameters that maximize certain functions. We chose τ in eq. (6.2) as a test object precisely because we know its maximum value at all times, yet it can still be evaluated through an optimization. Two independent parameters $\vec{\varphi} = (\varphi_1, \varphi_2)$ are needed to evaluate τ, and its optimization takes the form

$$\tau(\rho) = \max_{\vec{\varphi}} \langle\phi_{\vec{\varphi}}|\rho|\phi_{\vec{\varphi}}\rangle, \tag{6.3}$$

where $|\phi_{\vec{\varphi}}\rangle = \cos\varphi_1|0\rangle + e^{i\varphi_2}\sin\varphi_1|1\rangle$. For example, if the state ρ is the pure state $|\psi\rangle\langle\psi|$, where $|\psi\rangle = \frac{|0\rangle+|1\rangle}{\sqrt{2}}$, then the obvious choice of parameters that maximize τ are $\vec{\varphi} = (\frac{\pi}{4}, 0)$ such that $|\phi_{\vec{\varphi}}\rangle = |\psi\rangle$. As the state ρ evolves, the choice of optimal parameters $\vec{\varphi}$ will also change.

We first show how to keep track of $\vec{\varphi}(t)$ as $\rho(t)$ evolves under purely coherent dynamics, then show how optimal control can be applied when incoherent dynamics are considered.

6.1.1 Purely coherent dynamics

Suppose we have a given initial state ρ_0 of a system whose dynamics are completely determined, and we want to describe the dynamics of the functional $\tau(\rho(t))$. In this case, the functional is not a straightforward function of ρ, and full evaluation of τ at any given time t requires an optimization. Instead, we can use the methods presented in Chapter 5 to determine how the parameters $\vec{\varphi}$ evolve, such that the value of the functional is given by $\tau(\rho(t), \vec{\varphi}(t))$.

We first consider purely coherent dynamics of a single qubit, with a Hamiltonian $H_\mathrm{s} = a\sigma_x + b\sigma_y + c\sigma_z$, such that the dynamics of the system are governed by

$$\dot{\rho}(t) = -i[H_\mathrm{s}, \rho(t)]. \tag{6.4}$$

In this case, the evolution of the state is completely determined by the unitary operator $U(t) = e^{-iH_\mathrm{s}t}$, such that $\rho(t) = U(t)\rho_0 U^\dagger(t)$. For a given initial state, the state $\rho(t)$ and the dynamics $\dot{\rho}(t)$ are known for all times. A maximization can be performed to determine the optimal choice of parameters $\vec{\varphi}(0)$ to evaluate the functional of the initial state $\tau(\rho(0))$. In the single qubit case, this can be determined analytically.

Using the parametrization $|\phi_{\vec{\varphi}}\rangle = \cos\varphi_1|0\rangle + e^{i\varphi_2}\sin\varphi_1|1\rangle$ for the space of all possible pure states, the un-optimized functional of the state ρ with parameters $\vec{\varphi}$ is given by

$$\tau(\rho, \vec{\varphi}) = \cos^2\varphi_1\langle 0|\rho|0\rangle + \sin^2\varphi_1\langle 1|\rho|1\rangle + \cos\varphi_1\sin\varphi_1\left(e^{i\varphi_2}\langle 0|\rho|1\rangle + e^{-i\varphi_2}\langle 1|\rho|0\rangle\right). \tag{6.5}$$

To aid our calculations, we make use of the Bloch vector representation $\vec{R}$ for the state of a single qubit,

$$\rho = \frac{1}{2}\left(\mathbb{1} + R_1\sigma_x + R_2\sigma_y + R_3\sigma_z\right). \tag{6.6}$$

Inserting this into (6.5) yields

$$\tau(\rho, \vec{\varphi}) = \frac{1}{2}\left(1 + \cos\varphi_2\sin 2\varphi_1 R_1 + \sin 2\varphi_1\sin 2\varphi_2 R_2 + \cos 2\varphi_1 R_3\right). \tag{6.7}$$

To calculate the evolution of the parameters $\dot{\vec{\varphi}}$, we need the Hessian of the functional with respect to $\vec{\varphi}$ and the gradient $\vec{g}$, whose elements are given by

$$\Omega_{ij} = \frac{\partial^2 \tau}{\partial\varphi_i \partial\varphi_j} \qquad \text{and} \qquad g_i = \frac{\partial}{\partial\varphi_i}\langle\phi_{\vec{\varphi}}|\dot{\rho}|\phi_{\vec{\varphi}}\rangle. \tag{6.8}$$

According to our analysis in 5.2.1, the dynamics for the parameters $\vec{\varphi}$ are given by

$$\dot{\vec{\varphi}} = -\Omega^{-1}\vec{g}. \tag{6.9}$$

The dynamics of $\vec{\varphi}$ can be determined numerically. Explicitly, the elements of Ω are

$$\begin{aligned}
\Omega_{11} &= -2\left[\cos(\varphi_2)\sin(2\varphi_1)R_1 + \sin(2\varphi_1)\sin(\varphi_2)R_2 + \cos(2\varphi_1)R_3\right] \\
\Omega_{22} &= -\frac{1}{2}\sin(2\varphi_1)\left[\cos(\varphi_2)R_1 + \sin(\varphi_2)R_2\right] \\
\Omega_{12} = \Omega_{21} &= -\cos(2\varphi_1)\left[\sin(\varphi_2)R_1 - \cos(\varphi_2)R_2\right]
\end{aligned} \tag{6.10}$$

and the elements of $\vec{g}$ are

$$g_1 = \cos(2\varphi_1)\cos(\varphi_2)\dot{R}_1 + \cos(2\varphi_1)\cos(\varphi_2)\dot{R}_2 - \sin(2\varphi_1)\dot{R}_3 \tag{6.11}$$

$$g_2 = -\frac{1}{2}\sin(2\varphi_1)\left[\sin(\varphi_2)\dot{R}_1 - \cos(\varphi_2)\dot{R}_2\right]. \tag{6.12}$$

As a 2×2-matrix, Ω is invertible using formula

$$\left(\begin{smallmatrix} a & b \\ c & d \end{smallmatrix}\right)^{-1} = \tfrac{1}{ad-bc}\left(\begin{smallmatrix} d & -b \\ -c & a \end{smallmatrix}\right). \tag{6.13}$$

Since $\dot{\rho}(t)$ is known, we can solve the differential equations to determine $\rho(t)$ and $\dot{\rho}(t)$ for all times, which allows us to calculate Ω^{-1} and $\vec{g}$. Equation (6.9) is now a differential equation which we can solve numerically to determine the optimal parameters $\vec{\varphi}(t)$ for calculating the functional at all times.

We can now consider an example with a specific initial state ρ_0 and Hamiltonian H_s and determine how well our method for keeping track of $\vec{\varphi}$ works. The maximum eigenvalue of a pure state always has a value of 1. If we choose an initial pure state undergoing coherent dynamics, then the state of the system will stay pure. That is, our results should yield $\tau(\rho(t)) = 1$ for all t.

Consider a qubit in the initial state $\rho_0 = |\psi\rangle\langle\psi|$ with $|\psi\rangle = \frac{|0\rangle+|1\rangle}{\sqrt{2}}$ and system dynamics governed by the Hamiltonian $H_\mathrm{s} = \sigma_z + \frac{1}{2}\sigma_x$. Since the initial state is

$$\rho_0 = \frac{1}{2}\left(|0\rangle + |1\rangle\right)\left(\langle 0| + \langle 1|\right) = \frac{1}{2}\left(\mathbb{1} + \sigma_x\right), \tag{6.14}$$

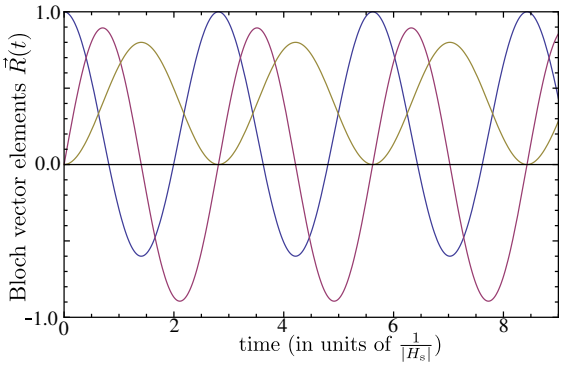

(a) Dynamics of the Bloch vector elements $\vec{R}(t)$.

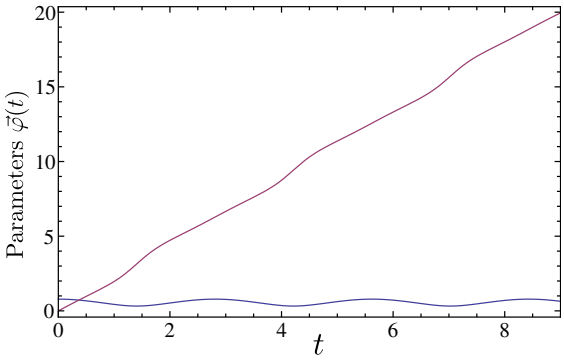

(b) Evolution of optimal parameters $\vec{\varphi}(t)$.

Figure 6.1: Coherent dynamics of a single qubit with $H_s = \sigma_z + \frac{1}{2}\sigma_x$, with initial state $\rho_0 = \frac{1}{2}(\mathbb{1} + \sigma_z)$. The actual value of the functional is constant, $\tau(\rho(t), \vec{\varphi}(t)) = 1$.

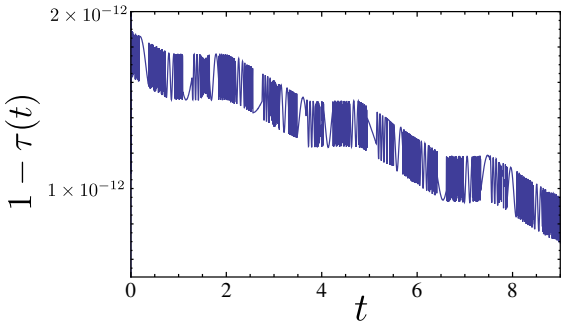

Figure 6.2: Value of $\tau(\rho(t), \vec{\varphi}(t))$ with ρ and $\vec{\varphi}$ determined by numerically solving differential equations and plotted in 6.1. Plot shows $1 - \tau \approx 10^{-12}$, so τ is always close to 1, which is the actual value of optimization. Thus, $\vec{\varphi}(t)$ is always optimal.

the Bloch vector at time $t = 0$ is given by $\vec{R}(0) = (1, 0, 0)$. The subsequent dynamics of the elements of $\vec{R}(t)$ are shown in Figure 6.1a. The initial optimal choice for the parameters is $\vec{\varphi}(0) = (\frac{\pi}{4}, 0)$, since this yields $\tau(\rho_0, \vec{\varphi}(0)) = 1$. Solving the differential equation in (6.9) gives a choice of parameters $\vec{\varphi}(t)$ for all times t. This solution is plotted in Figure 6.1b. To show that choice of parameters $\vec{\varphi}(t)$ are always optimal, we plot the deviation of $\tau(\rho(t), \vec{\varphi}(t))$ from unity in Fig. 6.2, which never drifts farther than 10^{-11} away from 1. This confirms that we can successfully keep track of the evolution of the optimal parameters without continuously needing performing optimizations to evaluate our target functionals.

6.1.2 Dephasing dynamics

Now that we have seen that this method successfully determines the evolution of the optimal parameters as the state of the system evolves in a simple case, we will now implement our control method to determine optimal control of a single qubit that undergoes dephasing. The uncontrolled dynamics of the system are now governed by the master equation that corresponds to the dephasing channel,

$$\dot{\rho} = \gamma(\sigma_z \rho \sigma_z - \rho), \tag{6.15}$$

where the constant γ describes the rate of dephasing. As in the previous section, the target functional is the maximal overlap with a pure state,

$$\tau(\rho) = \max_{|\phi\rangle} \langle\phi|\rho|\phi\rangle. \tag{6.16}$$

The three tunable parameters in the control are the amplitudes $k_{x,y,z}$ corresponding to the externally applied fields that govern the dynamics through a hamiltonian of the form

$$H_\mathrm{c} = k_x \sigma_x + k_y \sigma_y + k_z \sigma_z. \tag{6.17}$$

The full dynamics of the system at time t are given by

$$\dot{\rho} = -i[H_\mathrm{c}, \rho(t)] + \gamma(\sigma_z \rho(t) \sigma_z - \rho(t)). \tag{6.18}$$

The only pure states that are unaffected by the dynamics-induced dephasing channel in (6.15) are the eigenstates σ_z, i.e. $|0\rangle$ and $|1\rangle$. Thus, the only states that will remain unaffected are mixtures of the form $\alpha|0\rangle\langle 0| + (1-\alpha)|1\rangle\langle 1|$. Since the dephasing channel can only cause a decrease in the maximum eigenvalue of $\rho(t)$, the control that is calculated should drive the input state such that it is as close as possible to either $|0\rangle\langle 0|$ or $|1\rangle\langle 1|$.

In this simple example, we choose $\frac{|0\rangle+2|1\rangle}{\sqrt{5}}$ as our initial state, and the dynamics are determined by equation 6.18. Control is calculated using the scheme outlined in Chapter 5. We choose different maximum amplitudes for the control Hamiltonian in (6.17), and the dynamics of the functional are shown in Fig. 6.3. The uncontrolled dynamics are also shown, where the final state is $\frac{1}{2}\left(\mathbb{1} + \frac{3}{5}\sigma_x\right)$.

The control that is determined by our scheme in this case applies a strong σ_y-pulse, which pushes the system into a state close to $|1\rangle$. Once this is achieved, no more control is needed since the state of the qubit no longer changes under the dephasing channel.

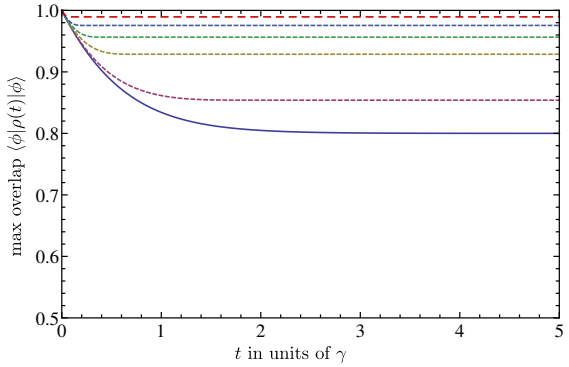

Figure 6.3: Maximum eigenvalue of dephasing qubit, with and without control. Control strengths $|H_c|$ are 0, 0.1γ, 0.5γ, γ, 2γ and 5γ. For uncontrolled dynamics (blue), dephasing leads to a final value of $\tau = \frac{4}{5}$. When strong control is used ($|H_c| = 5\gamma$, red dashed), the final state is reached after time $t = 0.1$ and the final value of τ is 0.94.

6.2 Controlling entanglement dynamics in two qubits

The previous example shows that our technique for determining optimal control indeed works for the most basic systems and target functionals that require an optimization over a real parameter space. Now we can move on to more complex systems of many qubits and use more complex target functionals in our optimal control methods.

To do so, we consider a system of two qubits, where we use τ_{gme} introduced in 3.2.5 as the target functional. The set of fully separable vectors that we use for optimizing τ_{gme} can be parametrized as

$$|\Phi\rangle = |\phi_1\phi_2\phi_1^\perp\phi_2^\perp\rangle \tag{6.19}$$

where $|\phi_1\rangle$, $|\phi_2\rangle$, $|\phi_1^\perp\rangle$ and $|\phi_2^\perp\rangle$ are parametrized by the four real parameters $\vec{\varphi} = \{\varphi_1, \varphi_2, \varphi_3, \varphi_4\}$, with

$$\begin{aligned} |\phi_1\rangle &= \cos(\varphi_1)|0\rangle + e^{i\varphi_2}\sin(\varphi_1)|1\rangle \qquad & |\phi_1^\perp\rangle &= -e^{-i\varphi_2}\sin(\varphi_1)|0\rangle + \cos(\varphi_1)|1\rangle \\ |\phi_2\rangle &= \cos(\varphi_3)|0\rangle + e^{i\varphi_4}\sin(\varphi_3)|1\rangle \qquad & |\phi_2^\perp\rangle &= -e^{-i\varphi_4}\sin(\varphi_3)|0\rangle + \cos(\varphi_3)|1\rangle. \end{aligned} \tag{6.20}$$

The functional τ_{gme} takes the form

$$\tau_{gme}(\rho, |\phi_1\phi_2\phi_1^\perp\phi_2^\perp\rangle) = \left|\langle\phi_1\phi_2|\rho|\phi_1^\perp\phi_2^\perp\rangle\right| - \sqrt{\langle\phi_1\phi_2^\perp|\rho|\phi_1\phi_2^\perp\rangle\langle\phi_1^\perp\phi_2|\rho|\phi_1^\perp\phi_2\rangle}. \tag{6.21}$$

Once the system Hamiltonian is given, optimal control is determined by the method outlined in Chapter 5.

In an examplary case, we use the interaction Hamiltonian $H_\mathrm{s} = J\sigma_z \otimes \sigma_z$ to produce the drift dynamics. To demonstrate the effectiveness of our control scheme, we use a fully separable initial state and derive control fields that take advantage of the existing interactions of the system to create a maximally entangled state. There are exceptional states for which the scheme does not work, however, since some would be unaffected by the dynamics. For example, the initial state $|0\rangle^{\otimes 2}$ is unaffected by H_s, and it rests on a saddle point with respect to the control, i.e.

$$\frac{\partial \ddot{\tau}}{\partial k_\lambda} = 0. \tag{6.22}$$

In this case, no control would be applied and the initial state would remain separable. If the initial state $|\psi_i\rangle$ were $\frac{|00\rangle+|11\rangle}{\sqrt{2}}$, however, the state would already be maximally influenced by the interaction hamiltonian, so no optimal control is needed. Thus, we chose the initial state

$$|\psi_i\rangle = \left(\frac{|0\rangle + 2|1\rangle}{\sqrt{5}}\right)^{\otimes 2} \tag{6.23}$$

to avoid these effects.

To demonstrate the effects of the interaction Hamiltonian on the initial state, we first allowed the state to evolve without external control. The resulting entanglement dynamics are shown in Figure 6.4. For the uncontrolled dynamics, τ_{gme} starts at zero since the initial state is separable. The interaction then induces a sinusoidal oscillation between different states, but a maximally entangled state is never reached.

We can produce highly entangled states by optimizing the dynamics, i.e. by applying our control scheme which maximizes the curvature of τ_{gme} through continuous application of the optimal local control Hamiltonians. Here, the maximum amplitude of the applied control was limited to five times the interaction strength of the system, i.e. $k_\mathrm{max} = 5|H_\mathrm{sys}|$. The entanglement dynamics of the optimally controlled system are given by the red curve in Figure 6.4.

We can analyze the control fields and the dynamics of the controlled system to gain an understanding of how the control scheme works. The amplitudes of the control and the overlap of the controlled system with some intermediate states are shown in Figure 6.5. At first, a short pulse is applied that drives the system into the state

$$|\psi_1\rangle = \tfrac{1}{\sqrt{2}}\left(|0\rangle + |1\rangle\right)^{\otimes 2}, \tag{6.24}$$

which is rapidly entangled by the interactions. For a short time, no control is needed as the interactions bring the system to a highly entangled state within the

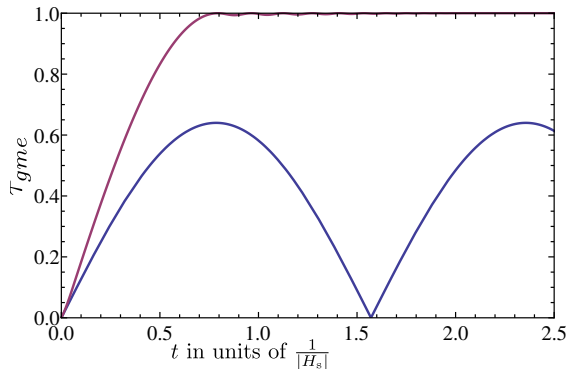

Figure 6.4: Entanglement evolution of the controlled (red) and uncontrolled (blue) dynamics of the two qubit system. Maximal entanglement is only produced on the time scale of the interaction.

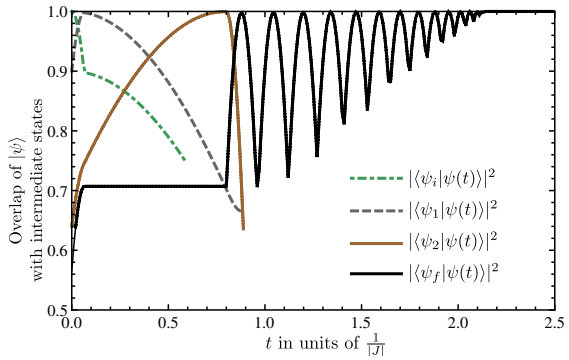

(a) Overlap of the state $|\psi(t)\rangle$ of the controlled system with the initial state $|\psi_i\rangle$, the intermediate states $|\psi_1\rangle$, $|\psi_2\rangle$ and the final state $|\psi_f\rangle$ during control. States $|\psi_i\rangle$ and $|\psi_1\rangle$ are separable, while $|\psi_2\rangle$ and $|\psi_f\rangle$ are maximally entangled. The final state $|\psi_f\rangle$ is unaffected by the dynamics of the system.

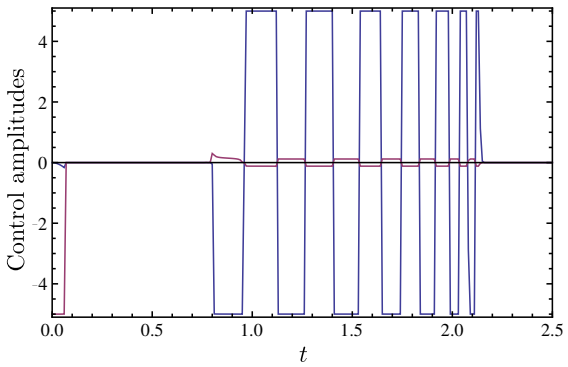

(b) Control fields applied to one qubit in the two-partite system. An initial short pulse pushes the system into a state that is most responsive to interactions, then H_{sys} drives the system into a highly entangled state. Finally, the control brings the system into a state that is still highly entangled, but unaffected by the interactions.

Figure 6.5: Dynamics of the control and the state of the controlled system of two qubits.

time scale of the interactions, i.e. $\frac{\pi}{4}/|H_{\text{sys}}|$. At this point, the state is approximately the intermediate state

$$|\psi_2\rangle = \tfrac{1}{2}\left(|00\rangle + |11\rangle - i|01\rangle - i|10\rangle\right), \tag{6.25}$$

which is susceptible to the interaction, although it is maximally entangled. The entanglement would disappear just as rapidly as it formed. Subsequently, the control oscillates, which can be seen in Figure 6.5b, until the final state of

$$|\psi_f\rangle = \tfrac{1}{\sqrt{2}}\left(|01\rangle + |01\rangle\right) \tag{6.26}$$

is reached. The systen then remains unaffected by the dynamics, but is still maximally entangled. After time $t \approx 2.0$, the system remains in state $|\psi_f\rangle$ which can be seen in Figure 6.5a.

6.3 Multipartite systems

We have now seen our control method sucessfully target highly entangled states in simple systems of two qubits where the target functional used was the gme-detection quantity τ_{gme}. When evaluation of the target functional requires an optimization over a parameter space, we can successfully keep track of the optimal choice of variables that optimize this functional.

In this section, we apply the same optimal control scheme in systems with more than two particles. We considered only Ising-type Hamiltonians as given in (6.1). With larger numbers of particles, we successfully used the maximal overlap functional to target W-like states. While targeting maximally entangled states in systems of two qubits works very well, we encountered issues in multipartite systems that hampered our control scheme's ability to produce dynamics that create highly entangled states. Efforts to produce GHZ-like states, as well as states that maximize τ_{gme}, are also reviewed in this section.

6.3.1 Targeting maximal-overlap functionals

Since we are interested in generating states with a high degree of genuine multipartite entanglement, one possible choice of target funcitonal is the maximal overlap functional τ_ψ introduced in Section 3.2.4. If the target state $|\psi\rangle$ is genuinely multipartite entangled, i.e. $|\text{W}\rangle$ or $|\text{GHZ}\rangle$, then a state that maximizes $\tau_\psi(\rho)$ will be LU-equivalent to $|\psi\rangle$ and thus genuinely multipartite entangled.

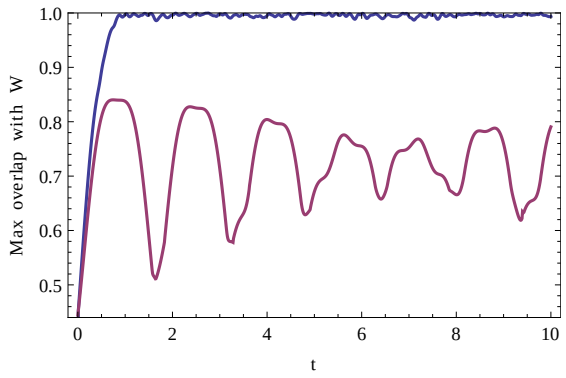

Figure 6.6: Time evolution of the maximal overlap with a W-state τ_{ψ_W} in an interacting system of three qubits, with and without control.

Targeting W-states

An example of successful control on one particular system is shown in Figure 6.6, where the maximal overlap with a W state is the target functional. The modeled system involves three interacting qubits with the interaction strengths

$$\lambda_{1,2} = 0.5, \quad \lambda_{1,3} = 0.48, \text{ and } \quad \lambda_{2,3} = 0.43. \tag{6.27}$$

We found that our control scheme has greatest success when the interaction strengths are similar in magnitude. The particular values in (6.27) are chosen to avoid degeneracy. That is, if the interaction strengths were all equal, perfect entanglement could be created by the system Hamiltonian alone.

The initial state is the product

$$|\psi_{\text{in}}\rangle = \tfrac{1}{\sqrt{2}}(|0\rangle + |1\rangle)^{\otimes 3}. \tag{6.28}$$

This is not an eigenstate of the interaction Hamiltonian H_{s}, so the system becomes entangled even without control. Entanglement dynamics of the uncontrolled system are given by the red curve in Figure 6.6. Initially, the state is fully separable and not very close to a W state. After some evolution, the value of the target functional increases. It then oscillates at a rate according to the interaction strengths, but never attains an optimal value.

We now include control with a maximal control amplitude of $k_{\max} = 5|H_{\text{s}}|$. The controlled entanglement dynamics are represented by the blue curve in Figure 6.6. Initally, the entanglement dynamics of the controlled system follow very close to those of the uncontrolled system. Local control cannot create entanglement on its own, so overlap with a W state at first increases at the same rate as in the uncontrolled dynamics. After $t \approx 1$ in Figure 6.6, the controlled dynamics diverge from the uncontrolled, since the control has driven the system into a state such that

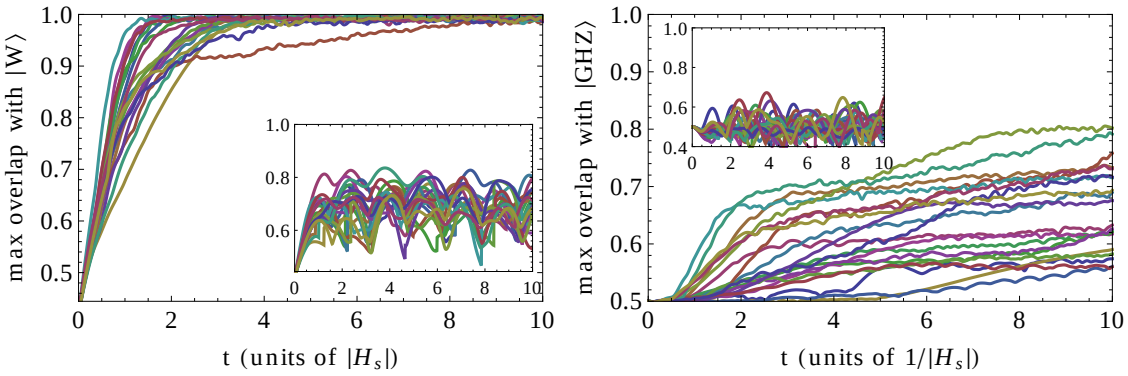

(a) Maximal overlap with W state as target functional.

(b) Maximal overlap with GHZ state as target functional.

Figure 6.7: Controlled and uncontrolled dynamics using the maximal overlap τ_ψ with different target states (see (3.24)) as the target functional. We consider 25 different systems with randomly generated interactions. In each case, a different interaction Hamiltonian was used with randomly chosen interaction strengths. The maximum control amplitude was always chosen to be $k_{\max} = 5|H_s|$. Uncontrolled dynamics for each case are shown in the inset. The success of targeting W-like states in systems of 4 qubits is independent of the interaction, whereas our control scheme is unable to generate GHZ states for any system with randomly chosen interaction strengths.

the interactions have the greatest entangling effect. After some time, the system reaches a state that maximizes the overlap with a locally equivalent W state, and the continued application of control allows this high value to be sustained.

In addition to this particular interaction Hamiltonian, we also considered many randomly generated interactions. The plot in Figure 6.7a shows the controlled entanglement dynamics of a four qubit system, each with a different randomly generated interaction Hamiltonian in the Ising form. The interaction strengths λ_{ij} were taken from a uniform distribution over the interval $[-1, 1]$. In each case, $|H_s|$ is defined by the largest interaction amplitude

$$|H_s| := \max_{\{i,j\}} \{|\lambda_{ij}|\}. \tag{6.29}$$

An optimal value for the maximal overlap with a W state is achieved for all of the randomly chosen interactions.

Targeting GHZ-states

We also considered the maximum overlap with a GHZ as a target state, but with less success. When the system is initially separable, our method of control is not

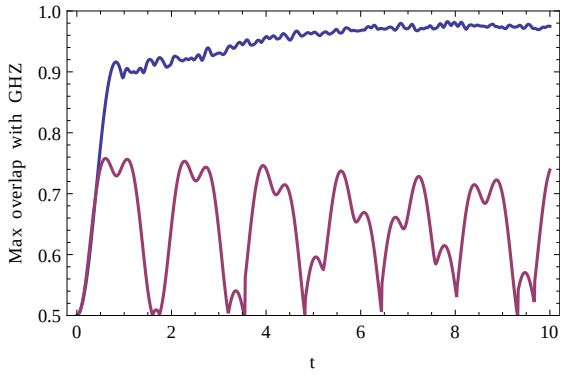

Figure 6.8: Time evolution of the maximal overlap with a GHZ-state $\tau_{\psi_{GHZ}}$ in an interacting system of four qubits, with (blue) and without (red) control.

successful creating states that maximize overlap with a GHZ state. Using the same interaction Hamiltonians with randomly generated interaction strengths as above, the initial state given in (6.28) was propagated with and without external control applied, shown in Figure 6.7b. Whereas maximum overlap with a W state was achieved in all of the random system of four qubits that we considered, our control method failed to generate a GHZ state when any of the interaction Hamiltonians were used.

In a system of three qubits, with the same initial state (6.28) and interaction strengths (6.27) as above, our control method was unable to drive the system into a state that maximized overlap with a GHZ state. The dynamics this system with (blue) and without (red) control are shown in Figure 6.8.

The failure of this control method to generate GHZ states might have something to do with the fact that our control scheme is not necessarily optimal. That is, control is only determined by how the target functional can be immediately increased rather than what is best for the long term. In each case of controlled dynamics in Figures 6.8 and 6.7b, we see that the target functional does typically increase with time because our control scheme derives control fields that maximize the time derivatives during the time-propagation. However, the control is not optimal in the since that the maximum of the target functional is not necessarily reached, as discussed in Chapter 4.

Future work may be done to characterize this behavior to understand why our control method fails when the maximal overlap with a GHZ state is chosen as the target functional.

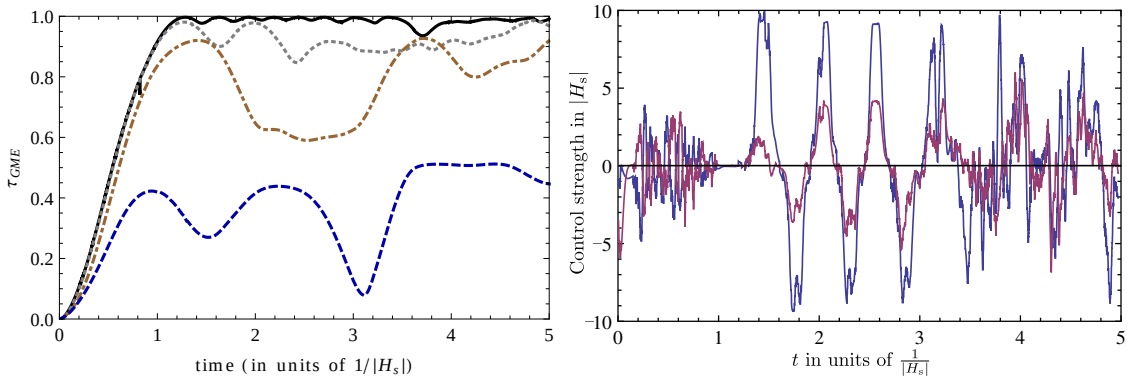

(a) (b)

Figure 6.9: (a) Time evolution of τ_{gme} for a separable initial state of 3 interacting qubits for various levels of control. The uncontrolled (blue dashed) dynamics are shown, as well as controlled dynamics with various levels of control amplitudes $k_{\max}$: $10|H_s|$ (solid), $5|H_s|$ (grey dotted), $|H_s|$ (brown dash-dotted). (b) The optimal time-local control fields $k_x^{(1)}$ (blue) and $k_y^{(1)}$ (red) addressing the first qubit are shown, where maximal control amplitude $k_{\max} = 10|H_s|$.

6.3.2 Targeting genuine multipartite entanglement

The main goal of this thesis is to implement the control scheme outlined in Chapter 5 using the gme-detection quantity τ_{gme} as a target functional. This was achieved in systems of two qubits, as shown in Section 6.2, and we show here our successes with targeting τ_{gme} in larger systems. Although we were also successful in implementing control on systems of four qubits, in this section we largely present our exemplary results for tripartite systems.

As in the previous examples, we consider a system of interacting spins with a system Hamiltonian H_s of the form given in (6.1). We were able to successfully control the dynamics where the interaction strengths are the same as in (6.27). The value of the largest interaction strength is therefore $|H_s| = 0.5$. We chose the initial state given in (6.28) for the evolutions.

Time evolution of τ_{gme} in the absence of control is shown by the dashed blue line in Figure 6.9. The system starts out in a fully separable state, so the initial amount entanglement is zero. As in the previous examples, some amount of genuine multipartite entanglement is generated due to the interactions, but this oscillates at low values and never attains the maximum value.

We now turn to the optimized entanglement dynamics, which are also shown in Figure 6.9. When the maximum control amplitude is selected to be $k_{\max} = 10 \cdot |H_s|$, a highly entangled state is quickly generated after a time of about $t \approx \frac{1}{|H_s|}$, and the control is able to maintain a highly entangled state for the remainder of the time.

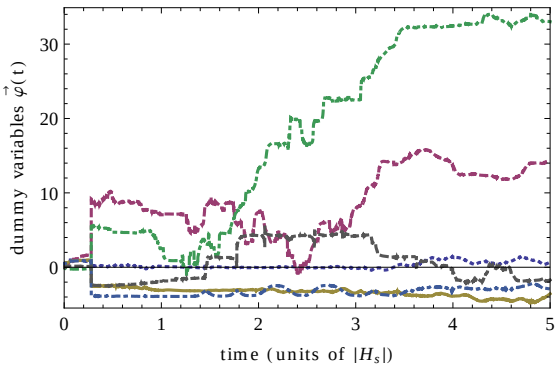

Figure 6.10: Dynamics of the choice of parameters $\vec{\varphi}(t)$ to evaluate $\tau_{gme}(\rho(t))$ for the optimally controlled system in Fig. 6.9.

If the control amplitudes are limited to smaller values, in this case $5|H_s|$ and $|H_s|$, the controlled dynamics are still an improvement on the uncontrolled dynamics, but persisting levels of high amounts of entanglement are unable to be generated.

For the case of $k_{\max} = 10 \cdot |H_s|$, the amount of control applied to the first spin is shown in Figure 6.9b. During part of this simulated time interval (between $t \approx 1$ and $t \approx 3.5$), there is a relatively clear pattern of pulses that should be applied to have optimal entanglement dynamics. The remainder of the control consists of high-frequency parts that make it difficult to interpret qualitatively what the control is doing.

Our method of determining optimal control depends on the fictitious parameters changing smoothly as the state evolves. Thus, it is important that we analyze the parameters in $\vec{\varphi}$ to verify that this is indeed the case. The plot in Figure 6.10 shows the value of the elements of $\vec{\varphi}(t)$ for the controlled system given in Figure 6.9 with a maximum control amplitude of $k_{\max} = 10|H_s|$. To ensure that the parameters $\vec{\varphi}$ are indeed optimal, an optimization is performed every few time steps of the evolution such that the nearest local maximum of τ with respect to the paremeters is obtained. Except for one "jump" toward the beginning of the dynamics, we see in Figure 6.10 that the choice of variables $\vec{\varphi}$ evolves continuously. This jump corresponds to a discontinuous shift of the global maximum of $\tau_{gme}(\rho, |\Phi\rangle)$ as the state evolves. Even though only the range $\varphi_j \in [0, 2\pi)$ must be considered to parametrize a local unitary, the full $\vec{\varphi} \in \mathbb{R}^6$ provides a continuous and smooth parametrization for the manifold of local unitary matrices. Considering the whole (although redundant) space $\mathbb{R}^6$ allows us perform the maximization without constraints and permits the parameters to change smoothly with the evolution of the state in question.

For the most part, we have limited our analysis to systems of three qubits to re-

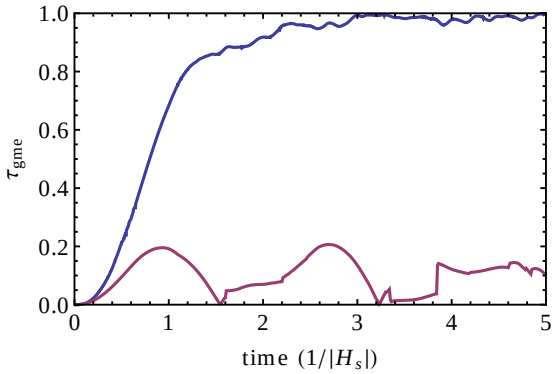

Figure 6.11: Time evolution of τ_{gme} for a separable initial state of 4 interacting qubits. The uncontrolled (red) dynamics are shown, as well as controlled dynamics with control amplitudes $k_{\mathrm{max}}= 10|H_{\mathrm{s}}|$ (blue).

duce computation times, since tripartite systems are the simplest systems in which the concept of genuine multipartite entanglement becomes relevant. However, to show that our control scheme achieves states that maximize τ_{gme} in systems of more particles, we also applied our control scheme to systems of four interacting qubits. In a system with an Ising-type Hamiltonian as in (6.1) with randomly generated interaction coefficients, Figure 6.11 shows the entanglement dynamics of the system with and without application of external control.

In the fully separable state $\left(\frac{|0\rangle+|1\rangle}{\sqrt{2}}\right)^{\otimes 4}$, the initial entanglement of the system is zero. In absence of control, the amount of genuine multipartite entanglement in the system oscillates at low levels, and τ_{gme} never exceeds 0.2. The non-smooth apperance of the curve is due to the fact that the evaluation of τ_{gme} is numerically more challenging in systems of four qubits. With the application of optimal control, we obtain states that maximize τ_{gme} on time scales corresponding to the interaction strengths of the system.

6.4 Control of dissipative systems

Up to this point, we have only considered the idealized case of a closed quantum system with purely unitary dynamics. In real experiments, it is never possible to shield a system entirely from environmental effects, and we must consider entanglement dynamics in open quantum systems. In the presence of such incoherent effects, we would like to not only be able to prepare highly entangled states, but also to preserve the entanglement over sufficiently long times such that it can be used for different tasks [85].

If the incoherent dynamics of a system are known or can be reliably modeled,

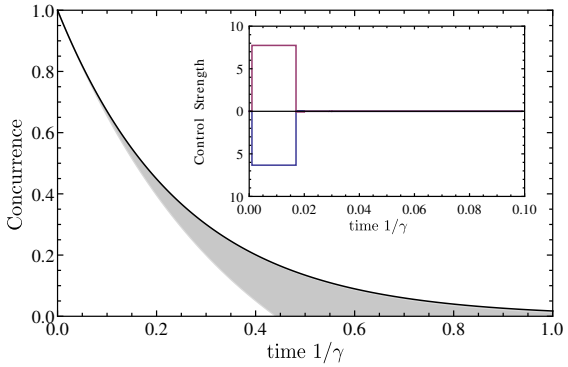

Figure 6.12: Time evolution of τ in a non-interacting system of two qubits under dephasing with rate γ. The grey area shows the evolution of 50 randomly generated locally equivalent maximally entangled states, and the black line shows the dynamics of one of these states under optimal control with amplitude $h_{\max} = 5\gamma$. Control amplitude shown in inset.

we can incorporate these dynamics into our calculations of $\ddot{\tau}$, which are needed to calculate the amplitudes for the optimal control. Markovian interactions with an environment can only decrease the value of entanglement in any state [74], but the entanglement in different states will not be equally affected by the decoherence. When the incoherent dynamics are included in the calculations, we can determine control amplitudes that will steer the system into states such that this decoherence has the smallest effect. This can also help us identify the highly entangled states that are most robust against decoherence present in a system.

The only type of incoherent dynamics that we consider in the following sections is the paradigmatic model of a dephasing environment. In particular, we consider the situation where each spin is coupled to a separate environment, but each with the same coupling strength γ. In this case, the Lindblad master equation has the form

$$\mathcal{L}(\rho) = \sum_i \gamma(\sigma_z^{(i)} \rho \sigma_z^{(i)} - \rho), \tag{6.30}$$

where $\sigma_z^{(i)}$ is the third Pauli matrix operating on the i^{th} qubit [74].

Here, we show how our control scheme can be used to determine which of the locally equivalent states of a given orbit exhibit entangnlement that is most robust against this model of decoherence.

6.4.1 Robust entangled states

Two qubits

As an exemplary case to show how our control methods can account for decoherence, we first consider a simple case with a system of two non-interacting qubits. We start with a set of randomly chosen maximally entangled states, and evolve them according to the dynamics given in (6.30). The resulting entanglement dynamics $\tau_{gme}(\rho(t))$ are shown in the grey area in Figure 6.12. We then pick one of these states as an initial state and use our control scheme to apply optimal control to the system. The resulting entanglement dynamics are depicted by the black curve. Here, the maximal control amplitude on the two qubits was chosen to be $k_{\max} = 5\gamma$. A short control pulse, shown in the inset in Fig. 6.12, is applied, which then guides the system into a state that is most robust against the dephasing dynamics.

Three qubits targeting τ_{gme}

Expanding on the case above with two qubits, we can perform this same analysis on larger systems. Here, we investigate the dynamics of three-qubit states that are locally equivalent to $|\mathrm{GHZ}\rangle = \frac{1}{\sqrt{2}}(|000\rangle + |111\rangle)$ as they undergo dephasing modeled by the Lindblad master equation in (6.30). The grey area of the plot in Figure 6.13 shows the entanglement dynamics of 50 randomly selected states of this form undergoing dephasing with a rate of γ.

As long as $\tau_{gme}(\rho)$ is positive, the state ρ retains some degree of genuine multipartite entanglement. Even though all of the initial states have equivalent entanglement properties, the entanglement in some states is more affected by the envoronmental dephasing than others. Indeed, as seen in Figure 6.13, the least robust states become separable after undergoing dephasing for a time of only $t \approx 0.25/\gamma$, whereas the most robust of the randomly selected states exhibit genuine multipartite entanglement past $t = 0.4/\gamma$.

Using our control scheme, we can apply local control that minimizes the detrimental effects of the decoherence on the value of $\tau_{gme}(\rho(t))$. Here, we randomly chose one state that is locally equivalent to a GHZ state, and implemented our control scheme on the system as we allowed it to dephase. We limit the strength of the control fields addressing each qubit to $k_{\max} = 5\gamma$. The resulting entanglement dynamics are depicted by the black curve in Figure 6.13. The system in which we implement the control exhibits genuine three-body entanglement until $t \approx 0.55/\gamma$, clearly longer than in any of the uncontrolled dynamics.

The control pulses that were calculated and applied on the system are shown in the inset of Figure 6.13. Our control scheme derived a short, constant pulse on each of the subsystems. Once the system reaches the state that is most robust

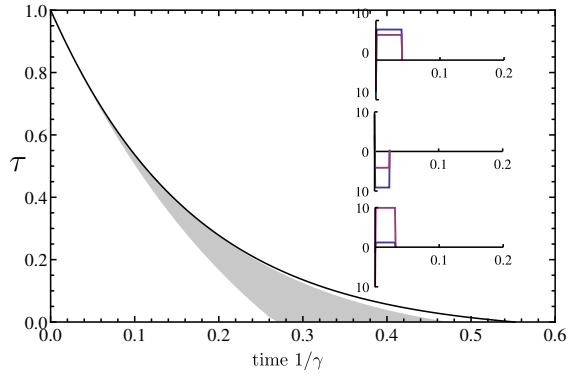

Figure 6.13: Time evolution of τ_{gme} in a non-interacting system of three qubits undergoing dephasing with rate γ. The grey area shows the evolution of 50 randomly generated locally equivalent GHZ states, and the black line shows the dynamics of one of these states under optimal control with amplitude $k_{\max} = 5\gamma$.

against this type of decoherence, no more control needs to be applied since no further improvements to the robustness can be made.

In principle, this method can be applied with any model of decoherence where the target functional is a measure of entanglement. Using our techniques to derive local control that minimizes the decrease in the target functional, we can identify the states of the local orbit that exhibit the largest values of the target functional for the longest amount of time.

Chapter 7

Conclusions

In conclusion, we have expanded on previous methods [27] for determining time-optimal control pulses of quantum systems for targeting highly entangled states in systems of many qubits. The methods presented here deterministically derive external control Hamiltonians that yield optimal increase in the target functional. This is done by determining the local control Hamiltonians that yield the largest time derivatives of the target functional. Most importantly, when these target functionals involve optimizations over a continuous parameter space, this thesis outlines a method to evaluate these time derivatives even when an analytic method of doing so is not available. This method can devise control that maximizes a functional as long as the functional is invariant under local unitary transformations and the parameter space is continuous. By taking into account how the optimal choice of parameters changes as the state ρ evolves when different parts of the control Hamiltonian are applied, we can determine the optimal amplitudes for the external control.

Above all, the control scheme presented here can be used as a valuable tool to gain insights into entanglement dynamics and its robustness against decoherence. We succeeded in creating genuinely multipartite entangled states when certain target functionals were used as objectives in a variety of modeled interactions. This was demonstrated when the target function that was employed was the maximal overlap with a locally equivalent W state, but also with a measure of genuine multipartite entanglement τ_{gme}. However, the failure of these methods to create highly entangled states when some target functionals were used, such as the maximal overlap with a GHZ state, is something that can still be analyzed. In addition to manipulating dynamics to create entanglement, this control method also succeeded in determining the states that are most robust against decoherence by maximizing an entanglement measure while the system undergoes dephasing.

Bibliography

[1] J. von Neumann, *Mathematische Grundlagen der Quantenmechanik*. Die Grundlehren der mathematischen Wissenschaften, Springer, 1932.

[2] A. Einstein, B. Podolsky, and N. Rosen, "Can Quantum-Mechanical Description of Physical Reality Be Considered Complete?," *Physical Review*, vol. 47, pp. 777–780, May 1935.

[3] E. Schrödinger, "Die gegenwärtige Situation in der Quantenmechanik," *Die Naturwissenschaften*, vol. 23, pp. 823–828, Dec. 1935.

[4] J. S. Bell, "On The Einstein-Podolsky-Rosen paradox," *Physics*, vol. 1, pp. 195–200, Dec. 1974.

[5] A. Aspect, P. Grangier, and G. Roger, "Experimental Realization of Einstein-Podolsky-Rosen-Bohm Gedankenexperiment: A New Violation of Bell's Inequalities," *Physical Review Letters*, vol. 49, pp. 91–94, July 1982.

[6] R. P. Feynman, "Simulating physics with computers," *International Journal of Theoretical Physics*, vol. 21, pp. 467–488, June 1982.

[7] C. H. Bennett, "Quantum Information," *Physica Scripta*, vol. T76, no. 1, p. 210, 1998.

[8] A. K. Ekert, "Quantum cryptography based on Bells theorem," *Physical Review Letters*, vol. 67, pp. 661–663, Aug. 1991.

[9] C. H. Bennett, G. Brassard, C. Crépeau, R. Jozsa, A. Peres, and W. K. Wootters, "Teleporting an unknown quantum state via dual classical and Einstein-Podolsky-Rosen channels," *Physical Review Letters*, vol. 70, pp. 1895–1899, Mar. 1993.

[10] C. H. Bennett, P. W. Shor, J. A. Smolin, and A. Thapliyal, "Entanglement-Assisted Classical Capacity of Noisy Quantum Channels," *Physical Review Letters*, vol. 83, pp. 3081–3084, Oct. 1999.

[11] M. A. Nielsen and I. L. Chuang, *Quantum computation and quantum information*. Cambridge University Press, Dec. 2010.

[12] P. W. Shor, "Polynomial-Time Algorithms for Prime Factorization and Discrete Logarithms on a Quantum Computer," *SIAM Journal on Computing*, vol. 26, pp. 1484–1509, Oct. 1997.

[13] R. Jozsa and N. Linden, "On the role of entanglement in quantum-computational speed-up," *Proceedings of the Royal Society A: Mathematical, Physical and Engineering Sciences*, vol. 459, pp. 2011–2032, Aug. 2003.

[14] D. Gottesman, "An Introduction to Quantum Error Correction and Fault-Tolerant Quantum Computation," p. 46, Apr. 2009.

[15] W. K. Wootters and W. H. Zurek, "A single quantum cannot be cloned," *Nature*, vol. 299, pp. 802–803, Oct. 1982.

[16] O. Gühne and G. Tóth, "Entanglement detection," *Physics Reports*, vol. 474, pp. 1–75, Apr. 2009.

[17] D. Leibfried, E. Knill, S. Seidelin, J. Britton, R. B. Blakestad, J. Chiaverini, D. B. Hume, W. M. Itano, J. D. Jost, C. Langer, R. Ozeri, R. Reichle, and D. J. Wineland, "Creation of a six-atom 'Schrödinger cat' state.," *Nature*, vol. 438, pp. 639–642, Dec. 2005.

[18] H. Häffner, W. Hänsel, C. F. Roos, J. Benhelm, D. Chek-al Kar, M. Chwalla, T. Körber, U. D. Rapol, M. Riebe, P. O. Schmidt, C. Becher, O. Gühne, W. Dür, and R. Blatt, "Scalable multiparticle entanglement of trapped ions.," *Nature*, vol. 438, pp. 643–6, Dec. 2005.

[19] R. Raussendorf, D. E. Browne, and H. J. Briegel, "Measurement-based quantum computation on cluster states," *Physical Review A*, vol. 68, Aug. 2003.

[20] H. J. Briegel and R. Raussendorf, "Persistent Entanglement in Arrays of Interacting Particles," *Physical Review Letters*, vol. 86, pp. 910–913, Jan. 2001.

[21] J. Zhu, S. Kais, A. Aspuru-Guzik, S. Rodriques, B. Brock, and P. J. Love, "Multipartite Quantum Entanglement Evolution in Photosynthetic Complexes," p. 37, Feb. 2012.

[22] L. Vandersypen and I. Chuang, "NMR techniques for quantum control and computation," *Reviews of Modern Physics*, vol. 76, pp. 1037–1069, Jan. 2005.

[23] C. Altafini, "On the generation of sequential unitary gates from continuous time Schrodinger equations driven by external fields," *Quantum Information Processing*, vol. 1, pp. 207–224, Mar. 2002.

[24] V. Ramakrishna, K. Flores, H. Rabitz, and R. Ober, "Quantum control by decompositions of SU(2)," *Physical Review A*, vol. 62, p. 053409, Oct. 2000.

[25] D. D'Alessandro, *Introduction to quantum control and dynamics*. Chapman & Hall/CRC Applied Mathematics and Nonlinear Science Series, Taylor & Francis, 2008.

[26] N. Khaneja, T. Reiss, C. Kehlet, T. Schulte-Herbrüggen, and S. J. Glaser, "Optimal control of coupled spin dynamics: design of NMR pulse sequences by gradient ascent algorithms.," *Journal of magnetic resonance*, vol. 172, pp. 296–305, Feb. 2005.

[27] F. Platzer, F. Mintert, and A. Buchleitner, "Optimal Dynamical Control of Many-Body Entanglement," *Physical Review Letters*, vol. 105, p. 020501, July 2010.

[28] G. Vidal and R. Tarrach, "Robustness of entanglement," *Physical Review A*, vol. 59, pp. 141–155, Jan. 1999.

[29] C. Bennett, D. DiVincenzo, J. Smolin, and W. Wootters, "Mixed-state entanglement and quantum error correction," *Physical Review A*, vol. 54, pp. 3824–3851, Nov. 1996.

[30] S. Roman, *Advanced linear algebra*. Graduate Texts in Mathematics, Springer, 2nd ed., 2005.

[31] R. F. Werner, "Quantum states with Einstein-Podolsky-Rosen correlations admitting a hidden-variable model," *Physical Review A*, vol. 40, no. 8, pp. 4277–4281, 1989.

[32] L. Gurvits, "Classical deterministic complexity of Edmonds' Problem and quantum entanglement," in *Proceedings of the thirty-fifth ACM symposium on Theory of computing - STOC '03*, (New York, New York, USA), pp. 10–19, ACM Press, Mar. 2003.

[33] R. Horodecki, M. Horodecki, and K. Horodecki, "Quantum entanglement," *Reviews of Modern Physics*, vol. 81, pp. 865–942, June 2009.

[34] E. Schmidt, "Zur Theorie der linearen und nichtlinearen Integralgleichungen," *Mathematische Annalen*, vol. 63, pp. 433–476, Dec. 1907.

[35] G. W. Stewart, "On the early history of the singular value decomposition," *SIAM review*, vol. 35, no. 4, pp. 551–566, 1993.

[36] R. E. Edwards, *Functional Analysis, Theory and Application.* New York: Hold, Rinehart and Winston, 1965.

[37] M. Horodecki, P. Horodecki, and R. Horodecki, "Separability of mixed states: necessary and sufficient conditions," *Physics Letters A*, vol. 223, pp. 1–8, Nov. 1996.

[38] M. Horodecki, P. Horodecki, and R. Horodecki, "Separability of n-particle mixed states: necessary and sufficient conditions in terms of linear maps," *Physics Letters A*, vol. 283, pp. 1–7, May 2001.

[39] M. Barbieri, F. De Martini, G. Di Nepi, P. Mataloni, G. DAriano, and C. Macchiavello, "Detection of Entanglement with Polarized Photons: Experimental Realization of an Entanglement Witness," *Physical Review Letters*, vol. 91, pp. 1–4, Nov. 2003.

[40] M. Bourennane, M. Eibl, C. Kurtsiefer, S. Gaertner, H. Weinfurter, O. Gühne, P. Hyllus, D. Bruß, M. Lewenstein, and A. Sanpera, "Experimental Detection of Multipartite Entanglement using Witness Operators," *Physical Review Letters*, vol. 92, pp. 1–4, Feb. 2004.

[41] M. Nielsen and I. Chuang, *Quantum Computation and Quantum Information.* Cambridge University Press, 10th anniv ed., 2010.

[42] A. Peres, "Separability Criterion for Density Matrices," *Physical Review Letters*, vol. 77, pp. 1413–1415, Aug. 1996.

[43] P. Agrawal and A. K. Pati, "Probabilistic quantum teleportation," *Physics Letters A*, vol. 305, pp. 12–17, Nov. 2002.

[44] M. Horodecki, "Entanglement measures," *Quantum Information and Computation*, vol. 1, no. 1, pp. 3–26, 2001.

[45] M. B. Plenio and S. Virmani, "An introduction to entanglement measures," *Quantum Information & Computation*, vol. 7, pp. 1–51, Apr. 2005.

[46] M. Choi, "Completely positive linear maps on complex matrices," *Linear Algebra and its Applications*, vol. 10, no. 3, pp. 285–290, 1975.

[47] M. A. Nielsen and G. Vidal, "Majorization and the interconversion of bipartite states," *Quantum information and computation*, vol. 1, no. 1, pp. 76–93, 2001.

[48] C. H. Bennett, D. P. DiVincenzo, J. A. Smolin, and W. K. Wootters, "Mixed-state entanglement and quantum error correction.," *Physical review. A*, vol. 54, pp. 3824–3851, Nov. 1996.

[49] A. Uhlmann, "Entropy and optimal decompositions of states relative to a maximal commutative subalgebra," *Open Systems & Information Dynamics*, vol. 5, pp. 209–228, Apr. 1998.

[50] W. K. Wootters, "Entanglement of Formation of an Arbitrary State of Two Qubits," *Physical Review Letters*, vol. 80, pp. 2245–2248, Mar. 1998.

[51] D. M. Greenberger, M. A. Horne, and A. Zeilinger, "Going beyond Bell's theorem," in *Bell's theorem, quantum theory and conceptions of the universe* (M. Kafatos, ed.), no. 3, pp. 69–72, Dordrecht: Kluwer, Dec. 1989.

[52] A. Zeilinger, M. A. Horne, and D. M. Greenberger, "Higher-Order Quantum Entanglement," in *Workshop on Squeezed States and Uncertainty Relations* (D. Han, Y. S. Kim, and W. W. Zachary, eds.), p. 73, Washington, D.C.: National Aeronautics and Space Administration, 1992.

[53] W. Dür, G. Vidal, and J. I. Cirac, "Three qubits can be entangled in two inequivalent ways," *Physical Review A*, vol. 62, p. 062314, Nov. 2000.

[54] O. Gühne and M. Seevinck, "Separability criteria for genuine multiparticle entanglement," *New Journal of Physics*, vol. 12, p. 053002, May 2010.

[55] M. Huber, F. Mintert, A. Gabriel, and B. C. Hiesmayr, "Detection of High-Dimensional Genuine Multipartite Entanglement of Mixed States," *Physical Review Letters*, vol. 104, p. 210501, May 2010.

[56] M. Seevinck and J. Uffink, "Partial separability and entanglement criteria for multiqubit quantum states," *Physical Review A*, vol. 78, p. 032101, Sept. 2008.

[57] B. C. Hiesmayr and M. Huber, "Two distinct classes of bound entanglement: PPT-bound and 'multi-particle'-bound," p. 4, June 2009.

[58] F. Levi and F. MIntert, "A Hierarchy of Entanglement," *arXiv:1204.5322 [quant-ph]*, 2012.

[59] A. Gabriel, B. C. Hiesmayr, and M. Huber, "Criterion for K-separability in mixed multipartite states," *Quantum information and computation*, vol. 10, no. 9, pp. 829–836, 2010.

[60] M. Blasone, F. DellAnno, S. De Siena, and F. Illuminati, "Hierarchies of geometric entanglement," *Physical Review A*, vol. 77, pp. 1–15, June 2008.

[61] A. R. R. Carvalho, F. Mintert, and A. Buchleitner, "Decoherence and Multipartite Entanglement," *Physical Review Letters*, vol. 93, p. 230501, Dec. 2004.

[62] F. Mintert, A. R. R. Carvalho, M. Kuś, and A. Buchleitner, "Measures and dynamics of entangled states," *Physics Reports*, vol. 415, pp. 207–259, Aug. 2005.

[63] L. Aolita, A. Buchleitner, and F. Mintert, "Scalable method to estimate experimentally the entanglement of multipartite systems," *Physical Review A*, vol. 78, pp. 3–6, Aug. 2008.

[64] F. Mintert, M. Kuś, and A. Buchleitner, "Concurrence of Mixed Multipartite Quantum States," *Physical Review Letters*, vol. 95, pp. 1–4, Dec. 2005.

[65] F. Mintert and A. Buchleitner, "Observable Entanglement Measure for Mixed Quantum States," *Physical Review Letters*, vol. 98, p. 140505, Apr. 2007.

[66] T.-C. Wei and P. M. Goldbart, "Geometric measure of entanglement and applications to bipartite and multipartite quantum states," *Physical Review A*, vol. 68, p. 042307, Oct. 2003.

[67] K. Uyanik and S. Turgut, "Geometric measures of entanglement," *Physical Review A*, vol. 81, p. 032306, Mar. 2010.

[68] D. Buhr, M. E. Carrington, T. Fugleberg, R. Kobes, G. Kunstatter, D. McGillis, C. Pugh, and D. Ryckman, "Geometrical entanglement of highly symmetric multipartite states and the Schmidt decomposition," *Journal of Physics A: Mathematical and Theoretical*, vol. 44, p. 365305, Sept. 2011.

[69] Z.-H. Ma, Z.-H. Chen, J.-L. Chen, C. Spengler, A. Gabriel, and M. Huber, "Measure of genuine multipartite entanglement with computable lower bounds," *Physical Review A*, vol. 83, p. 062325, June 2011.

[70] Z.-H. Chen, Z.-H. Ma, J.-L. Chen, and S. Severini, "Improved lower bounds on genuine-multipartite-entanglement concurrence," *Physical Review A*, vol. 85, p. 062320, June 2012.

[71] M. Bourennane, M. Eibl, C. Kurtsiefer, S. Gaertner, H. Weinfurter, O. Gühne, P. Hyllus, D. Bruß, M. Lewenstein, and A. Sanpera, "Experimental Detection of Multipartite Entanglement using Witness Operators," *Physical Review Letters*, vol. 92, pp. 2–5, Feb. 2004.

[72] B. Röthlisberger, J. Lehmann, and D. Loss, "Numerical evaluation of convex-roof entanglement measures with applications to spin rings," *Physical Review A*, vol. 80, p. 042301, Oct. 2009.

[73] J. A. Miszczak, "Generating and using truly random quantum states in Mathematica," *Computer Physics Communications*, vol. 183, pp. 118–124, Jan. 2012.

[74] H.-P. Breuer and F. Petruccione, *Theory of open quantum systems*. New York: Oxford University Press, 2002.

[75] R. Brocket and N. Khaneja, "On the stochastic control of quantum ensembles," in *System Theory: Modeling, Analysis, and Control* (T. E. Djaferis and I. C. Schick, eds.), pp. 75–96, Dorcrecht: Kluwer, 1st ed., 1999.

[76] D. Dong and I. R. Petersen, "Quantum control theory and applications: A survey," *Control Theory & Applications, IET*, vol. 4, no. 12, pp. 2651 – 2671, 2010.

[77] V. Vedral, M. B. Plenio, M. A. Rippin, and P. L. Knight, "Quantifying Entanglement," *Physical Review Letters*, vol. 78, pp. 2275–2279, Mar. 1997.

[78] R. Judson, K. Lehmann, H. Rabitz, and W. Warren, "Optimal design of external fields for controlling molecular motion: application to rotation," *Journal of Molecular Structure*, vol. 223, pp. 425–456, June 1990.

[79] C. Brif, R. Chakrabarti, and H. Rabitz, "Control of quantum phenomena: past, present and future," *New Journal of Physics*, vol. 12, p. 075008, July 2010.

[80] D. Goswami, "Optical pulse shaping approaches to coherent control," *Physics Reports*, vol. 374, pp. 385–481, 2003.

[81] I. I. Maximov, J. Salomon, G. Turinici, and N. C. Nielsen, "A smoothing monotonic convergent optimal control algorithm for nuclear magnetic resonance pulse sequence design.," *The Journal of chemical physics*, vol. 132, p. 084107, Feb. 2010.

[82] B. Schneider, C. Gollub, K.-L. Kompa, and R. de Vivie-Riedle, "Robustness of quantum gates operating on the high frequency modes of MnBr(CO)5," *Chemical Physics*, vol. 338, pp. 291–298, Sept. 2007.

[83] F. Mintert, "Smooth, optimal control," *arXiv:1205.5142v1 [quant-ph]*, 2012.

[84] S. Grivopoulos and B. Bamieh, "Optimal population transfers for a quantum system in the limit of large transfer time," in *Proceedings of the 2004 American Control Conference*, pp. 2481–2486, American Automatic Control Council, 2004.

[85] F. Mintert, "Robust entangled states," *Journal of Physics A: Mathematical and Theoretical*, vol. 43, p. 245303, June 2010.

[86] F. Platzer, *Optimal Dynamical Control of Many-Body Entanglement*. Diplom thesis, Albert-Ludwigs-Universität Freiburg, 2010.

[87] F. Lucas, F. Mintert, and A. Buchleitner, "Tailoring many-body entanglement through local control," *arXiv:1204.0388v1 [quant-ph]*, Apr. 2012.

[88] S. N. Walck and D. W. Lyons, "Maximum stabilizer dimension for nonproduct states," *Physical Review A*, vol. 17003, no. August, pp. 1–6, 2007.

[89] H. A. Carteret and A. Higuchi, "Multipartite generalization of the Schmidt decomposition," *Journal of Mathematical Physics*, vol. 41, no. 12, pp. 7932–7939, 2000.

[90] M. M. Sinolecka, K. Zyczkowski, and M. Kuś, "Manifolds of interconvertible pure states," *arXiv:quant-ph/0110082v2*, Oct. 2001.

[91] H. A. Carteret, N. Linden, S. Popescu, and A. Sudbery, "Multiparticle Entanglement," *Foundations of Physics*, vol. 29, no. 4, pp. 527–552, 1999.

[92] P. Cappellaro and M. Lukin, "Quantum correlation in disordered spin systems: Applications to magnetic sensing," *Physical Review A*, vol. 80, p. 032311, Sept. 2009.

[93] P. Neumann, N. Mizuochi, F. Rempp, P. Hemmer, H. Watanabe, S. Yamasaki, V. Jacques, T. Gaebel, F. Jelezko, and J. Wrachtrup, "Multipartite entanglement among single spins in diamond.," *Science*, vol. 320, pp. 1326–9, June 2008.

[94] L. Robledo, H. Bernien, I. van Weperen, and R. Hanson, "Control and Coherence of the Optical Transition of Single Nitrogen Vacancy Centers in Diamond," *Physical Review Letters*, vol. 105, p. 177403, Oct. 2010.

Appendix A

Orbit parametrization

Excluding a global phase factor, any arbitrary unitary on a two-dimensional quantum system can be parameterized by

$$U_j = \begin{pmatrix} \cos\theta_j e^{i\varphi_j} & \sin\theta_j e^{i\phi_j} \\ -\sin\theta_j e^{-i\phi_j} & \cos\theta_j e^{-i\varphi_j} \end{pmatrix}. \tag{A.1}$$

This can be factored into a product of two matrices

$$U_j = V_j \begin{pmatrix} e^{i\varphi_j} & 0 \\ 0 & e^{-i\varphi_j} \end{pmatrix} \tag{A.2}$$

where the matrix on the right can be written as $e^{i\sigma_z\varphi_j}$ and V_j is the unitary

$$V_j = \begin{pmatrix} \cos\theta_j & \sin\theta_j e^{i\phi'_j} \\ -\sin\theta_j e^{-i\phi'_j} & \cos\theta_j \end{pmatrix} \tag{A.3}$$

defined by only two parameters and we set $\phi'_j = \phi_j - \varphi_j$. Thus, an arbirary local unitary on a system of N qubits can be factored as

$$\begin{aligned} U = U_1 \otimes \cdots \otimes U_N &= \bigotimes_{j=1}^{N} U_j \\ &= \left(\bigotimes_{j=1}^{N} V_j\right)\left(\bigotimes_{j=1}^{N} e^{i\sigma_z\varphi_j}\right) \end{aligned} \tag{A.4}$$

These facts can be used to assist us in parameterizing orbits of states under local unitaries.

Orbit of GHZ states

An arbitrary state in the LU-orbit of the GHZ state is given by

$$U|\mathrm{GHZ}\rangle = \bigotimes_{j=1}^{N} U_j|\mathrm{GHZ}\rangle = \frac{1}{\sqrt{2}}\left(\bigotimes_{j=1}^{N} V_j\right)\left(\bigotimes_{j=1}^{N} e^{i\sigma_z\varphi_j}\right)\left(|0\cdots 0\rangle + |1\cdots 1\rangle\right). \tag{A.5}$$

Now, $|0\rangle$ and $|1\rangle$ are eigenvectors of $e^{i\sigma_z\varphi_j}$ with eigenvalues $e^{i\varphi_j}$ and $e^{-i\varphi_j}$, so we have

$$\begin{aligned} U|\mathrm{GHZ}\rangle &= \frac{1}{\sqrt{2}}\left(\bigotimes_{j=1}^{N} V_j\right)\left(e^{i\sum_j\varphi_j}|0\cdots 0\rangle + e^{-i\sum_j\varphi_j}|1\cdots 1\rangle\right) \\ &= \left(V_1 e^{i\sigma_z\left(\sum_j\varphi_j\right)}\right)\otimes V_2\otimes\cdots\otimes V_N|\mathrm{GHZ}\rangle. \end{aligned} \tag{A.6}$$

Each V_j requires only two parameters to define. One extra parameter defined by $\sum_j \varphi_j$ is also needed. Thus, we can parameterize an arbitrary state in the GHZ-orbit with $2N+1$ parameters, as given in (5.61) in Chapter 5.

Orbit of W states

An arbitrary state in the LU-orbit of the W state is given by

$$\begin{aligned} U|\mathrm{W}\rangle &= \frac{1}{\sqrt{N}}\left(\bigotimes_{j=1}^{N} V_j\right)\left(\bigotimes_{j=1}^{N} e^{i\sigma_z\varphi_j}\right)\sum_{k=1}^{N}|\{2^{k-1}\}\rangle \\ &= \frac{1}{\sqrt{N}}\left(\bigotimes_{j=1}^{N} V_j\right)\sum_{k=1}^{N} e^{i(-\varphi_k+\sum_{j\neq k}\varphi_j)}|\{2^{k-1}\}\rangle \\ &= \underbrace{e^{i\sum\varphi_j}e^{-2i\varphi_N}}_{e^{i\chi}}\frac{1}{\sqrt{N}}\left(\bigotimes_{j=1}^{N} V_j\right)\sum_{k=1}^{N} e^{i2(\varphi_N-\varphi_k)}|\{2^{k-1}\}\rangle \\ &= e^{i\chi}\left(\bigotimes_{j=1}^{N} V_j\right)\left(e^{i\sigma_z\varphi'_1}\otimes\cdots\otimes e^{i\sigma_z\varphi'_{N-1}}\otimes\mathbb{1}\right)|\mathrm{W}\rangle \end{aligned} \tag{A.7}$$

where the leading factor is an unimportant global phase factor and $\varphi'_k = 2(\varphi_N - \varphi_k)$. Thus, we have

$$U|\mathrm{W}\rangle = e^{i\chi}(V_1 e^{i\sigma_z\phi'_1})\otimes\cdots\otimes(V_{N-1}e^{i\sigma_z\phi'_{N-1}})\otimes V_N|\mathrm{W}\rangle. \tag{A.8}$$

Each V_j requires only two parameters to define. Additionally, $N-1$ extra parameters φ'_j are also needed to describe an arbitrary state in $\mathcal{O}(\mathrm{W})$. Thus, we can parameterize an arbitrary state in the W-orbit with $3N-1$ parameters, as given in (5.70).